

**Mechanisms of spike timing-dependent LTP in CA1
region of the hippocampus induced with a low
repeat of coincident pre- and postsynaptic spiking**

Dissertation

zur Erlangung des akademischen Grades

Doctor rerum naturalum

(Dr. rer. nat.)

genehmigt durch die Fakultät für Naturwissenschaften
der Otto-von-Guericke-Universität Magdeburg

von **M.Sc., B.Sc. Efrain Augusto Cepeda-Prado**

geb. am **23.11.1976** in **Bogotá, Colombia.**

Gutachter: **Prof. Dr. Volkmar Leßmann**
Prof. Dr. Christian Lohmann

eingereicht am: **19.06.2018**

verteidigt am **12.09.2019**

Table of contents

Abbreviations.....	v
List of figures.....	vii
Abstract.....	ix
Zusammenfassung.....	x
1. Introduction.....	12
1.1 The hippocampal formation and memory processing.....	12
1.2 Synaptic transmission.....	13
1.3 Synaptic plasticity as a substrate of learning and memory.....	15
1.4 Spike timing-dependent plasticity.....	18
1.4.1 Molecular mechanisms of LTP.....	19
1.5 Modulation of synaptic plasticity.....	23
1.5.1 Dopamine.....	23
1.5.2 The functional consequences of DA signals.....	23
1.5.3 Brain-derived neurotrophic factor.....	25
1.6 Rationale.....	26
2. Material and Methods.....	28
2.1 Animals.....	28
2.2 Preparation of hippocampal slices.....	28
2.3 Electrophysiological recordings.....	30
2.4 Induction of spike timing-dependent plasticity.....	35
2.5 Pharmacological tools.....	36
2.6 Data acquisition.....	37
2.7 Statistical analysis.....	38
3. Results.....	40
3.1 Induction of spike timing-dependent plasticity at Schaffer collateral-CA1 synapses.....	40
3.2 Timing dependent-LTP at Schaffer collateral-CA1 synapses requires only six single spike pairings.....	41
3.3 Incorporation of multiple postsynaptic spikes into a low repeat STDP paradigm.....	44
3.4 Low repeat STDP induces associative t-LTP, but not t-LTD.....	45
3.5 Single and multiple postsynaptic action potentials influence the locus of t-LTP expression.....	49
3.6 Distinct calcium sources are activated by low repeat STDP paradigms.....	56
3.7 Dopamine receptor dependence of t-LTP induced with low repeat STDP protocols.....	61
3.8 Influence of BDNF/TrkB signaling on t-LTP induced with only six pre-post pairings.....	67
4. Discussion.....	74
4.1 Response of hippocampal Sc-CA1 synapses to different numbers of single pre-post pairings.....	74
4.2 Cellular mechanisms underlying the expression of low repeat t-LTP at hippocampal Sc-CA1 synapses.....	75
4.3 Low repeat t-LTP induced with single and multiple postsynaptic spikes recruit distinct calcium signals.....	77

4.4	Dopaminergic modulation of low repeat t-LTP.....	80
4.5	Contribution of BDNF/TrkB signaling to low repeat t-LTP induction.....	82
4.6	General conclusion.....	82
5.	References	85
6.	Appendix.....	102

Abbreviations

Δt	delta-time, spike timing in ms
AC	adenylyl cyclase
ACSF	artificial cerebrospinal fluid
AMPA	α -amino-3-hydroxy-5-methylisoxazole-4-propionic acid receptor
ANOVA	analysis of variance
AP	action potential
BDNF	brain-derived neurotrophic factor
BLA	basolateral amygdala
CA1	cornu ammonis 1
CA2	cornu ammonis 2
CA3	cornu ammonis 3
CaMKII	calcium/calmodulin-dependent protein kinase II
CB1R	cannabinoid type 1 receptor
CP-AMPA	calcium-permeable AMPA receptor
CREB	cAMP response element-binding protein
CSK	C-terminal Src kinase
DA	dopamine
DG	dentate gyrus
DL-APV	DL-2-amino-5-phosphonopentanoic acid
DMSO	dimethyl sulfoxide
EC	entorhinal cortex
eCB	endocannabinoid
ERK	extracellular related kinase
EPSP	excitatory postsynaptic potential
GABA	gamma-aminobutyric acid
GPCRs	G protein-coupled receptors
HFS	high frequency stimulation
IP3	inositol phosphate 3
ISI	interstimulus intervals
IQR	interquartile range
KO	knock out
LC	locus coeruleus
LFS	low frequency stimulation
LJP	liquid junction potential
LTD	long-term depression
LTP	long-term potentiation
L-LTP	late long-term potentiation
MAPK	mitogen-activated protein kinase
MMP	matrix metalloproteinases
mGluR	metabotropic glutamate receptor
NA	noradrenaline
NaCl	sodium chloride

NaOH	sodium hydroxide
NMDA	N-methyl- D-aspartate
NMDAR	N-methyl- D-aspartate receptor
PI3K	phosphatidylinositol 3-kinase
PKA	protein kinase A
PKC	protein kinase C
PPR	paired-pulse ratio
PSD	postsynaptic density
PTP	post-tetanic potentiation
R _{in}	input resistance
RMP	resting membrane potential
Sc	Schaffer collateral
Sc-CA1	Schaffer collateral - Cornu Ammonis 1 synapse
SCH23390	R-(+)-7-Chloro-8-hydroxy-3-methyl-1-phenyl-2,3,4,5-tetrahydro-1H-3-benzazepine hydrochloride
SEM	standard error of the mean
STDP	spike timing-dependent plasticity
STP	short-term plasticity
TBS	Theta-burst stimulation
t-LTP	timing-dependent long-term potentiation
TrkB	tropomyosin receptor kinase B
VSCC	voltage-sensitive Ca ²⁺ Channels
VTA	ventral tegmental area
WT	wild type

List of figures

Figure 1. The basic hippocampal circuit.

Figure 2. Induction protocols for synaptic plasticity.

Figure 3. Preparation of acute hippocampal slices.

Figure 4. Patch-clamp setup.

Figure 5. Whole-cell patch-clamp recordings.

Figure 6. Paired-pulse ratio analysis.

Figure 7. INMDAR/IAMPAR ratio analysis.

Figure 8. Input resistance and EPSP slope measurements.

Figure 9. Experimental settings for the induction of STDP.

Figure 10. Induction threshold of 1:1 t-LTP at Sc-CA1 synapses in mice.

Figure 11. Induction threshold of 1:1 t-LTP at Sc-CA1 synapses in rats.

Figure 12. 1:4 protocol induces robust t-LTP at Sc-CA1 synapses.

Figure 13. Low repeat STDP paradigms induce long lasting changes in synaptic transmission.

Figure 14. The temporal window of low repeat STDP paradigms.

Figure 15. Cellular mechanisms of 6x 1:1 and 6x 1:4 t-LTP.

Figure 16. Changes in spontaneous and miniature excitatory postsynaptic currents in response to 6x 1:1 stimulation.

Figure 17. Role of retrograde endocannabinoid signaling in 6x 1:1 t-LTP.

Figure 18. IAMPAR/INMDAR ratio at Sc-CA1 synapses after t-LTP induction with low repeat STDP paradigms using horizontal hippocampal slices from mice.

Figure 19. IAMPAR/INMDAR ratio at Sc-CA1 synapses after t-LTP induction with a high number of spike pairings using transversal hippocampal slices from Wistar rats.

Figure 20. NMDARs contribution to low repeat t-LTP.

Figure 21. Activation of L-type Ca^{2+} channels is required for 6x 1:1 but not for 6x 1:4 t-LTP induction.

Figure 22. Antagonist for either mGluR_1 or mGluR_5 has no effects on 6x 1:4 t-LTP.

Figure 23. Postsynaptic $[\text{Ca}^{2+}]$ rise is critical for t-LTP induced with 6x 1:4 protocol.

Figure 24. Variation in the pattern and number of spike pairings leads to the activation of different DARs.

Figure 25. Dopamine uptake inhibitor leads to chemical LTP at Sc-CA1 synapses.

Figure 26. K252a blocks 6x 1:1 but not 6x 1:4 t-LTP.

Figure 27. BDNF/TrkB signaling is not required for t-LTP induced with low repeat STDP paradigms.

Figure 28. Low repeat t-LTP is not affected in BDNF $^{+/-}$ mice.

Figure 29. Zn^{2+} signals are not involved in the trans-activation of Trk receptors associated with the molecular mechanisms of 6x 1:1 t-LTP.

Figure 30. Co-existence of two different forms of synaptic plasticity in the same CA1 pyramidal neuron.

Abstract

In the hippocampus, the consolidation of long-term associative memories occurs rapidly and requires few or even only one-trial presentation of a learning task, suggesting that the encoding of memories occurs very fast at the cellular level. Spike timing-dependent plasticity (STDP) is considered one of the most suitable models to investigate learning and memory processes in the brain at the cellular level. It consists of the repetitive temporal correlation between one excitatory postsynaptic potential (EPSP) and either a single or a burst of postsynaptic action potentials (AP or spikes). In this dissertation the actions of endogenous dopamine and BDNF/TrkB signaling in t-LTP at hippocampal Schaffer collateral (Sc)-CA1 synapses, using two novel different STDP paradigms that consist of only six repeats (6x) of either 1EPSP/1AP or 1EPSP/4AP were investigated. Overall, 6x 1:1 t-LTP is likely to have a presynaptic locus of expression and requires the activation of NMDA receptors (R) and L-type Ca₂₊ channels. This type of plasticity was antagonized by the combination of both D1-like and D2-like dopamine receptor blockers. TrkB receptor seems to be also involved but not the BDNF release. In contrast, 6x 1:4 t-LTP has a postsynaptic expression locus triggering the trafficking of GluA2-lacking AMPARs into the membrane. However, it was unaffected by the presence of selective blockers for NMDAR, L-type Ca₂₊ channels, mGluR₁ or mGluR₅, but requires postsynaptic Ca₂₊ elevation. Activation of D2-like receptors showed to be critical for the induction of 6x 1:4 t-LTP but not BDNF/TrkB receptor signaling. Interestingly, STDP experiments using the same spike pattern but with a higher number of repeats (70x 1:1 and 35x 1:4) revealed a different outcome. T-LTP induced with 70x 1:1 relies on presynaptic mechanisms and requires only D1-like dopamine receptor but not TrkB receptor activation. However, 35x 1:4 t-LTP has postsynaptic locus expression and depends on BDNF/TrkB signaling. These two types of plasticity can be induced in the same cell, indicating that a single CA1 pyramidal neuron hosts multiple types of plasticity that can be triggered by the variation in the patterns and number of pre- and postsynaptic activation. These findings provide new insights into the processing properties and information storage at the single-cell level.

Zusammenfassung

Im Hippocampus erfolgt die Konsolidierung von langanhaltenden assoziativen Gedächtnis schnell und bedarf nur wenigen oder nur einer einzigen Präsentation des Lernreizes. Folglich muss auch die Einspeicherung des Gedächtnisinhaltes auf zellulärer Ebene sehr schnell erfolgen. Die Spike timing-dependent plasticity (STDP) wird dabei als eines der besonders geeigneten Modelle zur Untersuchung zellulärer Grundlagen von Lern- und Gedächtnisvorgängen im Gehirn angesehen. STDP wird durch eine wiederholte, fast zeitgleiche Auslösung von einem erregenden postsynaptischen Potential (EPSP) und entweder, einem einzelnen bzw. multiplen postsynaptischen Aktionspotentialen (APs oder Spikes) induziert. Hier wird der Einfluss von endogenem Dopamin und BDNF/TrkB-Signalwegen auf die t-LTP an Schaffer Kollateral-CA1 Synapsen des Hippocampus untersucht. Dabei werden 2 verschiedene STDP Paradigmen mit jeweils 6 Wiederholungen von 1EPSP/1AP oder 1EPSP/4AP verwendet.

Es konnte gezeigt werden, dass das 6x 1:1 t-LTP höchstwahrscheinlich präsynaptisch exprimiert wird und dass dabei sowohl NMDA Rezeptoren als auch L-Typ Ca_2^+ Kanäle beteiligt sind. Diese Plastizitätsform kann durch eine Kombination von D1- und D2-ähnlichen Dopaminrezeptor-Antagonisten blockiert werden. Weiterhin wurde eine TrkB-Rezeptorbeteiligung in Abwesenheit von BDNF festgestellt. Im Gegensatz dazu hat das 6x 1:4 t-LTP einen postsynaptischen Expressionsort, der durch Einbau von GluA2-freien AMPA Rezeptoren in die Membran ausgelöst wird. Diese LTP ist unabhängig von NMDAR, L-Typ Ca_2^+ Kanäle, mGluR1 oder mGluR5, bedarf aber dennoch einer postsynaptischen Erhöhung des Ca_2^+ Levels. Die Aktivierung von D2-ähnlichen Rezeptoren ist für die Expression des 6x 1:4 t-LTP wichtig, während der BDNF/TrkB-Signalweg nicht aktiviert wird. Interessanterweise, wiesen STDP Experimente mit demselben Paarungsmuster aber höherer Anzahl von Wiederholungen (70x 1:1 und 35x 1:4) einen anderen molekularen Mechanismus auf. Die 70x 1:1 t-LTP hat zwar einen präsynaptischen Expressionsort, wird allerdings alleinig von D1-ähnlichen Rezeptoren ohne eine zusätzliche Beteiligung von BDNF oder TrkB Rezeptoren gesteuert. Die 35x 1:4 t-LTP hat einen postsynaptischen Expressionsort und ist

abhängig vom BDNF/TrkB-Signalweg. Diese zwei Typen von Plastizität können in einer Zelle nacheinander ausgelöst werden, d.h. eine CA1-Pyramidenzelle kann verschiedene Plastizitätsformen ausprägen, die durch unterschiedliche Variationen von Stimulationsmustern und -wiederholungen von prä- und postsynaptischer Aktivierung ausgelöst werden. Diese Befunde lassen Rückschlüsse auf die Verarbeitung und Prozessierung von Gedächtnisinhalten auf dem Level einer Einzelzelle zu.

1. Introduction

1.1 The hippocampal formation and memory processing

The hippocampus is located in the medial temporal lobe of the mammalian brain. It is subdivided into three *Cornu ammonis* (CA) subfields: CA1, CA2, and CA3, which together with the dentate gyrus (DG), the subicular complex (the parasubiculum, presubiculum, and subiculum), and the entorhinal area (lateral and medial entorhinal cortices) form the so-called hippocampal formation (Witter, 1993; Golgi *et al.*, 2001). The general anatomical organization of the connectivity between entorhinal cortex (EC) and the different hippocampal subfields has been classically schematized into an excitatory tri-synaptic circuit as depicted in **Figure 1**.

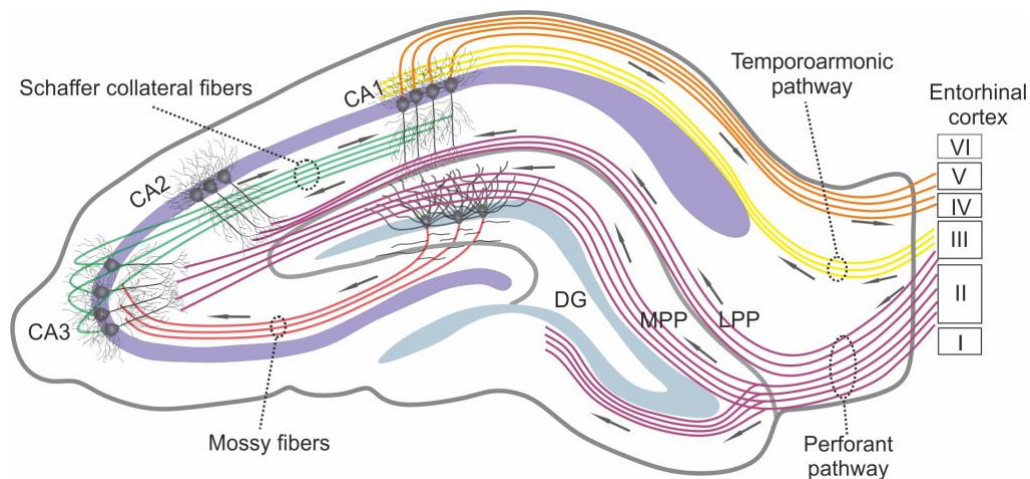


Figure 1. The basic hippocampal circuit. The schematic representation of hippocampus shows its connectivity with adjacent cortical areas. Granular cells in the DG and pyramidal neurons in CA2 region receive direct inputs from neurons located at the layer II and III of the entorhinal cortex (EC) via medial (MPP) and lateral perforant pathway (LPP), respectively. Granule cells located in DG contact CA3 pyramidal neurons via mossy fibers. CA3 pyramidal neurons project to the CA1 subfield through Schaffer collateral fibers. CA1 pyramidal neurons project back to the layers IV and V of EC to complete the loop, which represents the primary output of the hippocampal network. Reciprocally, neurons from layer III of EC also send direct inputs to CA1 via a temporoammonic pathway. The arrows indicate the direction of the flow of the information through the hippocampal formation.

The hippocampus has been extensively investigated from functional, electrophysiological, and behavioral points of view, since the establishment of its direct connection with memory formation in the early 1960s (Scoville and Milner, 1957). Thus, there is general agreement that an essential function of the hippocampal formation is encoding associations between non-spatial or semantic information (e.g., object properties) and its spatiotemporal context (e.g., location) (Eichenbaum and Lipton, 2008). The hippocampus thereby constitutes a very attractive brain region to understand how the brain encodes and stores memories (Witter *et al.*, 1988; Witter, 1993; Lavenex and Amaral, 2000; Witter *et al.*, 2000).

1.2 Synaptic transmission

Since its discovery in 1894 by Santiago Ramon y Cajal, **the synapse** has been considered an essential piece in our understanding about the information processing in the brain (reviewed in (Markram *et al.*, 2011)). The synapse is a specialized junction between a presynaptic axonal terminal also called active zone and a postsynaptic membrane of a neighboring neuron separated by a small space known as synaptic cleft. **The chemical synaptic transmission** requires a signal released from the active zone called **neurotransmitter**, which binds and activates its specific receptor located at the postsynaptic membrane.

The release of neurotransmitter is triggered by the elevation of presynaptic calcium concentration ($[Ca_{2+}]$) caused by the **action potential (AP)** initiation at the initial axon segment. Then, the AP propagates forward along the axon mediated by voltage-activated Na^+ channels causing a depolarization of the presynaptic axonal terminal, and resulting in the activation of voltage-activated Ca_{2+} channels (e.g., N and Q/P type Ca_{2+} channels) (Del Castillo and Katz, 1954; Luebke *et al.*, 1993; Reuter, 1995). Thus, the transient increase in presynaptic $[Ca_{2+}]$ is rapidly buffered by activity-dependent Ca_{2+} regulators of exocytosis that mediate the fusion of the readily releasable pool of vesicles to the presynaptic membrane. This process occurs in milliseconds (Sudhof, 2013; Schneggenburger and Rosenmund, 2015). Neurotransmitter release can also take place in the absence of presynaptic

evoked AP. This release is caused by the spontaneous vesicle fusion in response to sub-threshold elevation of $[Ca^{2+}]$ in the presynaptic axonal terminal, resulting in small fluctuations in the postsynaptic membrane potential so-called **mini excitatory postsynaptic currents (mEPSCs)** (Katz and Miledi, 1967).

Most of the excitatory presynaptic axonal terminals in the brain including the hippocampus are connecting to dendritic spines, tiny membranous protrusions composed of a head (diameter $\sim 1\mu\text{m}$) attached to the dendritic shaft by a spine neck (diameter $\sim 0.2\mu\text{m}$) (Yuste *et al.*, 2000; Megias *et al.*, 2001). They have multiple sizes and shapes classified by their structure as filopodial and thin commonly called small spines, whereas stubby, fenestrated, and mushrooms-shape are all known as large spines (Hering and Sheng, 2001). Dendritic spines are characterized by the presence of a specialized electron-dense region known as postsynaptic density (PSD), which is composed by hundreds of membranous and cytoplasmic proteins (Kennedy, 2000; Boeckers, 2006; Okabe, 2007).

In excitatory synapses the principal neurotransmitter is glutamate. The electro-responsiveness of the glutamatergic synapses depends primarily on two ionotropic glutamate receptors located at the PSD, α -amino-3-hydroxy-5-methyl-4-isoxazolepropionic acid (AMPA) and N-methyl-D-aspartate (NMDA) receptor (R) (Bekkers and Stevens, 1989). AMPARs are the primary responsible for fast excitatory synaptic transmission. The binding of glutamate to the AMPAR causes conformational changes resulting in the ion-channel opening and subsequent influx of Na^+ ions, which produces a brief depolarization of postsynaptic membrane known as **excitatory postsynaptic potential (EPSP)**.

NMDARs are composing by one obligatory homodimer GluN1 subunit plus either a homo or heterodimer of GluN2 or GluN3 subunits (Laube *et al.*, 1998; Kennedy, 2000; Traynelis *et al.*, 2010). NMDARs containing di-heteromeric GluN1/GluN2A, GluN1/GluN2B, and triheteromeric GluN1/GluN2A/GluN2B are considering as the most common at CA1 pyramidal neurons (Tovar *et al.*, 2013). Even though NMDAR activation also depends on glutamate release, it does not contribute considerably to the basal transmission. That is mainly due that NMDAR has slow kinetics and its

responsiveness is limited by the voltage-dependent Mg^{2+} block, which directly interferes with the flow of ions (K^+ , Na^+ , and Ca^{2+}) through the receptor voltage-gated pore. The opening of the voltage-gated pore of the NMDAR is determined by coincidence between the glutamate binding to the receptor, and the relief of the Mg^{2+} block caused by strong postsynaptic depolarization (Nowak *et al.*, 1984; Collingridge *et al.*, 1988). There is a general agreement that the influx of Ca^{2+} via NMDAR is an essential step required for the regulation of the enzymatic machinery that enables the synapse undergoes structural and functional modifications, leading to changes in strengthening and efficacy of AMPAR-mediated synaptic transmission so-called **synaptic plasticity**.

1.3 Synaptic plasticity as a substrate of learning and memory

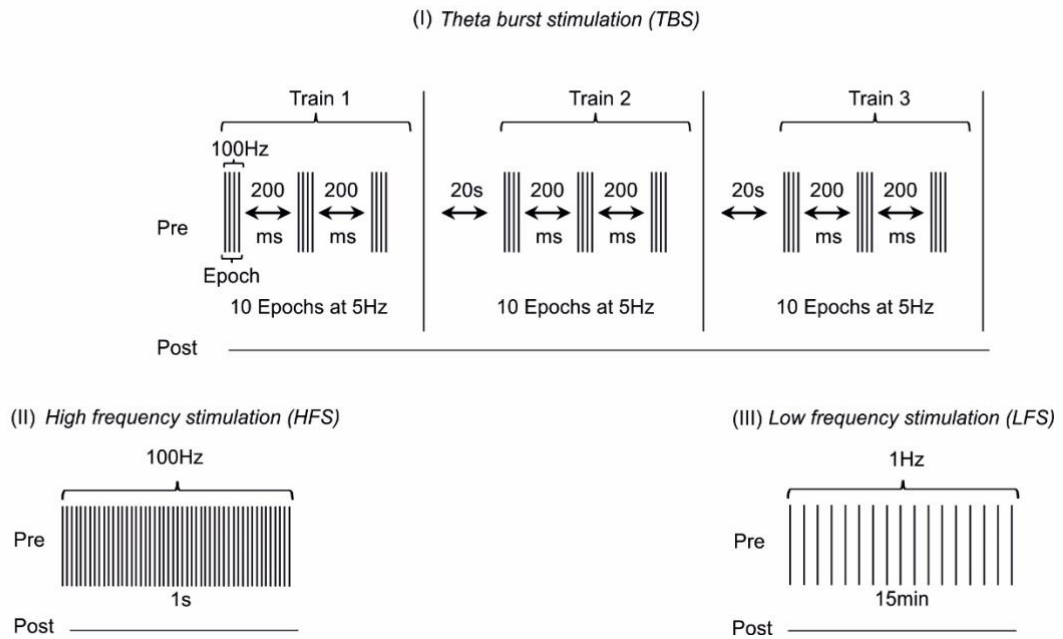
The theoretical conceptualization of the role of synaptic plasticity in memory formation was enormously influenced by the work of the neuropsychologist Donald Hebb, who postulated the associative learning rule: *“When an axon of cell A is near enough to excite a cell B and takes part in firing it, some growth process or metabolic change takes place in one or both cells such that A’s efficiency, as one of the cells firing B, is increased”* or so-called Hebbian learning rule (reviewed in (Markram *et al.*, 2011)).

It was not until 1973 when Bliss and Lømo showed the first experimental evidence of Hebb’s associative learning rule. They report that a high-frequency stimulation at the synapses between entorhinal cortex and granule cells in hippocampus results in persistent increase of synaptic transmission so-called **long-term potentiation (LTP)** (Lømo, 1966; Bliss and Gardner-Medwin, 1973; Bliss and Lomo, 1973). Later on, Lynch and collaborators (1977) found the opposite effect in Schaffer collateral (Sc)-CA1 synapses, i.e., a decrease in synaptic transmission in response to low-frequency stimulation, known as **long-term depression (LTD)** (Lynch *et al.*, 1977).

Nowadays, multiple forms of activity-dependent synaptic modifications that differ in duration and mechanisms have been identified (Bliss and Collingridge, 1993; Citri and Malenka, 2008; Nicoll, 2017). Short-lasting forms, known as **short-term plasticity (STP)** mainly refers to changes in neurotransmitter release in response to synaptic stimulation, lasting from milliseconds to seconds even minutes. Commonly, short-term changes in synaptic transmission are observing by the electrophysiological protocol known as **paired-pulse facilitation or depression**. This protocol consists of a consecutive presynaptic depolarization induced by two electrical pulses delivered within an interstimulus interval (ISI) of few milliseconds. Overall, facilitation is defined when the peak amplitude of the second response is greater than the first one and, depression when the second response is smaller than the first one. Usually, paired-pulse facilitation occurs with long ISI (20 to 500ms), whereas shorter ISI (<20ms) leads to depression (Citri and Malenka, 2008). Another type of STP is the post-tetanic potentiation (PTP), which consists of a transient enhancement of neurotransmitter release commonly elicited right after high-frequency presynaptic stimulation that can last several minutes (Regehr, 2012).

For the induction of long-lasting changes in synaptic transmission, there is a broad spectrum of experimental protocols. In extracellular recordings, theta-burst stimulation (TBS; **Figure 2A, I**) or high-frequency stimulation (HFS; **Figure 2A, II**) are usually used to induce changes in local field potentials i.e., synaptic activity from a large population of neurons collected by an extracellular recording electrode (Larson and Munkacsy, 2015; Abrahamsson *et al.*, 2016). In contrast, low-frequency stimulation (LFS) is the most traditional protocol for LTD (**Figure 2A, III**). At the single-cell level, LTP is classically induced by synchronous activation of pre- and postsynaptic components using *theta-burst pairing* (**Figure 2B, I**) and *pairing protocols* (**Figure 2B, II**) (Gustafsson *et al.*, 1987; Liao *et al.*, 1995; Chen *et al.*, 1999).

A. Local field potentials (LFPs)



B. Intracellular recordings

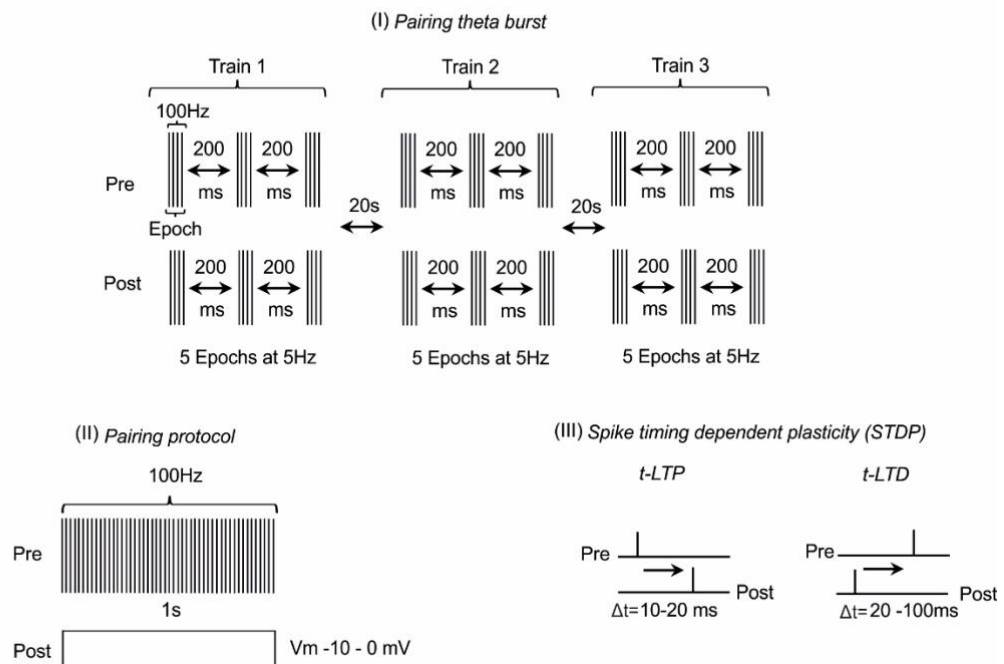


Figure 2. Induction protocols for synaptic plasticity. (A) Conventional protocols to induce LTP of the local field potentials: (I) *TBS*, a strong presynaptic (Pre) stimulation that usually uses three trains consisting of 10 epochs delivered at 5 Hz. Each epoch is composed

of four stimulations with a frequency of 100 Hz. (II) *HFS* is basing on multiple presynaptic evoked stimulations delivered at 100 Hz for 1s, repeated two or three times. (III) *LFS* consisting of 900 pulses delivered in 15 min, corresponding to 1 Hz, which is typically used to induce LTD. **(B)** The traditional protocols used to induce LTP at the single-cell level are: (I) *Theta-burst pairing* in which pre- and postsynaptic neurons are synchronously activated with three trains consisting of 5 epochs delivered at 5 Hz. Each epoch is composed of four stimulations with a frequency of 100 Hz. (II) *Pairing protocol*: HFS is pairing with strong postsynaptic (Post) depolarization to a holding potential -10 to 0mV, repeated two or three times. (III) STDP is eliciting by the repeated (60-100 times at 0.5-2 Hz) pairing of pre- and postsynaptic activations. The induction of timing-dependent (t)-LTP occurs when a presynaptic input precedes a single postsynaptic action potential (positive spike timing) within a delta-time/spike timing (Δt) of +10 to +20 ms, whereas the reverse order (negative spike timing) causes t-LTD, which is observing at longer Δt between -15 to -100 ms.

1.4 Spike timing-dependent plasticity

Spike timing-dependent plasticity (STDP) is another type of pairing protocol in which induction of LTP and LTD depends on the order and the timing between pre- and postsynaptic activation (**Figure 2B, III**). In the hippocampus, the presynaptic activation is given by the depolarization of the afferents arriving at the postsynaptic neuron (e.g., Schaffer collaterals fibers) to produce an EPSP or presynaptic input. The EPSP is paired with single or multiple postsynaptic APs, induced by somatic current injection, with a delay of 10 ms. The **back-propagation** of postsynaptic APs (bAP) from the soma along to apical dendrites via voltage-gated Na⁺ channels is considered a crucial postsynaptic signal for the STDP induction (Amitai *et al.*, 1993; Kim and Connors, 1993; Magee and Johnston, 1997; Larkum *et al.*, 1999; Kampa *et al.*, 2006; Hardie and Spruston, 2009). Moreover, under certain circumstances, the bAP can also causes strong dendritic depolarization leading to the initiation of regenerative local membrane potentials known as **dendritic spikes**, which are essential for STDP induction at distal dendrites (Jaffe *et al.*, 1992; Larkum *et al.*, 1999; Golding *et al.*, 2002; Chen *et al.*,

2006). Thus, STDP occurs by the repetitive coincidence between one EPSP and single or multiple action potentials within a time interval or delta-time (Δt) of ~ 10 ms (Debanne *et al.*, 1994; Debanne *et al.*, 1997; Markram *et al.*, 1997; Bi and Poo, 1998; Debanne *et al.*, 1998).

STDP has been tested *in vitro* and *in vivo* in several models of mammals including rodents, monkeys, and even humans (Dan and Poo, 2004; Dan and Poo, 2006; Caporale and Dan, 2008). The coincidence detection of spatiotemporal patterns of activity has also been used to create stochastic mathematical simulations to visualize the effects of STDP on cellular networks using computational modeling (Chistiakova *et al.*, 2015; Zenke and Gerstner, 2017).

1.4.1 Molecular mechanisms of LTP

The structural and functional modifications of pre- and postsynaptic compartments in response to a given LTP induction protocol requires the activation, mobilization, and synthesis of hundreds of molecules within precise spatial and temporal coordination. The series of the cellular and molecular events underlying such modifications are broadly categorized in different temporal phases known as induction, expression, and maintaining of LTP, as describe (Huang, 1998; Malenka and Bear, 2004; Citri and Malenka, 2008).

a. LTP Induction

Most of the forms of LTP described in hippocampus require postsynaptic Ca^{2+} elevation mediated by NMDAR activation (Collingridge *et al.*, 1983; Mayer *et al.*, 1984; Guthrie *et al.*, 1991; Alford *et al.*, 1993; Bliss and Collingridge, 1993; Bosch *et al.*, 2014), except for mossy fibers-CA3 synapses in which LTP is NMDAR-independent and relies on presynaptic mechanisms (Harris and Cotman, 1986; Nicoll and Schmitz, 2005).

Upon glutamate release, the influx of Ca^{2+} through activated NMDAR is following by a morphological reorganization of the dendritic spine, consisting in a head

enlargement together with the shrinking and swelling of the spine neck (Fifkova and Van Harrevel, 1977; Guthrie *et al.*, 1991). These structural modifications of the dendritic spines have an essential role in the regulation of calcium dynamics and the protein translocation into the spine to mediate subsequent postsynaptic modifications (Shi *et al.*, 2001; Lee *et al.*, 2009; Bosch *et al.*, 2014; Barcomb *et al.*, 2016).

One of the first steps within the molecular mechanisms associated to the regulation of calcium signals required for LTP induction is the activation of a serine/threonine-specific protein kinase known as Ca^{2+} /calmodulin kinase II (CaMKII) (Otmakhov *et al.*, 2004; Ahmed *et al.*, 2006; Rellos *et al.*, 2010; Lisman *et al.*, 2012). The influx of Ca^{2+} via NMDAR, after LTP induction, leads to the activation of Calmodulin, a diffusible Ca^{2+} binding protein, which activates CaMKII. The interaction between CaMKII and Ca^{2+} /calmodulin complex provoke conformational changes releasing the regulatory segment of the enzyme leading to the autophosphorylation of CaMKII (at Thr286 or Thr287), which is known as “autonomous” state or switching on. Whereas phosphorylation at Thr305 and Thr306 allows to the enzyme to come back to its original molecular conformation, preventing the binding of Ca^{2+} /calmodulin complex, switching off its kinase activity (Miller and Kennedy, 1986; Chao *et al.*, 2011). Upon autonomous state, CaMKII moves into the PSD, where interacts with NMDAR and L-type Ca^{2+} channels having a persistent kinase activity that can lasts ~45s even hours (Miller and Kennedy, 1986; Leonard *et al.*, 1999; Zhang *et al.*, 2008; Lee *et al.*, 2009; Barcomb *et al.*, 2016). Such persistent activity of CaMKII allows the enzyme the biochemical integration of several Ca^{2+} signals and the regulation of critical molecular processes associated with early and even late LTP (Lisman *et al.*, 2012).

b. Expression LTP

It refers to the synaptic modification associated with the initial (30-60 min) increase in synaptic transmission after LTP induction. The locus expression of LTP has been subject of intense debate for years and is still controversial. The big question is whether LTP expression depends primarily on pre- or postsynaptic

mechanisms, or both together (Malenka and Bear, 2004; Costa *et al.*, 2017b; Lisman, 2017).

In general, changes in AMPAR properties such as the increase in open probability and conductance of AMPAR ion channel as well as enhancement of AMPAR translocation to the postsynaptic membrane have been proposed as signatures of postsynaptic forms of LTP (Benke *et al.*, 1998; Penn *et al.*, 2017). AMPARs are composed of four subunits GluA1-4 expressed throughout the brain. It is known that the permeability and trafficking of AMPARs rely on their subunit composition (Shi *et al.*, 2001). Under resting conditions, there is dynamic recycling of AMPAR containing GluA2 subunits at the postsynaptic membrane. These receptors are permeable to Na⁺ and K⁺ and primary support basal synaptic transmission. While the incorporation of AMPAR containing homomers of GluA1, GluA3, or GluA4 subunits known as AMPAR GluA2-lacking Ca²⁺ permeable (Cp)-AMPARs is activity-dependent (Chen *et al.*, 2000; Shi *et al.*, 2001; Brecht and Nicoll, 2003; Ashby *et al.*, 2006). Phosphorylation of C-terminal at Thr887 of GluR1 subunit followed the activation of CaMKII represents an essential step for the enhancement of Cp-AMPAR trafficking towards PSD. Interestingly, it has been shown that the insertion of Cp-AMPARs occurs right after LTP induction, and its presence lasts not more than 25 min. Then, Cp-AMPARs will be replaced by Ca²⁺ impermeable AMPAR contain GluA2 subunits, which should maintain the LTP expression (Plant *et al.*, 2006). Also, CaMKII enhances AMPAR conductance through the phosphorylation of the C-terminal of GluA1 subunit at Ser831. However, changes in the open probability of the AMPAR ion channel has been attributed to the phosphorylation the receptor at Ser845 by protein kinase A (PKA) (Benke *et al.*, 1998; Penn *et al.*, 2017).

On the other hand, changes in release properties such increase in probability of neurotransmitter release or the number of release sites, and elevation of cleft glutamate concentration that has been categorizing as typical signals associated with presynaptic modifications (Malinow, 1991). The presynaptic forms of LTP are usually dependent of retrograde messengers released from the postsynaptic neuron that bind specific receptors located on the presynaptic terminals, where

they mediate changes in the probability of neurotransmitter release (Pare, 2004; Andrade-Talavera *et al.*, 2016). Several molecules such as arachidonic acid (Williams *et al.*, 1989), nitric oxide (Padamsey *et al.*, 2017), and endocannabinoids (eCB) (Yang and Calakos, 2013) have been identified as retrograde messengers associated to the regulation of synaptic transmission efficacy.

b. Maintaining LTP

The integration of Ca²⁺ signals triggered by the synaptic stimulation during early phases of LTP is mediated by several kinases such as protein kinase A (PKA), CaMKII, CaMKIV, ERK1/2 (Chwang *et al.*, 2006; Citri and Malenka, 2008), and Ras/Raf1/MAPkinase pathway (Illario *et al.*, 2003; Bosch *et al.*, 2014). These molecular pathways converge in the activation of transcription factors, e.g., cAMP response element-binding protein (CREB), leading to the transcription of early genes including *cfos*, *bdnf*, *src*, and *zif268/egr-1*, which are involved in the structural modifications required for the maintenance of LTP (Jones *et al.*, 2001; Thomas and Huganir, 2004; Bliim *et al.*, 2016). Such modifications include an enlargement of PSD, due to the enrichment of the postsynaptic terminal with newly synthesized protein, which positively correlates with the size of the presynaptic bouton. Additionally, there is an increase in the expression of cell-adhesion molecules (e.g., N-cadherin, neuroligin, and ephrins) that contribute to the stabilization of the connection between pre- and postsynaptic terminals. Moreover, the expansion of the postsynaptic terminal could also lead to the splitting of the PSD into two new functional synapses (perforated synapses). The growth of entirely new dendritic spines is also part of the structural changes associated with the later phases of LTP (Nikonenko *et al.*, 2002; Matsuzaki *et al.*, 2004).

1.5 Modulation of synaptic plasticity

There is a large body of evidence indicating that neuromodulatory inputs directly influence the molecular components, shaping synaptic modifications at different timescales from short-term potentiation to early and late phases of LTP (Nadim

and Bucher, 2014; Fremaux and Gerstner, 2016). Neuromodulation has been proposed as an essential factor controlling synaptic efficacy in several brain regions (Seol *et al.*, 2007).

1.5.1 Dopamine

Dopamine (DA) is considering a powerful neuromodulator of synaptic plasticity in several brain regions (Geisler and Zahm, 2005). In the hippocampus, DA participates in the encoding of novelty and reward signals (Lisman and Grace, 2005; Bethus *et al.*, 2010; Brzosko *et al.*, 2015; Moreno-Castilla *et al.*, 2017), as well as spatial learning (Kempadoo *et al.*, 2016) and novel object recognition (Yang *et al.*, 2017). Activation of BDNF/TrkB signaling has been identified as important mediator of DA actions in synaptic plasticity (Iwakura *et al.*, 2008; Navakkode *et al.*, 2012) as well as regulator of dopaminergic signals through the modulation of DA release (Goggi *et al.*, 2002) and DARs expression (Do *et al.*, 2007). However, cellular and molecular processes that underlying DA actions are still not well understood (Edelmann and Lessmann, 2018)

1.5.2 The functional consequences of DA signals

For years, the *substantia nigra* and *ventral tegmental area* (VTA) at the midbrain have been considered as the primary dopaminergic input that innervates mainly subiculum and CA1 region of the ventral and dorsal hippocampus (Gasbarri *et al.*, 1994; Gasbarri *et al.*, 1996). Most recently, it has been demonstrated a co-release of noradrenaline and DA to the dorsal hippocampus through noradrenergic fibers coming from *locus coeruleus* (Smith and Greene, 2012; Kempadoo *et al.*, 2016; McNamara and Dupret, 2017). Despite the numerous studies confirming the critical role of DA in hippocampus-dependent memories, controversies remain about the role of DA inputs and their connectivity to the hippocampal circuit.

Regarding the DA receptors (Rs), the emerging picture seems to be more explicit. Five different receptors, widely distributed in the hippocampus, have been identified and classified into two classes: D1-like (D1 and D5) and D2-like (D2, D3,

and D4) DARs (Dewar and Reader, 1989; Kohler *et al.*, 1991). Those receptors have different sensitivities and affinities to the ligand. D1-like and D2-like DARs respond to high and low levels of DA, respectively (Richfield *et al.*, 1989). DARs are G-protein coupled receptors (GPCR) assembling as homo- or heterodimers (e.g., D1-D2, D1-D3, and D2-D4). Variations in the subunits of the G protein ($G\alpha$ and the complex $G\beta\gamma$) provide a broader spectrum of actions of the receptor (Oldham and Hamm, 2008). For instance, it is known that activation D1-like DARs coupled to $G\alpha_{s/olf}$ subunits positively modulate cyclic adenosine monophosphate/protein kinase A (cAMP/PKA) pathway, whereas activation of D2-like DARs coupled to $G\alpha_{i/o}$ induce inactivation cAMP/PKA pathway (Tritsch and Sabatini, 2012). Furthermore, mobilization of Ca^{2+} signals from internal stores can be regulated by homodimeric D1R or heterodimers such as D1-D2Rs via $G\alpha_q$ subunits, and its interaction with inositol trisphosphate (IP3)-PKC α signal-transduction pathway (Beaulieu and Gainetdinov, 2011; Tritsch and Sabatini, 2012). Additionally, D2-like DARs, via protein kinase C-alpha (PKC α) and CaMKII signaling through $G\beta\gamma$ subunits, modulate several conductances including voltage-dependent Na^+ channels, T-type Ca^{2+} and A-type K^+ channels, having effects on the generation and propagation of APs (Hoffman and Johnston, 1999), and influencing intrinsic neuronal excitability (Edelmann and Lessmann, 2011).

Dopamine also promotes t-LTP instead of t-LTD in the hippocampus (Kuczewski *et al.*, 2010; Pawlak *et al.*, 2010). Bath application of DA facilitates LTP and enhances synaptic efficacy via D1-like DARs at hippocampal Sc-CA1 synapses (Brzosko *et al.*, 2015). On the other hand, the role of D2-like DARs in synaptic plasticity is less well understood. Particularly, it has been shown that D4Rs expressed in interneurons in the *stratum oriens* can cause changes in synaptic strength on pyramidal neurons through the modulation of the feed-forward inhibition (Herwerth *et al.*, 2012; Navakkode *et al.*, 2017). To date, DA is generally accepted as being critical for the modulation of different forms of synaptic plasticity (Hansen and Manahan-Vaughan, 2014). However, the mechanisms are still not well understood.

1.5.3 Brain-derived neurotrophic factor

Brain-derived neurotrophic factor (BDNF) is a member of the neurotrophins protein family, which has a widespread expression in the central nervous system. It is recognized as an essential modulator of synaptic development and plasticity having effects on pre- and postsynaptic compartments (Gottmann *et al.*, 2009; Ohno-Shosaku and Kano, 2014). The synthesis of mature BDNF (mBDNF) rely on the proteolytic cleavage of BDNF precursor pro-BDNF, which occurs through two distinct mechanisms: (i) intracellularly via furins in the *trans-Golgi* network and by pro-protein convertase 1/3 (PC1/3) in secretory granules (Mowla *et al.*, 2001), or (ii) extracellularly by the action of matrix metalloproteases (Hwang *et al.*, 2005; Ethell and Ethell, 2007; Lessmann and Brigadski, 2009). While pro-BDNF is implicating in LTD via p75 neurotrophin receptors (p75^{NTR}) activation; Leal *et al.*, 2017), mBDNF is gating and facilitating long-lasting changes in synaptic plasticity through its interacts with tropomyosin receptor kinase B (TrkB) (Figurov *et al.*, 1996; Edelman *et al.*, 2014; Lu *et al.*, 2014; Edelman *et al.*, 2017), Furthermore, BDNF/TrkB signaling promotes the expression and trafficking of NMDARs and AMPARs (Caldeira *et al.*, 2007a; Caldeira *et al.*, 2007b), and the enhancement of neurotransmitter probability release (Lessmann *et al.*, 1994; Kang and Schuman, 1995),

The release of BDNF and subsequent activation of TrkB receptor is an activity-dependent process (Lessmann, 1998; Hartmann *et al.*, 2001) that involves primary three molecular pathways: phospholipase C-gamma (PLC- γ), phosphatidylinositol 3-kinase (PI3K)/Akt protein kinase, and Ras/Raf/MEK/ERK (Poo, 2001; Leal *et al.*, 2014). Interestingly, TrkB receptors can also be activated independently of BDNF, a process known as transactivation, which can be mediated by GPCRs such as D1-like or D2-like DARs and adenosine A2A receptors (Rajagopal *et al.*, 2004; Swift *et al.*, 2011), and has been implicated in synaptic plasticity in hippocampal mossy fiber-CA3 synapses (Huang *et al.*, 2008) and CA3-CA1 synapses (Mohajerani *et al.*, 2007).

1.6 Rationale

For years, hippocampal synaptic modifications have been classically studied *in vivo* and *in vitro* using a plethora of protocols, which are consisting of many APs delivered at high or low frequency (**Figure 2**). However, such strong stimulation can lead to an overload of the neuronal networks, resulting in a disruption of the cell capacity to express further LTP, a phenomenon known as LTP-saturation. It has been demonstrated that LTP-saturation impairs memory formation in the hippocampus rather than contribute to its consolidation (Holscher, 1997; Moser *et al.*, 1998).

On the other hand, behavioral experiments have shown that consolidation of long-term associative memories occurs rapidly and requires few or even only one-trial presentation of a learning task (Tse *et al.*, 2007), suggesting that memories are encoded very fast at the cellular level. Theoretical studies have proposed that *in vivo*, changes in synaptic strength could occur with ≤ 10 correlations between pre-postsynaptic spikes (Yger *et al.*, 2015), which have been already demonstrated in hippocampal cultured neurons after exogenous application of DA (Zhang *et al.*, 2009), as well as at layer 2/3 synapses in visual cortex (Froemke *et al.*, 2006) and corticostriatal synapses in the striatum (Cui *et al.*, 2015), but it remains unexplored in hippocampal Sc-CA1 synapses.

On the other hand, previous studies in our group showed that a BDNF-independent t-LTP at Sc-CA1 synapses can be induced by the correlation of one presynaptic input with a single action potential, which is repeated 70-100 times (70x 1:1) within 10 ms time window. In contrast, when the presynaptic input was pairing with a postsynaptic burst (four spikes at 200 Hz) and repeated 25-35 times (35x 1:4), a BDNF-dependent t-LTP was elicited (Edelmann and Lessmann, 2011; Edelmann *et al.*, 2015). In the light of those findings, in this dissertation, the following **hypothesis** was tested:

The number and pattern of spike pairings heavily influence the cellular and molecular mechanisms underlying t-LTP, leading to multiple types of synaptic plasticity in hippocampal Sc-CA1 synapses.

Therefore, the **specific aims** of this dissertation were:

1. Determine whether t-LTP can be induced with ≤ 10 spike pairings at hippocampal Sc-CA1 synapses.
2. Evaluate the influence of single and multiple postsynaptic spikes on the magnitude as well as the cellular and molecular mechanisms underlying LTP at hippocampal Sc-CA1 synapses.

2. Material and Methods

2.1 Animals

For this study, two lines of juvenile (P28-P35 days old) male mice were using: C57BL/6J wild-type (WT) and BDNF heterozygous knockout (BDNF^{+/-}) animals with its corresponding WT littermates (Korte *et al.*, 1995). BDNF^{+/-} mice were breeding on the C57BL/6J genetic background. The genotype of the transgenic animals was confirmed using polymerase chain reaction (PCR). The DNA was obtaining from ear biopsies taken from three weeks old animals by an ear punch. Additional tissue samples from the tails were taken from sacrificed animals on the day of the experiment to confirm the genotype. For some experiments, juvenile (P15–P23) Wistar rats (Charles River, Sulzfeld) were using.

All the animals were housing in standard cages supplied with nesting material, food, and water *ad libitum* and maintained at the local conventional animal facility with a constant room temperature of 21 ± 0.3 °C, the humidity of $55 \pm 10\%$, and 12 h light-dark cycle. All experiments were conducted following the European Committee Council Directive (86/609/EEC) on the protection and ethical guidelines for experimental animal methods approved by the local animal care committee (Landesverwaltungsamt Sachsen-Anhalt).

2.2 Preparation of hippocampal slices

STDP experiments were performing in the CA1 region of acute horizontal hippocampal slices prepared from four weeks old WT, BDNF^{+/-}, and littermates C57BL/6J mice. For some experiments, transversal hippocampal slices from juvenile Wistar rats were used. Briefly, the animals were decapitating under deep anesthesia with isoflurane (Sigma, Germany) and the brain was rapidly dissected and transferred into ice-cold artificial cerebrospinal fluid (ACSF) cutting buffer containing (in mM): 125 NaCl, 2.5 KCl, 0.8 NaH₂PO₄, 25 NaHCO₃, 25 Glucose, 6 MgCl₂, 1 CaCl₂; pH 7.4; ~303 mOsmol/kg, saturated with 95% O₂ and 5% CO₂. Both

hemispheres were split up and sliced separately. The cerebellum and olfactory bulb were removed to create a tissue block from each hemisphere that was horizontally sectioned (350-400 μm thick) using a vibratome (Leica-VT 1200 S, Leica Biosystems, Germany). All electrophysiological experiments were carried out in intermediate slices (**Figure 3A-B**), since in horizontal slices at this level all structures of hippocampal formation can be easily identified (**Figure 3C**). Slices were then transferred into a handmade interface chamber containing a hydrophilic membrane (0.4 μm Millicell culture insert, PICMORG50, Millipore, Germany) submerged in carboxygenated ACSF cutting buffer in which the slices were incubated for 25 min at 32°C into a water bath. Then, the slices were kept at room temperature ($\sim 21^\circ\text{C}$) for at least 60 min before the recording started. The GABAergic inhibitory input was partially blocked by adding a specific GABA_A inhibitor (picrotoxin 100 μM ; Sigma, Germany) to the carboxygenated ACSF buffer to facilitate LTP induction. The epileptiform discharges resulting from the presence of the GABA_A blocker were prevented by cutting Schaffer collateral (Sc) fibers at the CA2 region (**Figure 3C**), silencing the spontaneous excitatory activity coming from CA3 area.

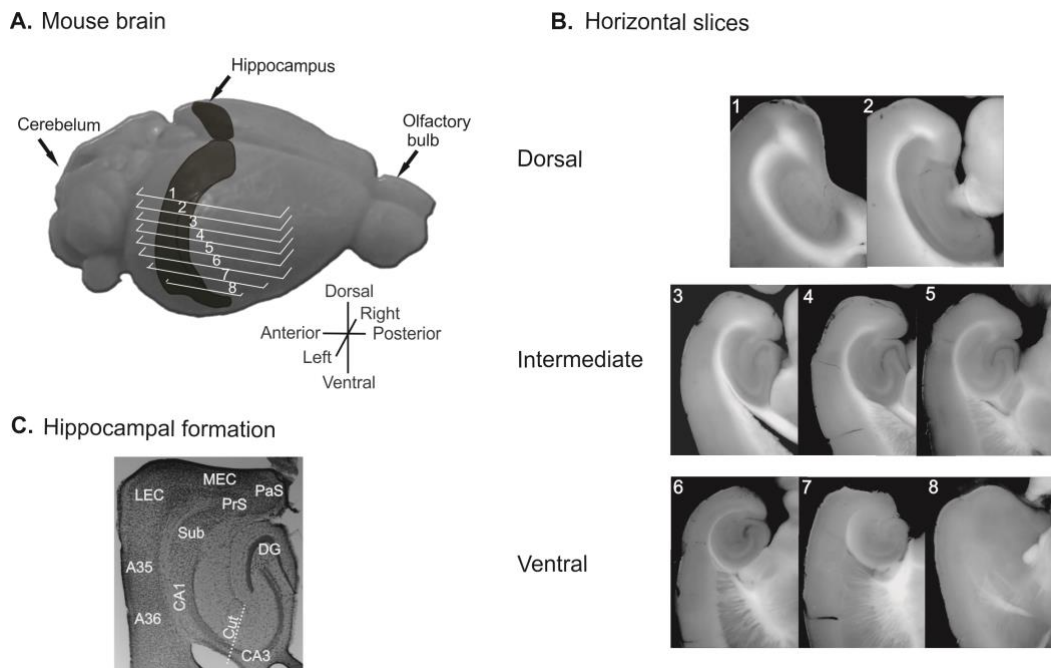


Figure 3. Preparation of acute hippocampal slices.

Continuation of Figure 3. (A) Picture of a mouse brain schematizes the slice-cutting angle. **(B)** The number on the microphotograph indicates the level from which the series of slices were taking from one single hemisphere – see A. **(C)** Nissl staining of a typical acute horizontal hippocampal slice containing: CA1, CA3, and DG; Sub: subiculum, Prs: pre-subiculum and PaS: para-subiculum; MEC: medial entorhinal cortex, LEC: lateral entorhinal cortex, and the perirhinal cortex (consisting of Brodmann areas A35 and A36). The microphotograph also indicates the localization of the cut between CA1 and CA3 region mentioned in the text (dot line).

2.3 Electrophysiological recordings

After 60 min of incubation, a slice was transferred to the submerged recording chamber of electrophysiological setup. The slice was under continuous perfusion (1-2 ml per min) with warmed ($30 \pm 0.2^\circ\text{C}$) carboxygenated ACSF buffer containing (in mM): 125 NaCl, 2.5 KCl, 0.8 NaH_2PO_4 , 25 NaHCO_3 , 25 Glucose, 1 MgCl_2 , 2 CaCl_2 ; pH 7.4; ~ 303 mOsmol/kg, saturated with 95% O_2 and 5% CO_2 . The recording setup was equipped with a fixed stage Zeiss microscope (Carl Zeiss, Jena, Germany,) coupled to a charge-coupled device (CCD)-infrared (IR) camera (PCO AG, Kelheim, Germany) that was connected to a monitor. The recording and stimulation electrodes were under the control of two micromanipulators (HEKA, Lambrecht/Pfalz, Germany). These electrodes were made from borosilicate glass filaments (outside 1.5 mm, inside 1.05 mm diameter; Science products, Hofheim am Taunus, Germany) using a two-step puller (Narishige Scientific Instrument Lab, Tokyo, Japan). The electrophysiological recordings were performing with a patch-clamp EPC-8 amplifier controlled by PATCHMASTER software (HEKA, Lambrecht/Pfalz, Germany) via a data interface (IntruTECH LIH 8+8, HEKA, Lambrecht/Pfalz, Germany). A stimulator device (Model 2100, A-M Systems, USA) was using to command the frequency and strengthening of the pulses delivered through the stimulation electrode. All electrical events were constantly monitored using a Tektronix TDS210 oscilloscope (Tektronix, Inc. Oregon, USA). The direction of the electrical signals flowing through the electrophysiological setup is shown in **Figure 4**. Once the slice was placed into the recording chamber, an anchor with

parallel Nylon threads was used to stabilize it. Then, under visual control, a glass stimulation electrode (resistance 0.7-0.9 M Ω) was positioned in the *striatum radiatum* in CA1 region to depolarize the Sc fibers.

The whole-cell patch-clamp recordings were performed from pyramidal neurons in the CA1 region of the hippocampus. A 60x water immersion objective was used to select a target cell. Then, a recording pipette (resistance 5-7 M Ω) filled with an internal solution containing (in mM): 10 HEPES, 20 KCl, 115 potassium gluconate, 0.001 CaCl₂, 10 Na phosphocreatine, 0.3 Na-GTP, and 4 Mg-ATP; pH 7.4, 285-290 mOsmol/kg was placed in the pipette holder. Under focus, the tip of the pipette went down until it overlapped with the shadow of the cell (**Figure 5**, step 1). At this point, slight positive pressure was applied using a 1ml syringe coupled to a three-way valve connected to the pipette holder through a plastic tube (**Figure 4**).

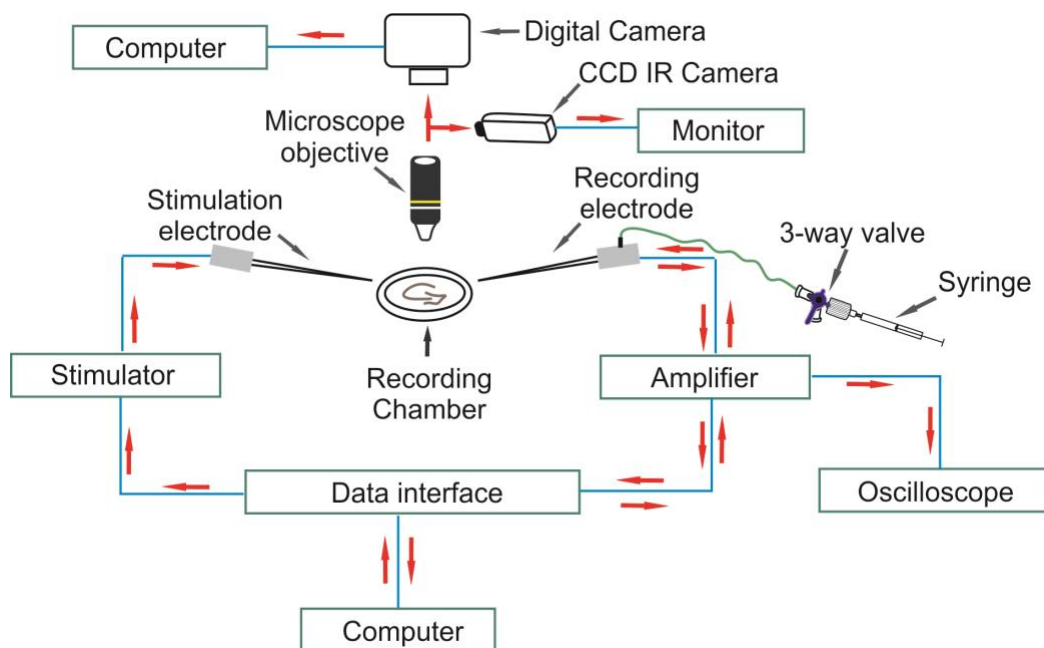


Figure 4. Patch-clamp setup. Schematic representation of the electrophysiological setup used for this project. The scheme shows the interconnectivity among the different devices that compose the electrophysiological setup. The red arrows show how the electrical signals flow through the system.

The pipette was moved slowly down until it touches the cell body making a dimple due to the positive pressure inside the pipette. Immediately, the positive pressure

was released, and negative pressure rapidly applied until reach 200 mega-ohms ($M\Omega$), then the negative pressure was released. As a consequence, the resistance started to increase quickly until it reaches one gigaohm ($G\Omega$), also known as gigaseal (**Figure 5**, step 2). At this point, the amplified was set up at -70 mV in voltage-clamp mode, taking into account -10 mV of liquid junction potential (LJP), i.e., the potential difference at the boundary between K-Gluconate pipette and extracellular solution (carboxygenated ACSF buffer). To break into the cell, once again slow negative pressure was applied, in this case, the pressure was constant, until open the cell to finally have the whole-cell patch-clamp configuration (**Figure 5**, step 3). Finally, electrical signals were recording.

At the beginning and the end of the whole-cell patch-clamp recording, regular spiking characteristics of pyramidal neurons were assessing for each cell using steps of steady depolarizing current (20 pA for 1 sec) in current-clamp mode. For some experiments, the action potential properties were used to analyze possible variations in AP firing in response to different pharmacological interventions. The features analyzed were the peak amplitude, half-width, rise and decay time and rheobase of AP, together with the early and late phase of spike frequency adaptation of the neuronal firing mode. For this analysis, the spike detection algorithm from Minianalysis software (Synaptosoft, USA) and action potential analysis from FITMASTER software (HEKA, Lamprecht, Germany) were used. Furthermore, amplitude and frequency of spontaneous/minis excitatory postsynaptic currents (sEPSC) were recorded in the voltage-clamp mode for 3 min, and digitized at 5 KHz using PATCHMASTER software (HEKA, Lamprecht, Germany). These recordings were carried out at the beginning and the end of LTP recordings.

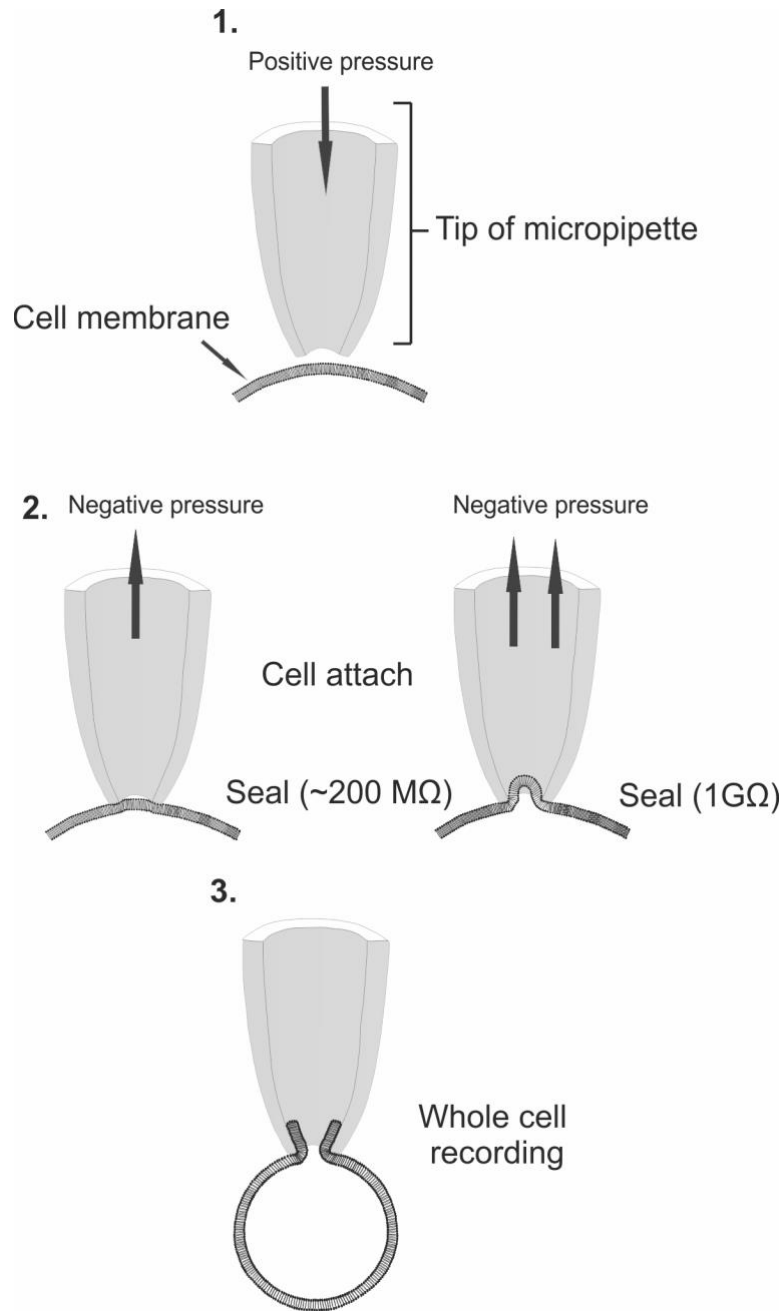


Figure 5. Whole-cell patch-clamp recordings. Step 1. Approaching the cell with the recording pipette with positive pressure inside. Step 2. Touch the cell with the tip pipette and release the positive pressure sucking the cell membrane. Then apply negative pressure until reaching the giga-seal. Step 3. Increase the negative pressure to break into the cell.

Changes in synaptic strength were monitored by the depolarization of Sc fibers using a glass electrode placed at the *stratum radiatum*. The stimulus duration was set to 0.7 ms, with intensities ranging from 90 to 700 μA . The stimulus intensity was adjusted to evoke synaptic responses of 4-5 mV, corresponding to 30-50% of maximal EPSP amplitudes.

Paired-pulse ratio (PPR) was measured to observe changes in P_r glutamate release before and after t-LTP. It consists of the depolarization of Sc fibers with two consecutive electrical pulses within an inter-stimulus interval of 50 ms, and the elicited EPSCs were recorded at -70 mV in voltage-clamp mode. This protocol was repeated three times, and the average response was used to calculate the ratio defined as the peak amplitude of the second evoked response divided by the peak amplitude of the first one (**Figure 6**).

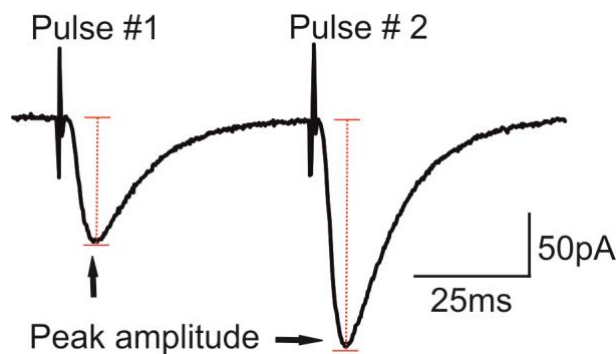


Figure 6. Paired-pulse ratio analysis. Original traces of two evoked EPSCs elicited within a time interval of 50ms. Red lines represent the points from which the peak amplitude of each EPSC was measured.

For some experiments, changes in AMPAR properties after t-LTP were assessed by the calculation of the ratio between AMPAR and NMDAR currents ($I_{\text{NMDAR}}/I_{\text{AMPA}}$ ratio), which are based on changes in the peak amplitude of evoked AMPAR-mediated current relative to NMDAR-mediated current as is shown in **Figure 7**.

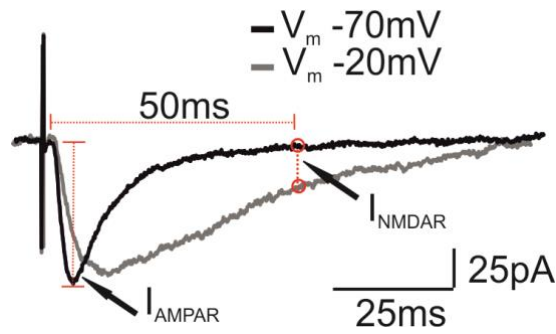


Figure 7. $I_{\text{NMDAR}}/I_{\text{AMPA}}$ ratio analysis. Original trace in black represents the AMPAR mediated evoked EPSC component elicited at the holding potential of -70 mV in voltage-clamp mode. To measure the NMDAR mediated component, a second EPSC was evoked but at the holding potential -20 mV, which is mediated by a dual-component consisting in a fast AMPAR current lasting not more than 50 ms together with NMDAR current lasting 100 ms. Then a pure NMDAR current can be calculated after 50 ms from the onset of EPSC.

2.4 Induction of spike timing-dependent plasticity

Spike timing-dependent plasticity (STDP) was induced by pairing a single EPSP elicited by presynaptic stimulation with either one or four postsynaptic spikes (spike frequency 200 Hz) delivered every 2 sec within a time interval (spike timing, Δt) of 10 ms. Variation in the pre- and postsynaptic pairings number was used to create different STDP paradigms (see **results - section 3.2**). Changes in the synaptic strength were monitored every 20 sec (0.05 Hz) for 10 min baseline. Then, the STDP paradigm was executing at time point 0 min and changes in the EPSP slope were recording for 30-60 min post-conditioning. As a negative control, recordings consisting in a single EPSP evoked every 20 sec were conducting for 40 min in the absence of the STDP induction protocol.

The bidirectionality of STDP was assessed using positive intervals (pre-post pairings) to elicit timing-dependent long-term potentiation (t-LTP) or negative intervals (post-pre) to elicit timing-dependent long-term depression (t-LTD). The temporal specificity of t-LTP was evaluated by using longer spike timing Δt ranging between 20-40 ms.

2.5 Pharmacological tools

To investigate whether a rise of postsynaptic Ca^{2+} concentration is required for low repeat t-LTP induction at Sc-CA1 synapses, a selective chelator of intracellular Ca^{2+} (10 mM BAPTA; Sigma, Germany) was added to the internal solution. Furthermore, the role of NMDARs was evaluated by bath application of an NMDAR antagonist (50 μ M DL-APV, DL-2-Amino-5-phosphonopentanoic acid; Tocris, Bristol, UK). The requirement of L-type Ca^{2+} channel activation for STDP was assessed using the selective blocker Nifedipine (25 μ M; Sigma, Germany). Moreover, the possible contribution of group I metabotropic glutamate receptors (mGluR₁ and mGluR₅) to low repeat t-LTP was tested using specific antagonists for mGluR₁ (1 μ M YM298198; Tocris, Bristol, UK) and mGluR₅ (10 μ M MPEP; Tocris, Bristol, UK).

Dopaminergic modulation of low repeat t-LTP was investigated by bath applications of D1-like (10 μ M SCH23390; Sigma, Germany) and D2-like DARs antagonists (10 μ M Sulpiride; Sigma, Germany). In some experiments, a selective DA reuptake inhibitor known as GBR-12783 (5 μ M; Tocris, UK) was used. In addition, the role of the endocannabinoid system was also evaluated by bath application of AM251 (3 μ M; Tocris, UK), a selective cannabinoid type 1 receptor antagonist.

Furthermore, the role of BDNF signaling was examined by using a recombinant human TrkB-Fc chimera (R&D Systems, USA) to scavenge the BDNF released endogenously. Before the recording, the slices were pre-incubated with 5 μ g/ml of TrkB-Fc for at least three hours. Then, the whole record was carried out under continuous presence of TrkB-Fc scavenger at 100 ng/ml (diluted in ACSF). Additional experiments were conducted with bath application of an unspecific tyrosine kinase inhibitor (200 nM K252a; Alomone labs, Israel) that interferes with the phosphorylation of the intracellular domain of Trk receptors, which is an essential step for its activation. Transactivation of TrkB receptors mediated by zinc signals was investigated by bath application of TPEN (10 μ M; Tocris, UK), an

intracellular membrane-permeable ion chelator with high-affinity for heavy metal ($Zn^{2+} > Fe^{2+} > Mn^{2+}$).

Bath application of either NBQX (10 μ M; Tocris, UK) or DL-APV (50 μ M; Tocris, UK) to block AMPARs and NMDARs, respectively were used to confirm the readout of AMPAR and NMDAR-mediated currents.

The corresponding control recordings were carried out with a similar concentration of the vehicle. Dimethyl sulfoxide (DMSO) was used to dilute Nifedipine, K252a, and TPEN, keeping the DMSO final concentration at 0.05%. Additionally, all experiments were performing with ACSF supplemented with 100 μ M Picrotoxin (Sigma, Germany) diluted in 100% ethanol, in which the final concentration of ethanol was 0.2%. All other pharmacological compounds were diluted in distilled water.

2.6 Data acquisition

STDP recordings were performed in the current-clamp mode, whereas voltage-clamp mode was used for PPR, AMPAR/NMDAR ratio, and spontaneous EPSCs recordings. Data were filtered at 3 kHz using Patch-Clamp EPC-8 Amplifier (HEKA, Germany) connected to a LiH8+8 interface and digitized at 10 kHz using PATCHMASTER software (HEKA, Lamprecht, Germany). Data analysis was performing using FITMASTER software (HEKA, Lamprecht, Germany).

Changes in the slope were obtained from the initial 2 ms of the evoked EPSP onset and normalized to 100% (**Figure 8**). The magnitude of the changes in synaptic strength were determined by the difference between the average of EPSP slope during baseline and the last 10 min of the recording. Similarly calculations were used to evaluate changes in input resistance (R_{in}), which was monitored continuously by long hyperpolarizing steps (250 ms; 20 pA) presiding each evoked EPSP.

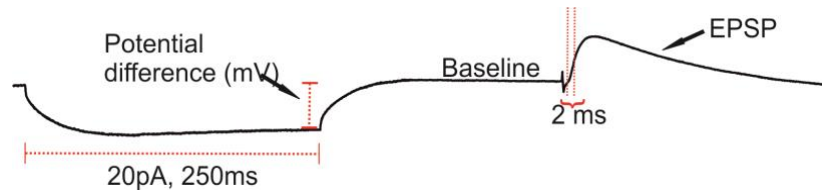


Figure 8. Input resistance and EPSP slope measurements. The input resistant (R_{in}) was calculated using Ohm's law current (I)= voltage (V) / resistance(R). Thus, the potential difference value (red lines) was defined as the amplitude of the membrane potential fluctuation resulting from a hyperpolarizing steady current. This value was divided by 20 pA, corresponding to the current applied to produce such fluctuation. Variation in the R_{in} usually is associated with instability of seal. EPSP slope was calculated using FITMASTER software by positioning two cursors (red lines) at the beginning of EPSP onset with a time interval of 2 ms.

For the STDP protocols, the time interval between pre- and postsynaptic activation (i.e., Δt in ms) were measuring from the beginning of the onset of the evoked EPSP to the peak of the first action potential. Experimental data were excluded from analysis when changes in input resistance exceed more than 25% between baseline and the last 10 min of the recording. Traces showing “run-up” or “run- down” during the baseline recording were also excluding.

2.7 Statistical analysis

Statistical analysis was performed using GraphPad Prism version 6.0 (GraphPad Software, California, USA). The data collected from at least three different animals presented in text and figures correspond to mean \pm standard error of the mean (SEM). All data were tested for normality using the Shapiro-Wilk normality test and analyzed as needed. Paired and unpaired Student's t-tests were used to compare two groups with a normal distribution; otherwise, nonparametric Mann-Whitney U-test was applied. Multiple comparisons were assessing with a one-way analysis of variance (ANOVA) followed by a post hoc Tukey test or Kruskal-Wallis test followed by post hoc Dunn's multiple comparisons test for parametric and

nonparametric data, respectively. Two samples Kolmogorov-Smirnov test was used to compare the cumulative distribution of EPSC frequencies and amplitudes before and after t-LTP.

In some cases, a one-sample t-test was used to determine the significant amount of synaptic potentiation in response to each paradigm. The statistical tests used are shown in the respective figure legends. A p-value < 0.05 was considered as a level of statistical significance. The respective number of experiments (n) and the number of animals (N) is reported in the figure legends.

3. Results

3.1 Induction of spike timing-dependent plasticity at Schaffer collateral-CA1 synapses

In this dissertation, whole-cell patch-clamp recordings were used to induce either timing-dependent (t-) LTP or t-LTD at Schaffer collateral-CA1 (Sc-CA1) synapses. The experiments were performed in acute horizontal and transversal hippocampal slices from young C57BL/6J mice and Wistar rats, respectively. Briefly, a stimulation electrode was positioned in the *stratum radiatum* to directly stimulate the Sc fibers (presynaptic input), which provide the primary excitatory afferents onto the apical oblique and basal dendrites of CA1 pyramidal neurons (Megias *et al.*, 2001). Long-lasting changes in synaptic strength were induced by the temporal coincidence of one evoked EPSP, with a single action potential (AP or spike) generated at the postsynaptic CA1 pyramidal neuron by somatic current injection (2-3 ms; 1 nA) within time delay (spike timing, Δt) of 10 ms. From here on, this protocol will be called 1:1 (1EPSP/1AP). Based on these experimental settings, t-LTP was inducing when the presynaptic input preceded the AP, whereas the reverse order led to t-LTD (**Figure 9B**).

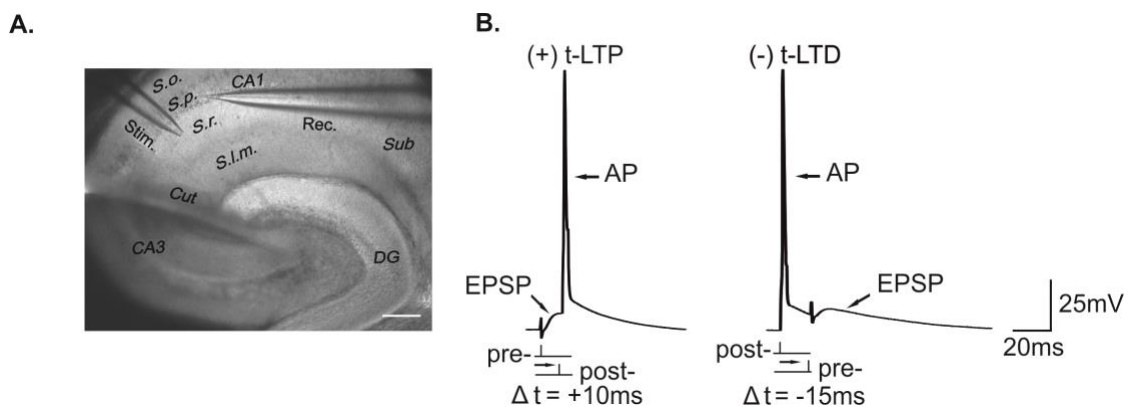


Figure 9. Experimental settings for the induction of STDP. (A) The microphotograph shows an arrangement of the recording and stimulating electrodes on a typical acute hippocampal slice. Scale bar 100 μm . Stim: stimulation electrode, Rec: recording electrode, DG, CA3 and CA1, S.o: *stratum oriens*, S.p: *stratum pyramidale*, S.r: *stratum radiatum*, S.l.m:

stratum lacunosum moleculare. **(B)** Original traces of single spike pairs used for t-LTP and t-LTD induction.

3.2 Timing dependent-LTP at Schaffer collateral-CA1 synapses requires only six single spike pairings

In vivo studies indicate that hippocampus-dependent associative memories can be formed rapidly, suggesting that the consolidation of long-lasting memories may need very few presentations of the stimulus (Tse *et al.*, 2007). Since activity-dependent synaptic plasticity represents the most suitable model to investigate memory processing at the cellular level, the primary aim was to determine the minimum number of repetitions of pre- and postsynaptic activation required to induce synaptic modifications at Sc-CA1 synapses. Then, the magnitude of synaptic strength was calculated in response to a gradual reduction of the number of 1EPSP:1AP pairings used for t-LTP induction (i.e., 100, 70, 50, 25, 12, 6, and 3) (**Figure 10A**). The results were compared with negative controls (called 0:0), in which none STDP protocol was executed.

STDP experiments conducted in mice showed that stimulation with 70x 1:1 induces a robust t-LTP at Sc-CA1 synapses ($166.9\% \pm 11.8\%$; $p < 0.01$) in comparison with 0:0 control ($105.0\% \pm 6.5\%$). In contrast, there was no significant synaptic potentiation after 50x 1:1 ($106.8\% \pm 19.04\%$), 25x 1:1 ($102.1\% \pm 14.2\%$), or 12x 1:1 stimulation ($146.1\% \pm 13.8\%$; $p < 0.05$). Surprisingly, a complete reestablishment of t-LTP was achieved with only 6x spike pairings of 1:1 protocol ($154.5\% \pm 8.2\%$; $p < 0.001$), whereas further experiments using 3x 1:1 protocol did not show reliable potentiation ($104.6\% \pm 22.3\%$; $p < 0.05$; **Figure 10B**). A representative single experiment for 0:0 control, 6x 1:1, 25x 1:1, and 70x 1:1 are presented in the **Figure 10C**. The resistant input resistance (R_{in}) showing accessing stability of the recordings is also presented.

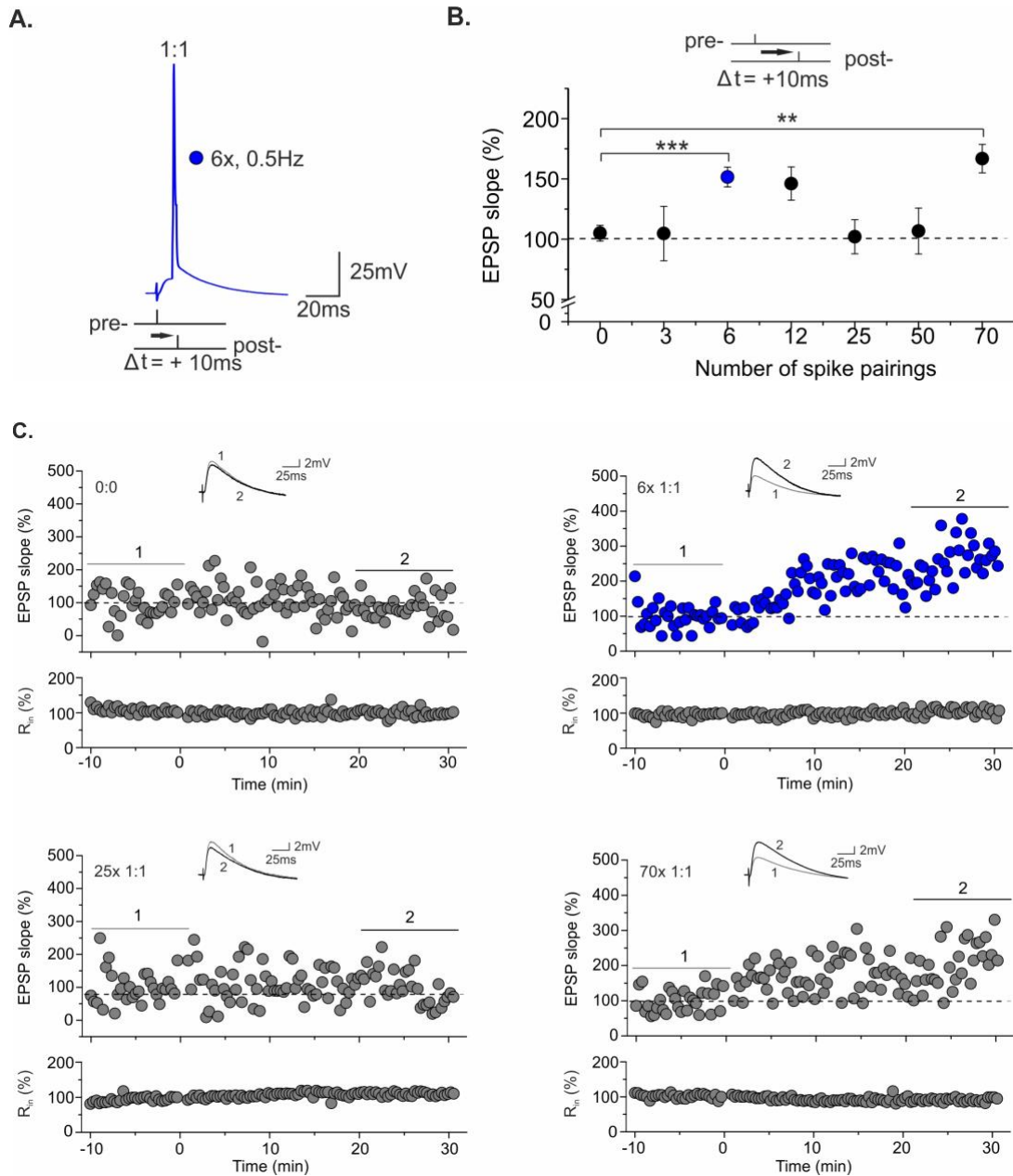


Figure 10. Induction threshold of 1:1 t-LTP at Sc-CA1 synapses in mice. (A) Original trace for 6x 1:1 protocol. **(B)** Variations in the magnitude of the synaptic plasticity in response to a different number of 1:1 spike pairings. The p-values were obtained using Kruskal-Wallis test $H_{(6)} = 32.74$; $p = 0.0001$ followed by Dunn's multiple comparison test post hoc analysis. ** $p < 0.01$, *** $p < 0.001$. Data shown are mean \pm SEM. **(C)** Typical time course of a single experiment for 0:0 negative control, 6x 1:1, 25x 1:1, and 70x 1:1. The inserts at the top of the graphs show the average EPSPs before (1) and after (2) t-LTP induction. The number of recorded cells and number of animals for each paradigm were: 0:0 ($n=23 / N=19$); 3x ($n=7 / N=6$); 6x ($n=59 / N=37$); 12x ($n=6 / N=5$); 25x ($n=11 / N=9$), 50x ($n=8 / N=7$), and for 70x ($n=10 / N=7$).

Interestingly, the data obtained from rats revealed a different outcome. The magnitude of t-LTP was robust with 1:1 protocol repeated 100x ($162.7\% \pm 14.2\%$; $p < 0.05$), 70x ($154.3\% \pm 8.2\%$; $p < 0.05$), 50x ($188.6\% \pm 18.9\%$; $p < 0.001$), and 12x ($164.7\% \pm 23.27\%$; $p < 0.01$). However, pairing with 6x 1:1 was not sufficient to produce reliable synaptic potentiation ($105.1\% \pm 13.9\%$; $p > 0.05$) in comparison with 0:0 control ($78.9\% \pm 7.2\%$; **Figure 11**).

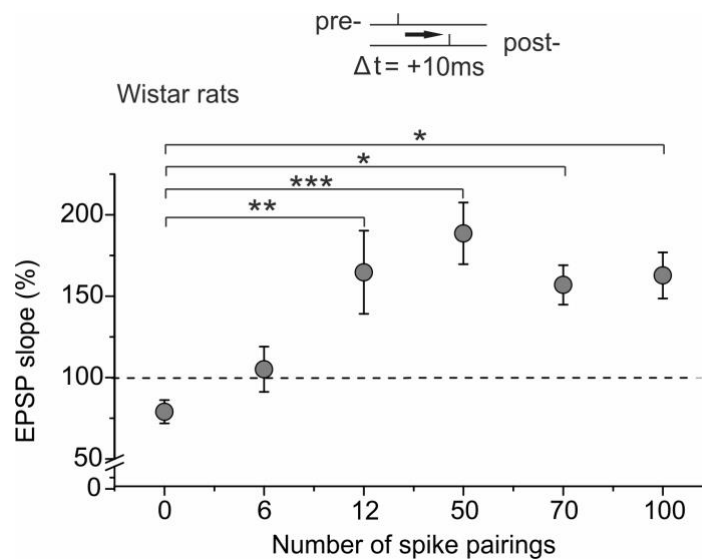


Figure 11. Induction threshold of 1:1 t-LTP at Sc-CA1 synapses in rats. The scatter plot shows the magnitude of t-LTP induced for each protocol. The number of recorded cells and number of animals for each paradigm were: 0:0 ($n = 5 / N = 5$); 6x ($n = 7 / N = 7$); 12x ($n = 7 / N = 5$); 50x ($n = 11 / N = 7$); 70x: ($n = 11 / N = 7$), and for 100x ($n = 6 / N = 6$). The p values were derived using ANOVA $F_{(5, 36)} = 6.863$; $p = 0.0001$ followed by Tukey's multiple comparison test post hoc analysis. * $p < 0.05$, ** $p < 0.01$, *** $p < 0.001$. Data are shown as mean \pm SEM.

To the best of our knowledge, this is the first report showing that only six spike pairings are sufficient to induce t-LTP at hippocampal Sc-CA1 synapses. From here on, this STDP paradigm will be called 6x 1:1 protocol or stimulation (in blue Figure 10), which represent a novel form of hippocampal LTP induction. Therefore, a series of experiments were performing to characterize locus of expression and the

potential contribution of dopaminergic and BDNF signaling. All these experiments were based on our previous STDP studies using a higher number of spike pairings (Edelmann and Lessmann, 2011; Edelmann et al., 2015), to evaluate whether high and low repeat STDP protocols rely on similar cellular and molecular mechanisms.

3.3 Incorporation of multiple postsynaptic spikes into a low repeat STDP paradigm

Previous studies conducted in our group revealed that 25-35 repeats of a presynaptic input paired with a postsynaptic burst (4 APs generated at 200 Hz), with a $\Delta t = 10$ ms, and repeated at 0.5 Hz resulted in BDNF-dependent t-LTP (Edelmann *et al.*, 2015). Hence, a comparable burst was incorporated into the 6x 1:1 paradigm described above (**Figure 10B**), creating a new paradigm that was called 6x 1:4 protocol to investigate the role of BDNF in low repeat t-LTP. Similarly than 1:1, this new paradigm was able to produce reliable t-LTP at Sc CA1 synapses (**Figure 12**).

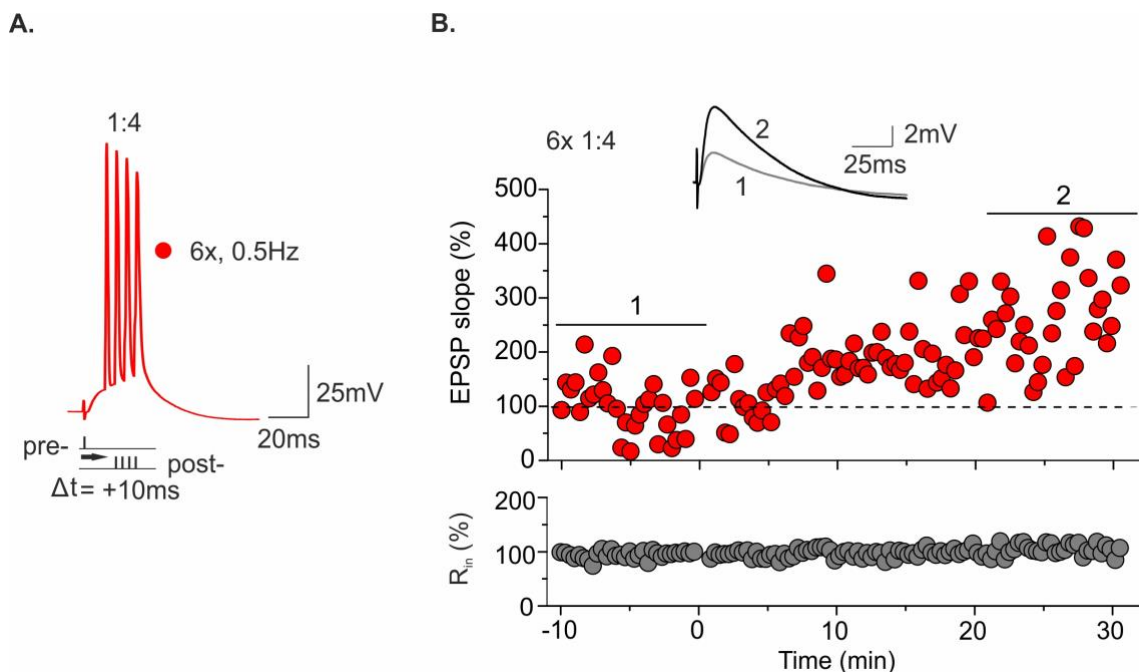
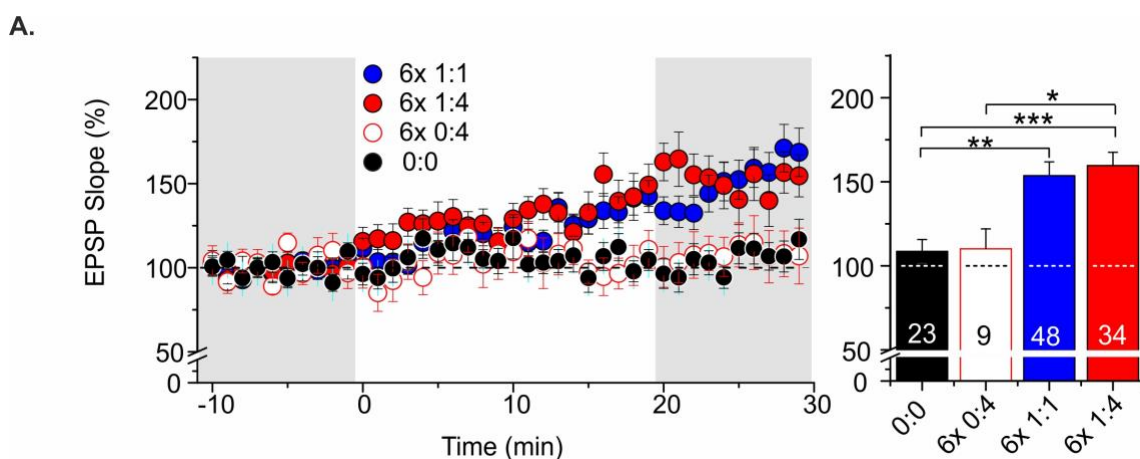


Figure 12. 1:4 protocol induces robust t-LTP at Sc-CA1 synapses.

Continuation of Figure 12. (A) Original trace of 6x 1:4 paradigm within a pre- and postsynaptic delta time of 10 ms. The four APs generated at the postsynaptic terminal were delivered at 200 Hz, and pre-postsynaptic pairings were executing every 2s. **(B)** Typical time course of a single experiment. The insert at the top of the graph shows the overlap between the EPSP average before (1) and after (2) t-LTP induction.

3.4 Low repeat STDP induces associative t-LTP, but not t-LTD.

Further experiments indicated that both 6x 1:1 (154.5% \pm 8.2%) and 6x 1:4 protocol (159.6% \pm SEM 8.0%) induced similar levels of t-LTP magnitudes ($p > 0.05$; **Figure 13A**) and no differences in basal electrophysiological properties were found among conditions (**Table 1**). There is a general agreement that STDP represents an associative form of synaptic plasticity that depends on the activation of both pre and presynaptic components (Magee and Johnston, 1997). Following this principle, there were no changes in synaptic strength in response to the postsynaptic burst alone (6x 0:4, 110.1% \pm 11.9%), being comparable with 0:0 negative control (105.0% \pm 6.5%; $p > 0.05$, **Figure 13A**). Recordings for 1h after t-LTP induction were carried out to corroborate that the changes in synaptic strength induced with low repeat paradigms were also stable. As shown in **Figure 13B**, the increases in EPSP slope were persistent, reaching a plateau, and no sign of deterioration was detected all over the time.



B.

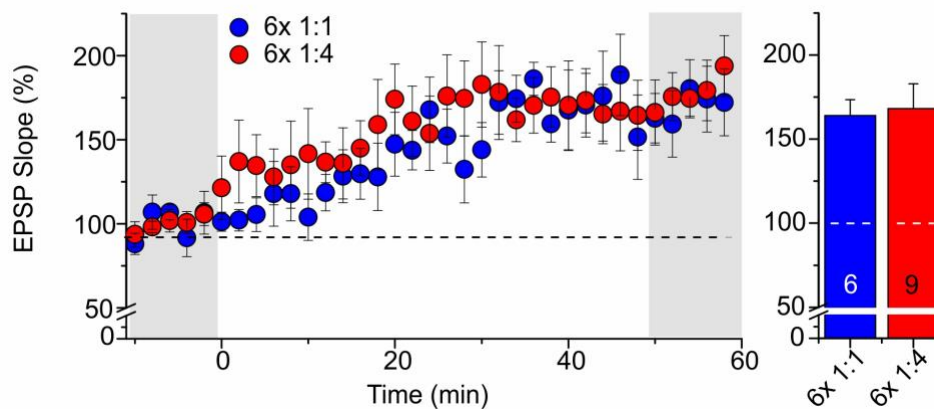


Figure 13. Low repeat STDP paradigms induce long-lasting changes in synaptic transmission. (A) Time course shows the average of the percentage of EPSP slope change in response to 6x 1:1, 6x 1:4, and 0:4 stimulation compared with 0:0 negative controls. Data quantification is shown as bars (right graph) for each time course. P values were derived using Kruskal-Wallis test $H_{(3)} = 24.0$; $p = 0.0001$, followed by Dunn's multiple comparison test post hoc analysis. The number of animals for each paradigm were: 6x 1:1 $N = 33$; 6x 1:4 $N = 27$; 6x 0:4 $N = 6$; 0:0 $N = 19$. The number of experiments is shown on the bars. **(B)** Recordings for 1h after t-LTP induction for both low repeat STDP paradigms. The number of animals for each paradigm were: 6x 1:1 $N = 3$ and 6x 1:4 $N = 6$. The number of experiments is shown on the bars. * $p < 0.05$, ** $p < 0.01$, *** $p < 0.001$. Data shown are mean \pm SEM.

At most glutamatergic synapses, t-LTP is eliciting when an EPSP precedes the postsynaptic AP while the reverse order leads to t-LTD. It has been described that the maximum delay (delta-time; Δt) between pre- and postsynaptic activation for t-LTP induction must be no longer than 20 ms, whereas for t-LTD the temporal window is broader, ranging from 10 to 100 ms (Markram *et al.*, 1997; Bi and Poo, 1998).

To investigate whether low repeat STDP paradigms also require a critical time window for induction of synaptic plasticity, experiments were carried out using positive (pre-before-post) and negative (post-before-pre) pairings with different spike timing (i.e., -15, +10 and +20, +30, +40 ms). The overall group of synaptic

responses in pyramidal neurons stimulated with 6x 1:1 protocol did not show significant t-LTP with Δt +20 ms, +30ms or +40 ms (one-sample Student's t-test: +20 ms $t_{(5)} = 0.154$, $p = 0.884$; +30 ms, $t_{(6)} = 1.399$, $p = 0.211$; +40 ms $t_{(6)} = 0.607$, $p = 0.566$; **Figure 14A**). Similarly results were found after 6x 1:4 stimulation using $\Delta t = +20$ ms and +40 ms (one-sample Student's t-test: +20 ms, $t_{(8)} = 1.735$; $p = 0.121$; +40 ms, $t_{(6)} = 1.296$; $p = 0.252$; **Figure 14B**). Nevertheless, a moderated potentiation was found in experiments carried out with $\Delta t = +30$ ms (one-sample Student's t-test: +30 ms, $t_{(7)} = 2.846$; $p = 0.025$; **Figure 14B**). Indeed, for all the spiking timings tested here, a robust potentiation was observed in some cells, suggesting that low repeat STDP paradigms are likely to respond to different temporal rules.

On the other hand, t-LTD induced with reversal order of either 6x 1:1 (one-sample Student's t-test: -15 ms, $t_{(7)} = 1.368$; $p = 0.214$; **Figure 14A**) or 6x 1:4 paradigms (one-sample Student's t-test: -15 ms, $t_{(6)} = 0.026$; $p = 0.980$; **Figure 14B**) did not show signs of t-LTD or t-LTP, indicating that t-LTD induction could require a higher number of spike pairings (Campanac and Debanne, 2008).

Table 1. Analysis of the basal cellular and synaptic properties of recorded CA1 pyramidal neurons.

Parameters	0:0	6x 1:1	6x 1:4	Statistical value	P-value ^a
	Mean ± SEM	Mean ± SEM	Mean ± SEM		
EPSP rise time (ms)	6.1 ± 0.3	5.8 ± 0.2	5.9 ± 0.1	F (2, 78) = 0.4123	0.661
EPSP decay time (ms)	61.1 ± 1.9	60.4 ± 1.3	59.9 ± 2.0	F (2, 95) = 0.1096	0.896
R_{in} MΩ	262 ± 12.60	261 ± 12.86	266 ± 11.80	F (2, 45) = 2.083	0.555
RMP (mV)	-67 ± 1.3	-66 ± 0.6	-64 ± 0.7	F (2, 93) = 0.4665	0.359

^aP-values were calculated using ANOVA test.

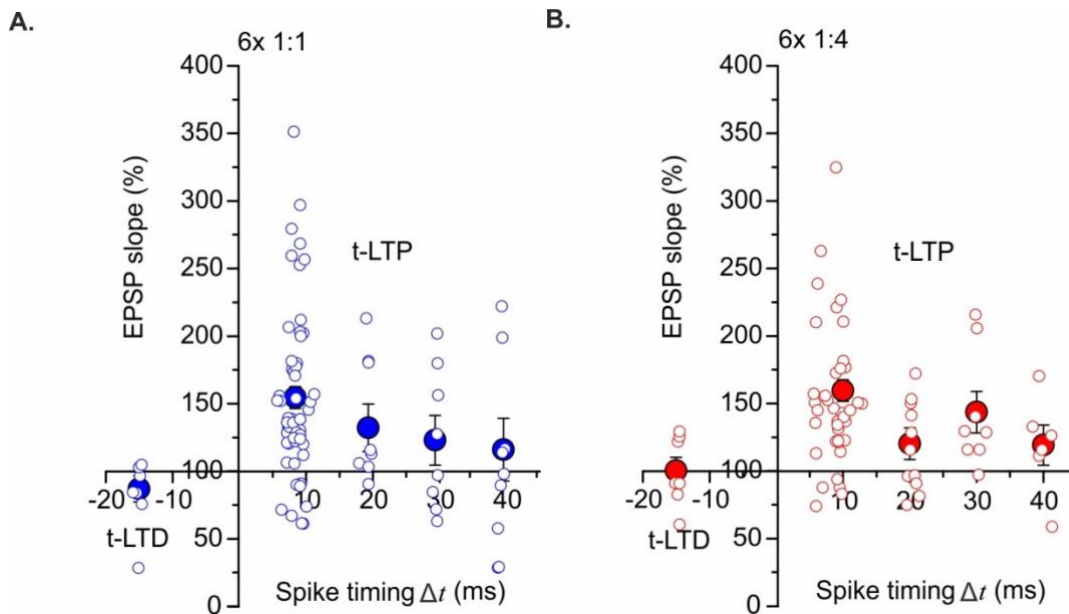


Figure 14. The temporal window of low repeat STDP paradigms. STDP plots showing the response of Sc-CA1 synapses after stimulation with pre-before-post ($+\Delta t$; right) and post-before-pre ($-\Delta t$; left) spike pairings at several Δt for 6x 1:1 (blue) **(A)** and 6x 1:4 (red) **(B)** t-LTP paradigms. Each open symbol depicts the individual pyramidal cell response. Close circles represent the mean \pm SEM.

3.5 Single and multiple postsynaptic action potentials influence the locus of t-LTP expression.

To investigate whether 6x 1:1 and 6x 1:4 have presynaptic or postsynaptic expression changes in glutamate release and AMPAR properties were examined.

The glutamate release properties were evaluated by changes in the paired-pulse ratio (PPR) calculated before and after t-LTP induction. For negative controls, the PPR changes before and after recording resulted in high variability between individual cells, whereas in stimulated cells, the response showed a clear trend. With the 6x 1:1 paradigm, the PPR after t-LTP increased in 90% of the evaluated cells (paired Student's t-test, $t_{(28)} = 5.03$; $p < 0.001$). In contrast, with 6x 1:4 stimulation only 55% of the cells showed a slight but not significant enhancement in the PPR after induction of t-LTP (paired Student's t-test, $t_{(26)} = 1.07$; $p = 0.296$; **Figure 15A**). As shown in **Figure 15B**, the values of PPR calculated before the t-LTP induction

were similar for both experimental groups (Kruskal-Wallis test, $H(2) = 0.059$; $p = 0.971$), indicating that the PPR effects described above occurred actively in response to the STDP paradigms and did not result from probable variations of the recording conditions.

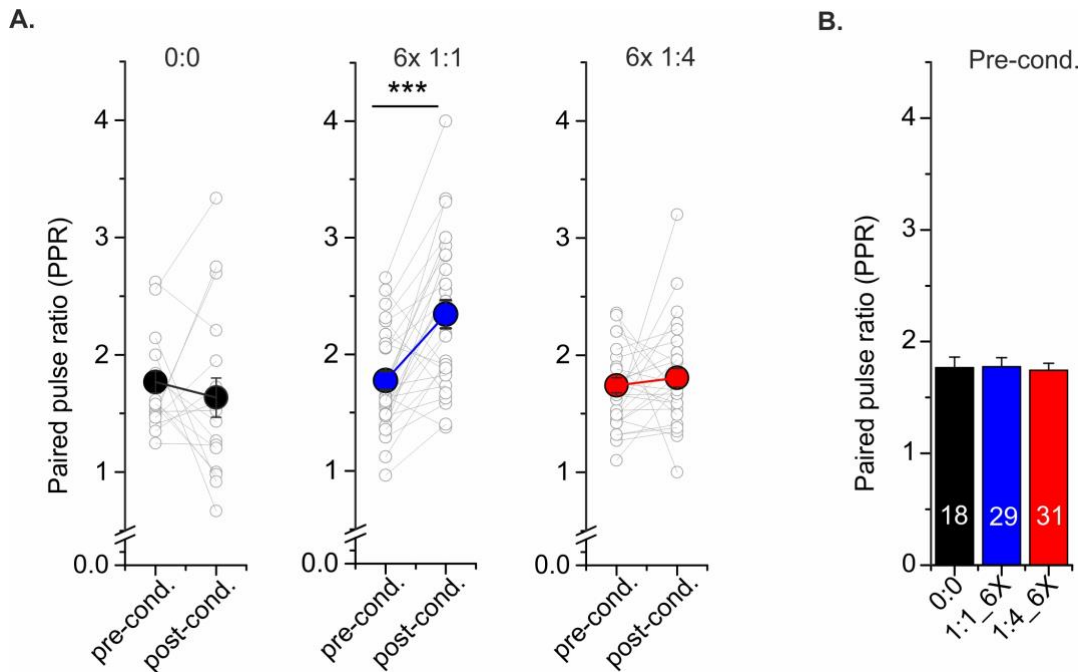


Figure 15. Cellular mechanisms of 6x 1:1 and 6x 1:4 t-LTP. (A) Changes in PPR before and after t-LTP induction. The open symbols depict results from individual cells. Closed symbols show mean \pm SEM. *** $p < 0.001$ using paired Student's t-test. **(B)** Bar graph comparing the mean of PPR calculated at the beginning of the experiments. The number of animals for each paradigm was: negative control (0:0; $N = 14$), 1:1 ($N = 24$) and 1:4 ($N = 24$). The number of recorded cells is shown on the bars. Data shown are mean \pm SEM.

In overall, the data indicated that 6x 1:1 stimulation produces changes in glutamate release properties, suggesting that this form of plasticity rely on presynaptic mechanisms. In contrast, 6 1:4 t-LTP is likely to have a postsynaptic locus expression.

To further investigate the possible effects of 6x 1:1 pairing on the presynaptic expression mechanisms, changes in frequency and amplitude of spontaneous and miniature excitatory postsynaptic currents (s/mEPSCs) at the beginning and the

end of 0:0 negative controls as well as before and after 6x 1:1 stimulation were measured. The distribution of the events was plotted and analyzed as a cumulative fraction function. In overall, the analysis of s/mEPSCs did not show changes in the mean amplitude (Mann-Whitney U test, $U_{(8)} = 10$; $p = 0.690$) or frequency (Mann-Whitney U test, $U_{(8)} = 12$; $p = 1.000$) for 0:0 negative controls. Similarly, for 6x 1:1 paradigm no differences in the mean of neither amplitude (Mann-Whitney U test, $U_{(8)} = 13$; $p = 0.490$) nor frequency (Mann-Whitney U test, $U_{(8)} = 10$; $p = 0.690$) were found. Nonetheless, the cumulative fraction analysis of 0:0 negative controls revealed a significant decrease of s/mEPSCs amplitudes (Kolmogorov-Smirnov test, $Z = 1.51$, $p = 0.020$, **Figure 16A**). While a significant increase in s/mEPSCs frequency was detected after 6x 1:1 stimulation (Kolmogorov-Smirnov test, $Z = 1.58$, $p = 0.010$, **Figure 16B**). These preliminary data suggest that 6x 1:1 protocol could increase probability of glutamate release supporting the findings in regard to PPR.

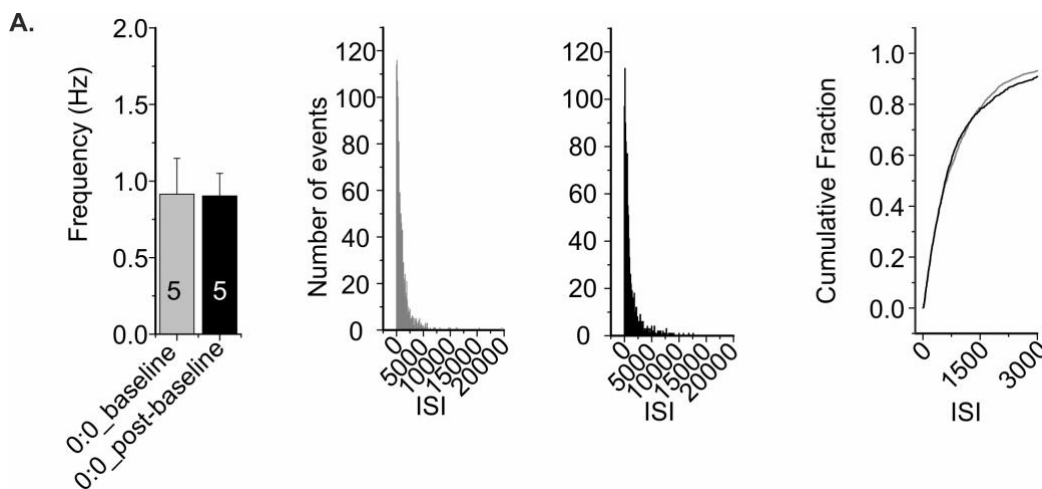


Figure 16. Continues on the next page.

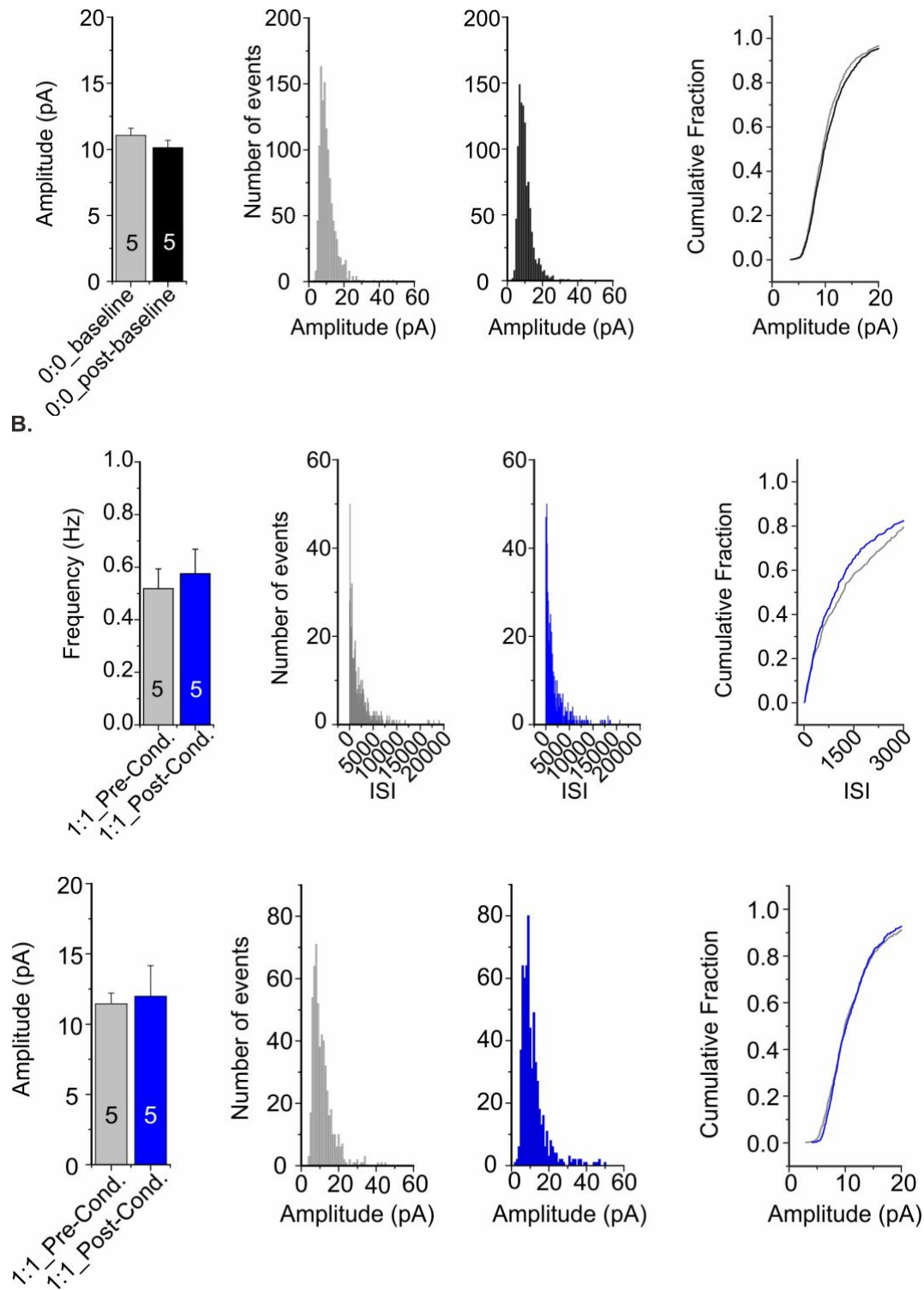


Figure 16. Changes in spontaneous and miniature excitatory postsynaptic currents in response to 6x 1:1 stimulation. Mean frequency and amplitude, as well as the cumulative fraction function of spontaneous mEPSCs, were calculated and analyzed for both **(A)** negative controls (0:0) and **(B)** 6x 1:1 stimulation. ISI: Interstimulus interval.

There is a general agreement that the presynaptic modification requires a retrograde messenger (Fitzsimonds and Poo, 1998; Blundon and Zakharenko, 2008), a role that can be played by endocannabinoids (eCB). Those are lipid-signaling molecules released postsynaptically, but with effects on presynaptic terminals via endocannabinoid type 1 (eCB1R) and type 2 (eCB2R) receptors (Castillo *et al.*, 2012). STDP experiments in corticostriatal synapses showed that activation of eCB1R could facilitate synaptic potentiation allowing the induction of t-LTP with only 5-10 spike pairings (Cui *et al.*, 2015; Cui *et al.*, 2016). Then, the rising question was whether the increase of the probability of glutamate release triggered by 6x 1:1 stimulation is mediated by the activation of eCB signaling as well. Hence, STDP experiments using 6x 1:1 protocol were carried out in the presence of an eCB1R antagonist known as AM251 (3 μ M). The results showed that AM251 did not affect 6x 1:1 t-LTP in comparison with DMSO control (Mann-Whitney U test, $U_{(16)} = 37$; $p = 0.9278$; **Figure 17**), suggesting that activation of eCB1R is not requiring for this type of plasticity.

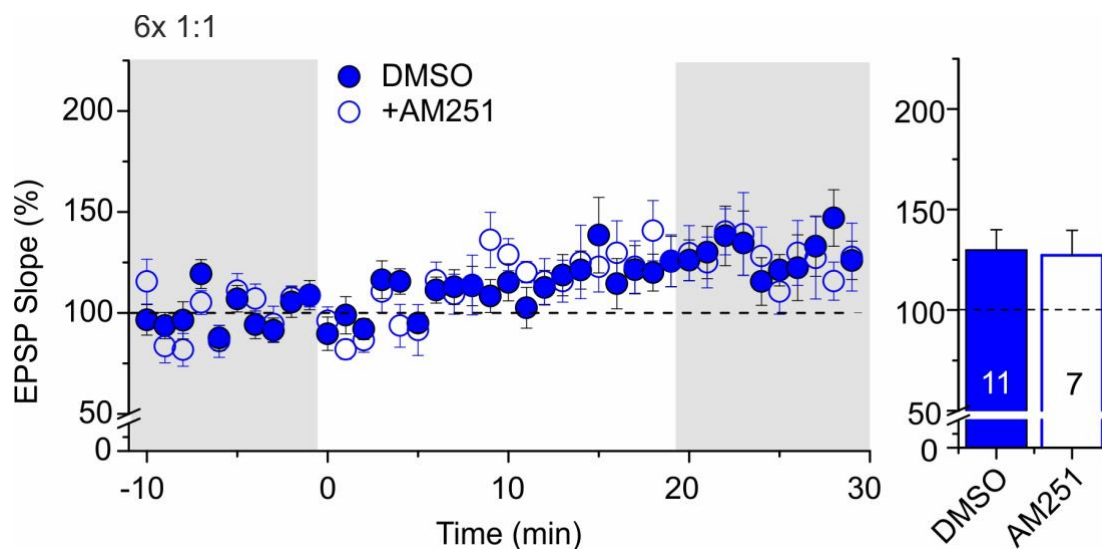


Figure 17. Role of retrograde endocannabinoid signaling in 6x 1:1 t-LTP. Time courses show the average of the normalized EPSP slopes in the presence of eCB1R antagonist (3 μ M AM251; open symbols) for 6x 1:1 protocol compared with untreated control (DMSO; closed

symbols). The number of recorded cells is indicated in the bars. The number of animals used for 6x 1:1 protocol was DMSO / AM251 (N= 4 / N= 3). Data are represented as mean \pm SEM.

To further investigate the expression locus of t-LTP, the variations in the $I_{\text{NMDAR}}/I_{\text{AMPA}}$ ratios were calculated after t-LTP induction with both 6x 1:1 and 6x 1:4 protocols, and compared with 0:0 negative controls. In agreement with the PPR findings and the preliminary data regarding to s/mEPSCs analysis described above, the $I_{\text{NMDAR}}/I_{\text{AMPA}}$ ratio calculated in cells conditioned with 6x 1:1 stimulation did not show significant differences in comparison with 0:0 negative controls (5.97 ± 0.64 vs. 7.18 ± 0.82 , respectively; $p > 0.05$). In contrast, a significant increase in the $I_{\text{NMDAR}}/I_{\text{AMPA}}$ ratio estimated after 6x 1:4 stimulation was observed (11.27 ± 1.48 ; $p < 0.01$; **Figure 18**), indicating that 6x 1:4, but not 6x 1:1, induces changes in AMPAR receptor properties.

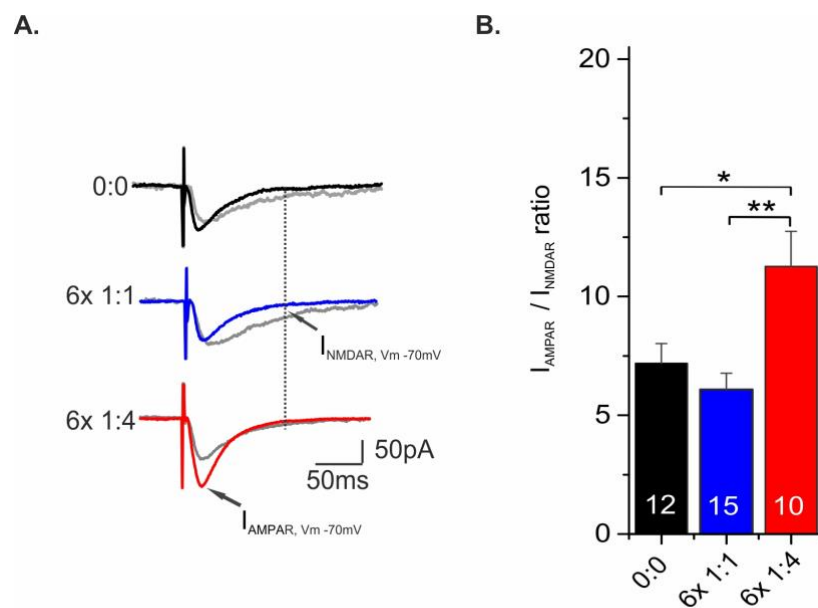


Figure 18. $I_{\text{AMPA}}/I_{\text{NMDAR}}$ ratios at Sc-CA1 synapses after t-LTP induction with low repeat STDP paradigms using horizontal hippocampal slices from mice. **(A)** Representative traces of AMPAR and NMDAR evoked EPSCs for each paradigm are shown. The dotted line shows the time point in which the slow NMDAR mediated component was calculated. **(B)** The ratios were calculated at the end of the recording for negative controls (0:0) and both 6x 1:1 and 6x 1:4 paradigms after t-LTP. The number of experiments is shown on the bars. The number of animals for each condition was: 0:0 N= 9; 6x 1:1 N= 15;

and 6x 1:4 N= 8. The p-values were derived using ANOVA $F_{(2,34)} = 7.98$; $p = 0.001$ followed by Tukey's multiple comparison test post hoc analysis. * $p < 0.05$, ** $p < 0.01$. Data are shown as mean \pm SEM.

Similar analyses were carried out in transversal acute hippocampal slices from Wistar rats but using a higher number of spike pairings, i.e., 70x 1:1 and 35x 1:4 protocols. Comparable to found in mice, the 35x 1:4 protocol significantly increased the $I_{\text{NMDAR}}/I_{\text{AMPA}}$ ratio, whereas no change was observed after 70x 1:1 stimulation (**Figure 19A**). In these experiments, the readout of AMPAR and NMDAR at the given holding potential was confirmed by bath application of either 10 μM NBQX or 50 μM DL-APV, respectively (**Figure 19B**).

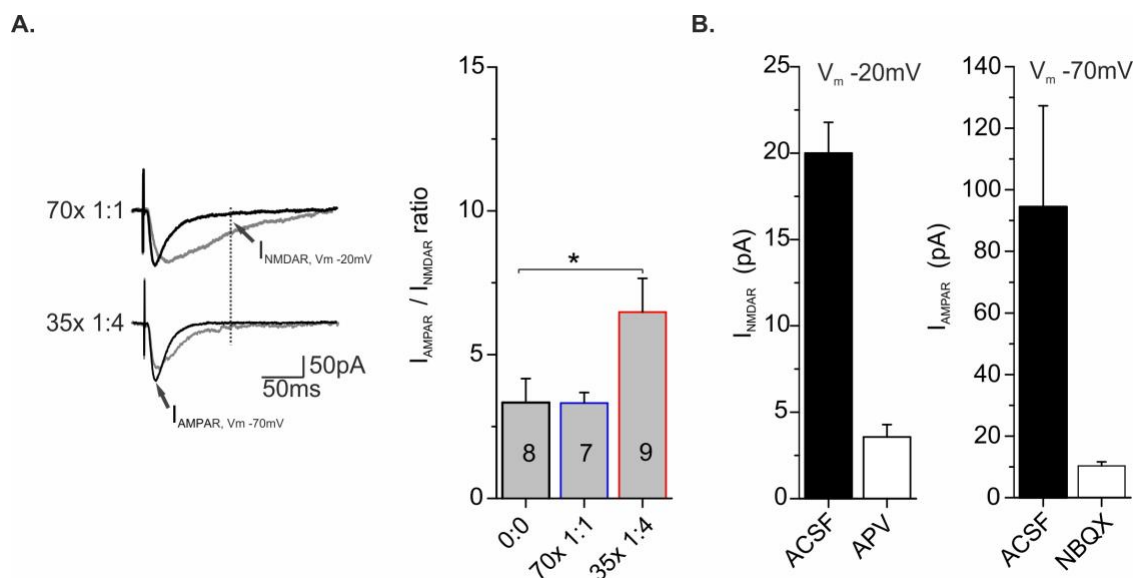


Figure 19. $I_{\text{AMPA}}/I_{\text{NMDAR}}$ ratio at Sc-CA1 synapses after t-LTP induction with a high number of spike pairings using transversal hippocampal slices from Wistar rats. (A) Representative traces of evoked AMPAR and NMDAR-mediated currents for each paradigm are shown in the insets. The $I_{\text{AMPA}}/I_{\text{NMDAR}}$ ratio was calculated (see **methods – section 2.3**) for negative controls (0:0) and after t-LTP induction with the 70x 1:1 and the 35x 1:4 protocol. The number of experiments is depicted in the bars. The p-values were derived using ANOVA $F_{(2,22)} = 8.489$, $p = 0.02$. The dotted line shows the time point in which the slow NMDAR component was calculated. **(B)** Pharmacological effects of 50 μM DL-APV and

10 μ M NBQX on the amplitude for AMPAR and NMDAR mediated currents, respectively, at the given holding potential. Data are represented as mean \pm SEM. * $p < 0.05$. Modified from (Edelmann *et al.*, 2015).

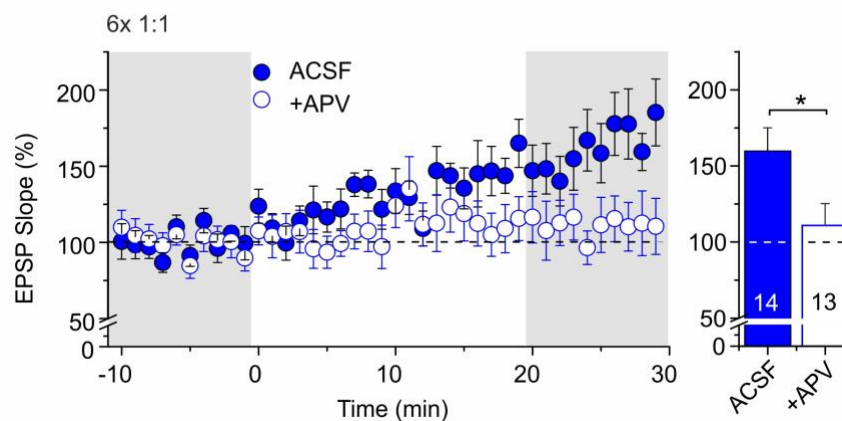
Taken together these data indicated that 6x 1:1 t-LTP is likely to be presynaptically expressed, whereas the 6x 1:4 t-LTP depends on postsynaptic mechanisms, which is consistent with previous reports of our group (Edelmann *et al.*, 2015).

3.6 Distinct calcium sources are activated by low repeat STDP paradigms.

There is a consensus that long-lasting changes in synaptic strength require the influx of Ca^{2+} ions into the dendritic spine via NMDARs (Bliss and Collingridge, 1993). Most recently, it has been described that voltage-gated Ca^{2+} channels (VGCC) and metabotropic glutamate receptors (mGluR) are also critical components for the induction of some types of synaptic plasticity (Tigaret *et al.*, 2016). Therefore, here, the role of NMDARs and L-type Ca^{2+} channels in low repeat t-LTP induction was investigated.

It was found that the bath application of 10 μ M DL-APV, an NMDAR antagonist, significantly decreased the t-LTP induced with 6x 1:1 protocol in comparison with ACSF control (unpaired Student's t-test, $t_{(26)} = 2.35$; $p = 0.03$; **Figure 20A**). Similar effects were observed after application of 25 μ M Nifedipine, a selective blocker for L-type Ca^{2+} channels (unpaired Student's t-test, $t_{(14)} = 4.25$; $p < 0.001$; **Figure 21A**).

A.



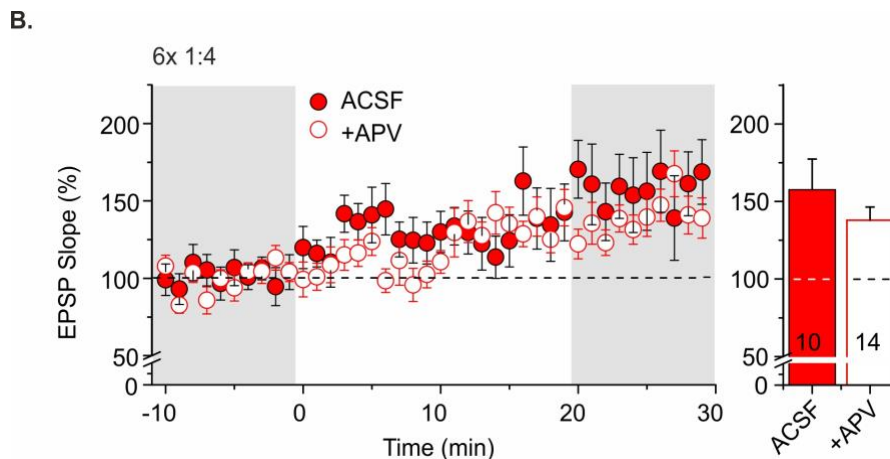


Figure 20. NMDARs contribution to low repeat t-LTP. Time courses show the average of the normalized EPSP slopes in the presence of the NMDAR antagonist (10 μ M DL-APV, open symbols) for 6x 1:1 (blue, **A**) and 6x 1:4 (red, **B**) protocols compared with untreated control (ACSF, closed symbols). The number of recorded cells is indicated in the bars. The number of animals used for 6x 1:1 protocol was ACSF / DL-APV (N= 11 / N= 11) and 6x 1:4 protocol ACSF / DL-APV (N= 6 / N= 9). Data are represented as mean \pm SEM. * $p < 0.05$ unpaired Student's t-test.

In contrast, neither DL-APV (unpaired Student's t-test, $t_{(22)} = 1.02$; $p > 0.05$; **Figure 20B**) nor Nifedipine (unpaired Student's t-test, $t_{(12)} = 0.70$; $p > 0.05$) had significant effects on the t-LTP induced with the 6x 1:4 protocol (**Figure 21B**). At this point, It is important to take into account that NMDARs and L-type Ca^{2+} channels are considered as the primarily Ca^{2+} sources for all forms of LTP at hippocampal Sc-CA1. Thus, the fact that 6x 1:4 t-LTP is completely independent of these two main Ca^{2+} sources, it is something that must to be confirmed with further experiments.

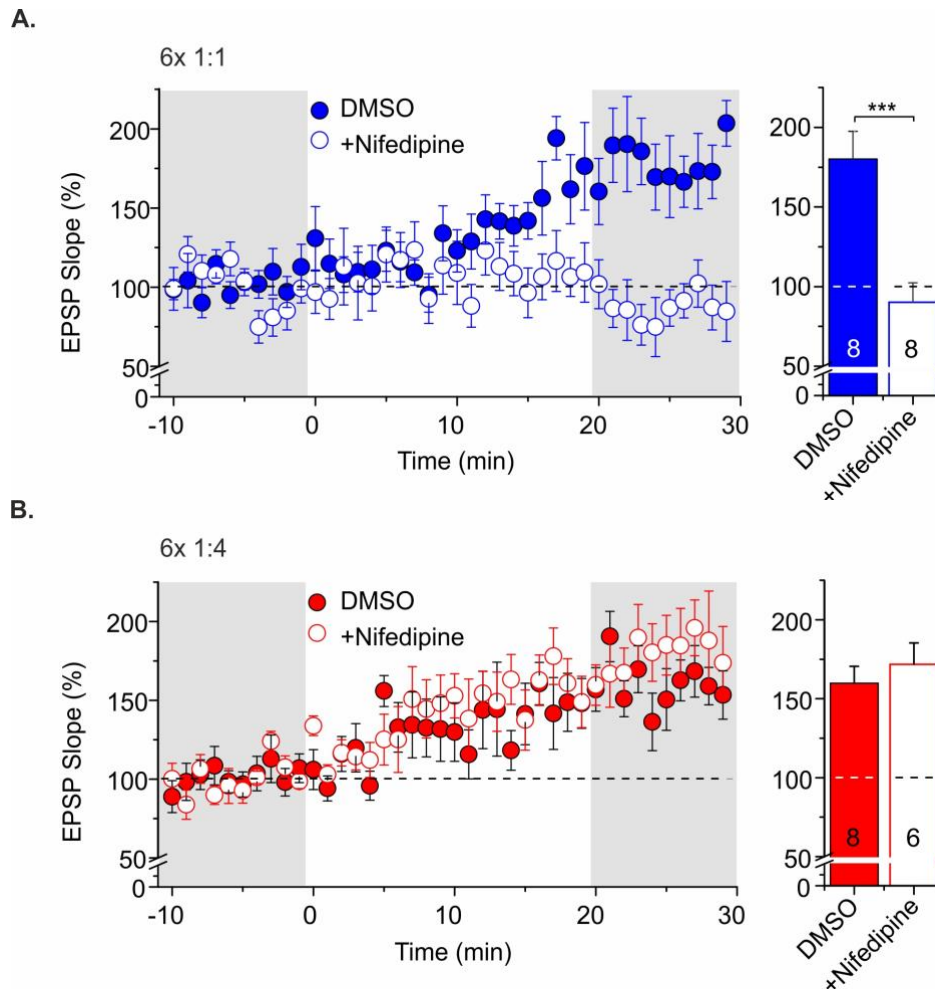


Figure 21. Activation of L-type Ca^{2+} channels is required for 6x 1:1 but not for 6x 1:4 t-LTP induction. Effects of the L-type Ca^{2+} channels blocker (25 μM Nifedipine; open symbols) on t-LTP induced with 6x 1:1 (blue, **A**) and 6x 1:4 (red, **B**) protocol compared to the negative control (0.05% DMSO; closed symbols). The number of recorded cells is indicated in the bars. The number of animals used for each condition was: 6x 1:1 DMSO / Nifedipine (N= 7 / N= 7) and 6x 1:4 DMSO / Nifedipine (N= 4 / N= 4). Data are represented as mean \pm SEM. *** $p < 0.001$.

Because, mGluRs have an essential role in the modulation of Ca^{2+} signals from internal stores (Hong and Ross, 2007), as well as in early and late phases of LTP and LTD in Sc-CA1 synapses (Anwyl, 2009; Neyman and Manahan-Vaughan, 2008). Therefore, the potential involvement of both mGluR1 and mGluR5 in 6x 1:4 t-LTP was examined. The data indicated that bath application of specific antagonists for either mGluR1 (10 μM YM-298198) or mGluR5 (10 μM MPEP) has no significant

effects on the magnitude of t-LTP induced with 6x 1:4 stimulations (Kruskal-Wallis test, $H_{(2)} = 0.277$; $p = 0.871$; **Figure 22**). Therefore, Ca^{2+} chelator BAPTA (10 mM) was added to the pipette solution to verify whether the impairment of postsynaptic Ca^{2+} mobilization affects the expression of low repeat t-LTP. Because, BAPTA has a negative charge, mainly due to the presence of four carboxylic acids in its structure, the loading of BAPTA into the cell was facilitated by somatic injection of negative pulses of -10pA for 250ms that were delivered at 0.05 Hz for 5 min.

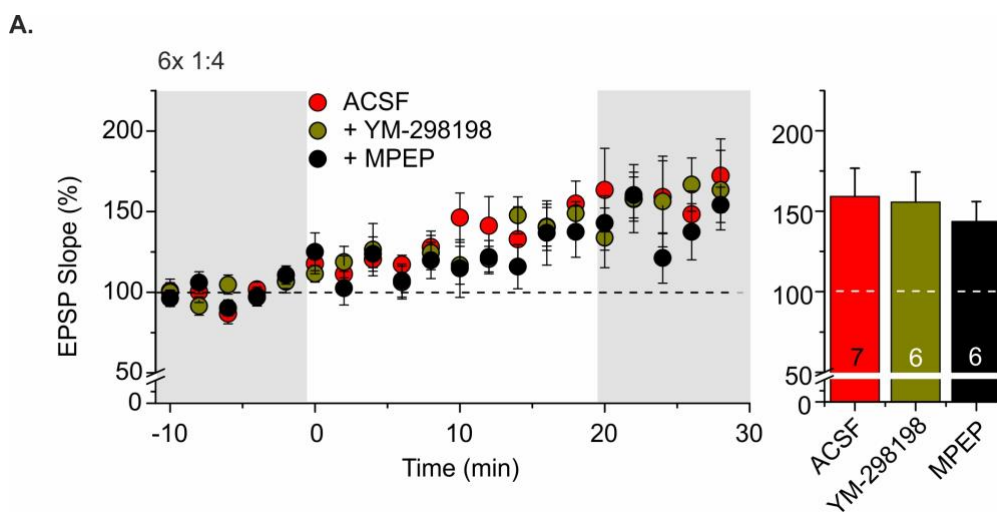


Figure 22. Blockage of either mGluR₁ or mGluR₅ has not effects on 6x 1:4 t-LTP. Time course shows the average of the normalized EPSP slopes in the presence of mGluR₁ and mGluR₅ blockers, 10 μ M YM-298198 (olive) and 10 μ M MPEP (black), respectively. The number of recorded cells is indicated on the bars. The number of animals used for each condition was: ACSF / YM-298198 / MPEP (N= 3 / N= 5 / N= 5). Data are represented as mean \pm SEM. $p > 0.05$.

The results showed that the intracellular infusion of BAPTA (iBAPTA) into the postsynaptic neuron did not have effects on 6x 1:1 t-LTP (Mann-Whitney U test, $U_{(10)} = 15$; $p = 0.699$; **Figure 23A**). In contrast, the 6x 1:4 t-LTP was completely blocked with iBAPTA (Mann-Whitney U test, $U_{(9)} = 3.0$; $p = 0.03$; **Figure 23B**).

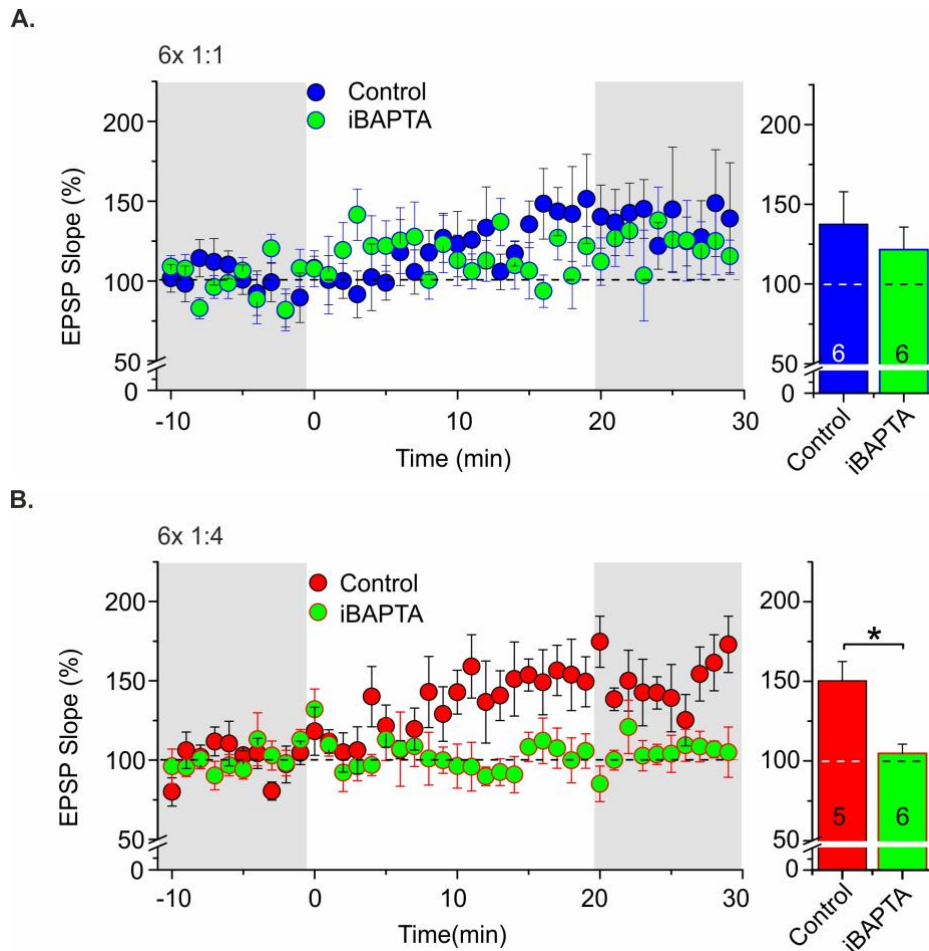


Figure 23. Postsynaptic $[Ca^{2+}]$ rise is critical for t-LTP induced with 6x 1:4 protocol.

Effects of the postsynaptic chelation of Ca^{2+} by infusion of BAPTA (10 mM, in the pipette) on t-LTP induced with 6x 1:1 (**A**) and 6x 1:4 (**B**) stimulations. Control corresponds to cells loaded with regular internal solution. The number of recorded cells is indicated on the bars. The number of animals used for each condition was: control / iBAPTA (N= 4 / N= 5). Data are represented as mean \pm SEM. * $p < 0.05$.

Together these data indicated that t-LTP induced with single and multiple postsynaptic spikes triggers different Ca^{2+} sources. On the one hand, 6x 1:1 t-LTP recruits NMDARs and L-type Ca^{2+} channels. However, in this case, the elevation of postsynaptic $[Ca^{2+}]$ seems to be not required. This finding opens the possibility that Ca^{2+} signals could operate at the presynaptic terminal (Tippens *et al.*, 2008; Bouvier *et al.*, 2018). On the other hand, although the suppression of postsynaptic Ca^{2+} elevation blocked 6x 1:4 t-LTP, the blockade of NMDARs, L-type Ca^{2+} channels or

mGluR₁ and mGluR₅ did not affect 6x 1:4 t-LTP. These data indicate that there are still other Ca₂₊ sources (e.g., activation of Ca₂₊ permeable-AMPA), which might be mediating the Ca₂₊ signals required for 6x 1:4 t-LTP. Then, further experiments are needed in this regard.

3.7 Dopamine receptor dependence of t-LTP induced with low repeat STDP protocols

The role of dopamine (DA) as a dominant neuromodulator gating synaptic plasticity at Sc-CA1 synapses has been very well documented (Pawlak *et al.*, 2010; Edelmann and Lessmann, 2018). Experimental evidence *in vivo* and *in vitro* indicated that DA actions on synaptic potentiation are mainly mediating by D1-like DA receptors (Rs) (Rozas *et al.*, 2015; Shivarama Shetty *et al.*, 2016). However, here, the potential contribution of both D1-like and D2-like DARs to the low repeat STDP induction was investigated.

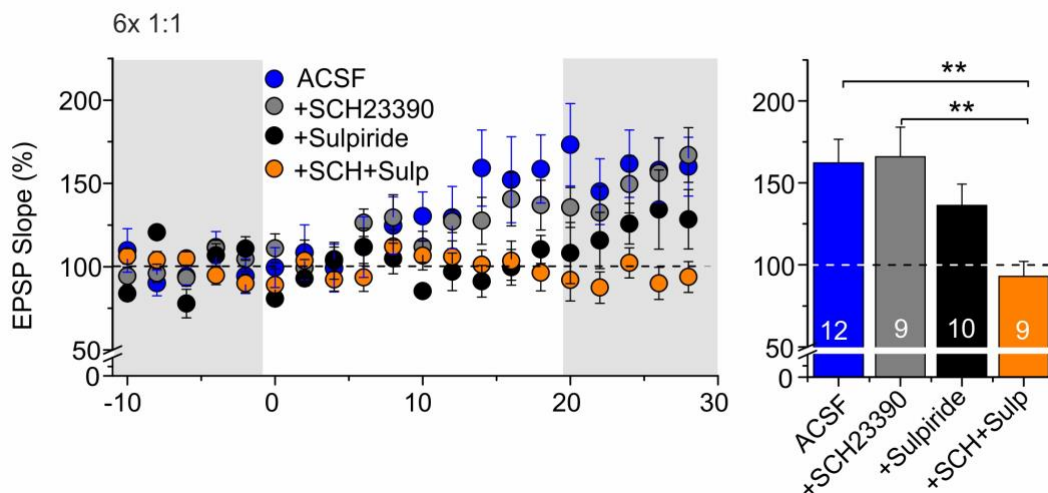
For that purpose, the bath application of SCH23390 (10 μ M) and Sulpiride (10 μ M), specific antagonists for D1-like DARs and D2-like DARs, respectively, were used. The data indicated that neither SCH23390 nor Sulpiride had a significant effect on the magnitude of 6x 1:1 t-LTP (SCH23390: 165.8% \pm 18.0%; $p > 0.05$; Sulpiride: 136.2% \pm 13.0%; $p > 0.05$) in comparison with ACSF controls (162.1% \pm 14.5%). Since it has been shown that D1-like and D2-like DARs can cooperate under certain conditions (Xu and Yao, 2010), a combination of both antagonists was used to verify whether co-activation of both receptors could be required for this type of plasticity. It was indeed the case for 6x 1:1 t-LTP, which was completely blocked when SCH23390 and Sulpiride were co-applied (93.0% \pm 9.0%; **Figure 24A**).

Similarly, the role of DA signaling was investigated for the 6x 1:4 protocol. The magnitude of t-LTP under control conditions (ACSF, 157.6% \pm 14.1%) was comparable with the t-LTP obtained in the presence of 10 μ M SCH23390 (153.6% \pm 14.5%, $p > 0.05$; **Figure 24B**). In contrast, experiments conducted in the presence of 10 μ M Sulpiride alone completely blocked 6x 1:4 t-LTP

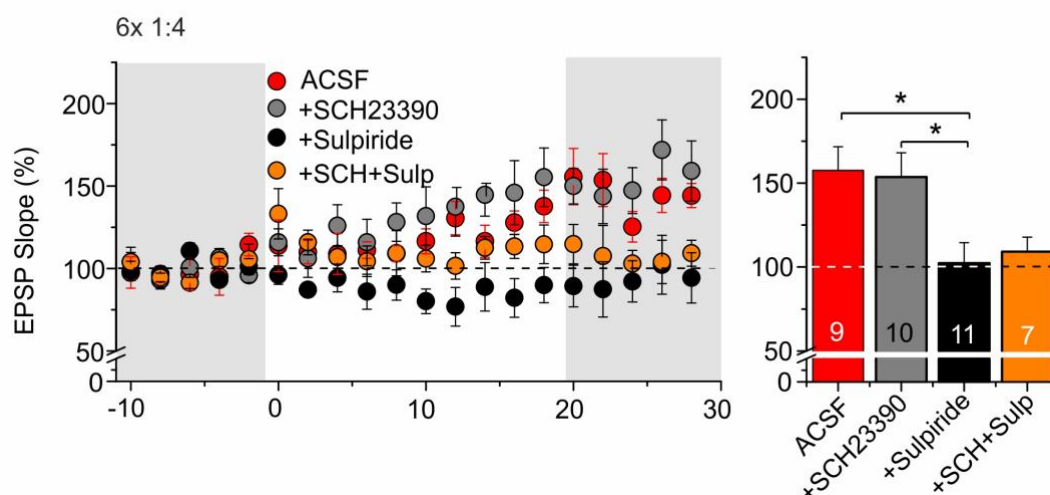
(102.3% ± 12.3%). Although the combination of both blockers shown a notable reduction in the magnitude of 6x 1:4 t-LTP, it was not statistically significant (108.7% ± 9.2%; $p > 0.05$).

The fact that the presence of 10 μM SCH23390 did not have effects on 6x 1:1 t-LTP was an expected result since a previous study in our group showed that the activation D1-like DARs is essential for 70x 1:1 t-LTP (Edelmann and Lessmann, 2011). However, it is important to take into account that in this study, transversal acute hippocampal slices from rats were used, and the number of spike pairings is higher. Then, to examine whether the role of D1-like DARs is related with possible intrinsic differences between animal species (rats vs. mice), cutting angle brain slices (transversal vs. horizontal) or to the difference in the number of spike pairings (6x vs. 70X) could be responsible for the results described here. Therefore, additional STDP experiments using 70x 1:1 protocol were conducted in horizontal acute hippocampal slices from mice. The data indicated that 70x 1:1t-LTP indeed requires the activation of D1-like DARs (**Figure 24C**), confirming previous findings (Edelmann and Lessmann, 2011).

A.



B.



C.

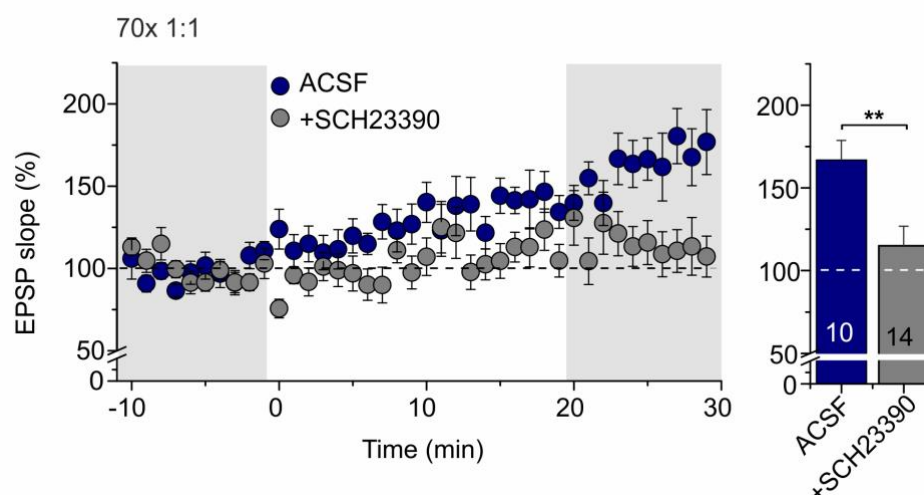


Figure 24. Variation in the pattern and number of spike pairings leads to the activation of different DARs. Experiments were carried out in the presence of either D1R (SCH23390, SCH; 10 μ M) or D2R (Sulpiride, Sulp, 10 μ M) antagonists, or by co-application of both antagonists. **(A)** 6x 1:1 (Kruskal-Wallis test, $H_{(3)} = 14.28$; $p = 0.003$) and **(B)** 6x 1:4 t-LTP (Kruskal-Wallis test $H_{(3)} = 12.65$; $p = 0.005$) in presence or absence of specific DAR antagonists. **(C)** 70x 1:1 t-LTP in presence or absence of SCH23390 (unpaired Student's t-test, $t_{(22)} = 3.03$; $p < 0.01$). The number of measured cells is indicated on the bars. The following number of animals was used for each condition: 6x 1:1: ACSF/SCH/Sulpiride (N = 9 / N = 6 / N = 8); 6x 1:4: ACSF/SCH/Sulpiride (N = 5 / N = 5 / N = 6); 70x 1:1 ACSF/SCH (N = 6 / N = 6). Data are presented as mean \pm SEM. * $p < 0.05$, ** $p < 0.01$.

Together these results indicated that different pattern and number of spike pairings used for t-LTP induction recruits distinct dopaminergic signals.

It is known that DA has an enormous influence on properties and propagation of the AP (Pedarzani and Storm, 1995; Hoffman and Johnston, 1998; Edelman and Lessmann, 2013; Bender and Trussell, 2009; Zhang *et al.*, 2009; Bender *et al.*, 2010; Edelman and Lessmann, 2011) Hence, in this dissertation, the effects of the DA antagonist application on the firing mode of CA1 pyramidal neurons in response to steps of somatic steady depolarizing current (20 pA for 1 sec) were investigated. All analyzed neurons showed a regular firing mode typically described for this type of neurons (Staff *et al.*, 2000), and there were no significant differences in the action potential properties between the different conditions. However, the AP rheobase showed a trend to decrease ($p=0.07$) in the presence of Sulpiride. Also, the data revealed that sulpiride alone and in combination with SCH23390 reduces the initial interspike interval or so-called early frequency adaptation of the action potential firing in CA1 pyramidal neurons (**Table 2**).

Table 2. Effects of DAR antagonists on action potential firing in CA1 pyramidal neurons from mice.

	ACSF	SCH	Sulpiride	SCH-Sulp	Statistical value	p-value
	Mean ± SEM	Mean ± SEM	Mean ± SEM	Mean ± SEM		
Amplitude (mV)	88.61 ± 2.4	89.2 ± 1.9	89.2 ± 1.9	83.9 ± 2.2	H ₍₃₎ = 4.496	p = 0.213
Half width (ms)	1.3 ± 0.03	1.4 ± 0.04	1.4 ± 0.03	1.3 ± 0.04	F _(3,70) = 8.489	p = 0.107
Rise time (ms)	0.3 ± 0.01	0.3 ± 0.01	0.3 ± 0.01	0.4 ± 0.02	H ₍₃₎ = 2.083	p = 0.555
Decay time (ms)	1.2 ± 0.04	1.2 ± 0.03	1.2 ± 0.03	1.2 ± 0.05	F _(3,61) = 0.424	p = 0.737
Rheobase (nA)	0.15 ± 0.01	0.17 ± 0.01	0.13 ± 0.07	0.16 ± 0.07	H ₍₃₎ = 7.182	p = 0.070
Early adaptation (ms)	70.5 ± 7.9	60.7 ± 9.7	47.8 ± 7.0*	32.79 ± 5.6**	H ₍₃₎ = 11.77	p = 0.008
Late adaptation (ms)	152.2 ± 9.4	158 ± 10.0	144.5 ± 9.7	148.0 ± 17.9	H ₍₃₎ = 1.546	p = 0.672

Analysis of action potential properties from CA1 pyramidal neurons evoked by somatic injection of 1s depolarizing current (60 pA) from the holding potential at -70 mV. All parameters were measured at the first AP of the sweep. Data are presented as mean ±SEM. Statistical values are H for Kruskal-Wallis test, F for ANOVA. P value in early adaptation corresponds to Dunn's multiple comparisons test post-hoc analysis.

In overall, the data presented here indicated that D2-like DARs have a dominant role in controlling the threshold of AP initiation in Sc-CA1 synapses (Stanzione *et al.*, 1984). It also suggests that Sc-CA1 synapses might receive a tonic DA input that maintains the constant activation of D2-like DARs, which should be required for the control of the synaptic efficacy at hippocampal Sc-CA1 synapses. Therefore, the raising question was whether the enhancement of endogenous DA concentration would enable the induction of t-LTP using an ineffective STDP paradigm (e.g., 3x 1:1 protocol - see **Figure 10B**).

Based on the scenario described above, the availability of free DA in the extracellular space was increased by bath application of a selective DA reuptake inhibitor known as GBR-12783 (5 μ M). In fact, the presence of GBR-12783 enables the potentiation of Sc-CA1 synapses in response to 3x 1:1 stimulation (3x 1:1 ACSF control: 106.1% \pm 22%; 3x 1:1 + GBR-12783: 194.8% \pm 25%). However, It has been shown that activation of DARs itself without any synaptic stimulation is sufficient to induce long-lasting changes in synaptic transmission (Stanzione *et al.*, 1984; Yang, 2000). Then, further experiments in the absence of pairing, i.e., 0:0 negative controls, but in the presence of GBR-12783 were conducted. The preliminary data indicate that the increase of endogenous DA concentration leads to chemical LTP (219.0% \pm 27.9%; **Figure 25**), suggesting that D2-like DARs control synaptic efficacy by tightly regulating DA release in CA1 region of hippocampus.

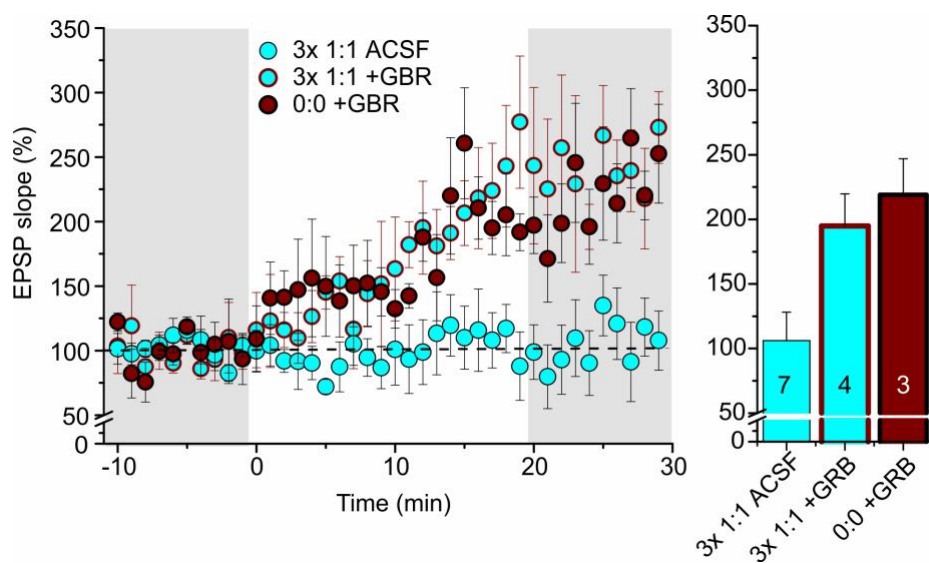


Figure 25. Dopamine uptake inhibitor leads to chemical LTP at Sc-CA1 synapses. Time course shows the average of the normalized EPSP slopes after 3x 1:1 protocol and 0:0 negative control in the presence of 5 μ M GRB-12783. The number of measured cells is indicated on the bars. The following number of animals was used for each condition: 3x 1:1: ACSF / GRB-12783 (N = 6 / N = 3); 0:0 (N = 2). Data are presented as mean \pm SEM.

3.8 Influence of BDNF/TrkB signaling on t-LTP induced with only six pre-post pairings

As mentioned before (**results - section 3.3**) one of the reasons to incorporate a postsynaptic burst into the t-LTP protocol was to investigate the putative function of brain-derived neurotrophic factor (BDNF) signaling in low repeat t-LTP. Then, the contribution of BDNF/TrkB signaling was evaluated by using three different approaches.

The first approach was bath application of 200 nM of a non-selective tyrosine kinase inhibitor (K252a) to block the Trk activation. The data revealed a significant decrease in 6x 1:1 t-LTP in the presence of K252a in comparison with DMSO control (Mann-Whitney U test, $U_{(23)} = 37$; $p = 0.031$; **Figure 26A**). In contrast, K252a did not affect the synaptic potentiation after 6x 1:4 protocol, which was comparable with DMSO control (Mann-Whitney U test, $U_{(10)} = 19$; $p = 0.9433$; **Figure 26B**). Thus, those data suggest that 6x 1:1 stimulation could require the activation of BDNF/TrkB signaling.

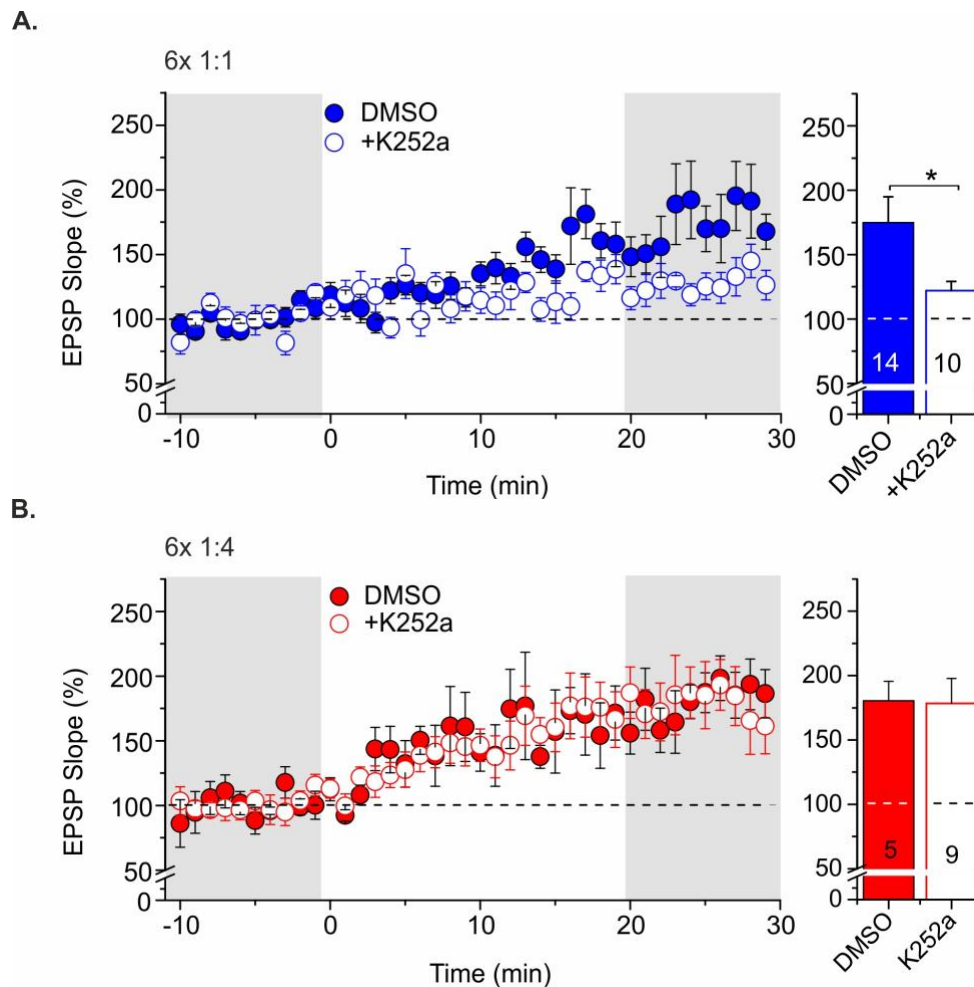


Figure 26. K252a blocks 6x 1:1 but not 6x 1:4 t-LTP. Time course of experiments and quantification are shown for the respective experiments. **(A)** Effects of K252a (200 nM, open symbols) on t-LTP induced with 6x 1:1 (blue) and **(B)** 6x 1:4 protocol (red) compared with DMSO controls (0.05% DMSO). The number of experiments is depicted on the bars. The following number of animals was used for each condition: 6x 1:1 DMSO/K252a (N= 4 / N= 6); and 6x 1:4 DMSO/K252a (N= 10 / N= 7). Data are presented as mean \pm SEM. * $p < 0.05$.

Then, a specific BDNF-scavenger was used to confirm the K252a data. For this, the acute hippocampal slices were pre-incubated for at least three hours with 5 μ g/ml TrkB-Fc, a specific BDNF-scavenger. Subsequently, all the recordings were performed in the continued presence of bath-applied TrkB-Fc (100 ng/ml); this procedure was shown previously to be effective inhibiting 35x 1:4 t-LTP in CA1 pyramidal neurons (Edelmann *et al.*, 2015). Unexpectedly, the magnitude of 6x 1:1

t-LTP was unaffected in the presence of the BDNF-scavenger (Mann-Whitney U test, $U_{(13)} = 13$; $p = 0.094$; **Figure 27A**). Likewise, the bath-applied TrkB-Fc treatment had no effect on t-LTP induced with the 6x 1:4 paradigm, being consistent with the results described above for K252a (Mann-Whitney U test, $U_{(12)} = 22$; $p = 0.805$; **Figure 27B**).

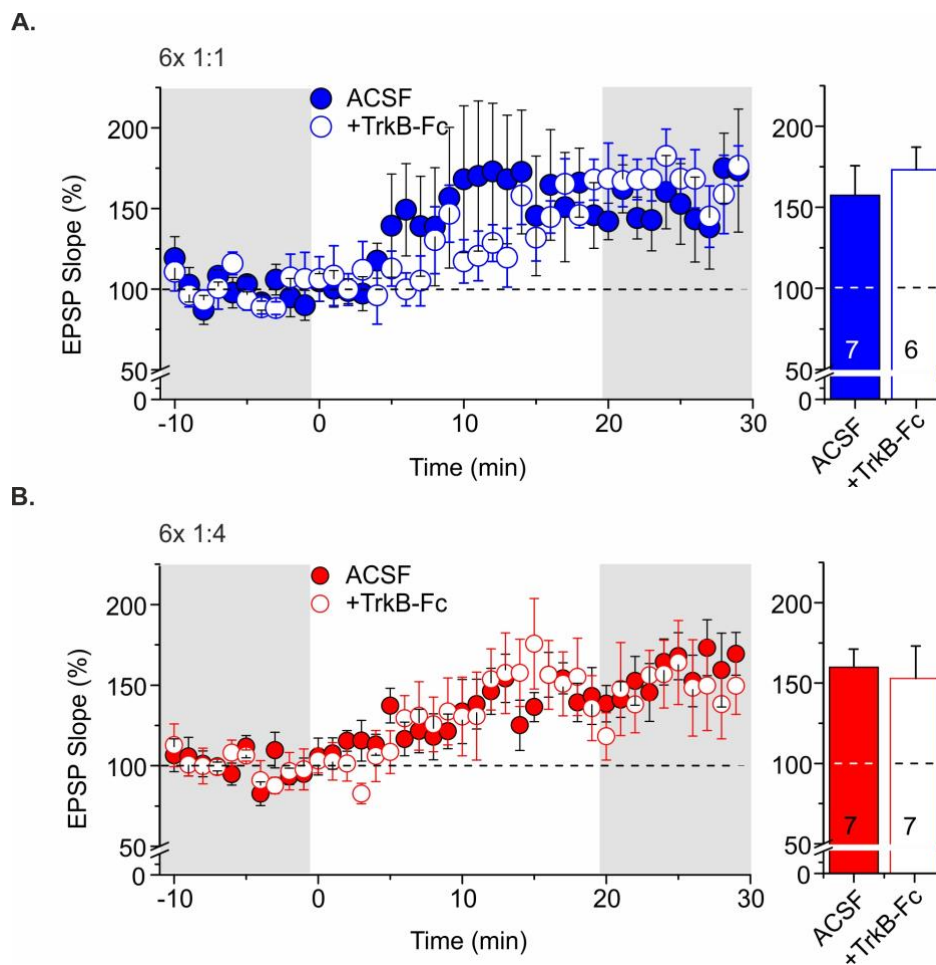


Figure 27. BDNF/TrkB signaling is not required for t-LTP induced with low repeat STDP paradigms. Time course of experiments and quantification are shown for the respective experiments. **(A)** Effects of TrkB-Fc (100 ng/ml; open symbols) on t-LTP induced with 6x 1:1 (blue) and **(B)** 6x 1:4 protocol (red). The number of experiments is indicated on the bars. The following number of animals was used for each condition: 6x 1:1 ACSF/TrkB-Fc (N= 6 / N= 5), and 6x 1:4 ACSF/TrkB-Fc (N= 6 / N= 6). Data are presented as mean \pm SEM.

Finally, to complement previous findings, acute hippocampal slices were prepared from a mouse model with chronically reduced BDNF levels (50%; heterozygous BDNF knockout mice; BDNF^{+/-}). The results revealed that the magnitude of t-LTP obtained in BDNF^{+/-} mice and wild-type littermates was comparable after both 6x 1:1 (Mann-Whitney U test, $U_{(13)} = 25$; $p = 0.779$; **Figure 28A**) and 6x 1:4 stimulation (Mann-Whitney U test, $U_{(10)} = 14$; $p = 0.589$; **Figure 28B**). These results indicate that reduced BDNF gene dosage in BDNF^{+/-} mice did not affect the efficacy of the 6x 1:4 t-LTP protocol in elicit long-lasting changes in synaptic transmission, being at variance with results observed for BDNF-dependent 35x 1:4 t-LTP (Edelmann *et al.*, 2015).

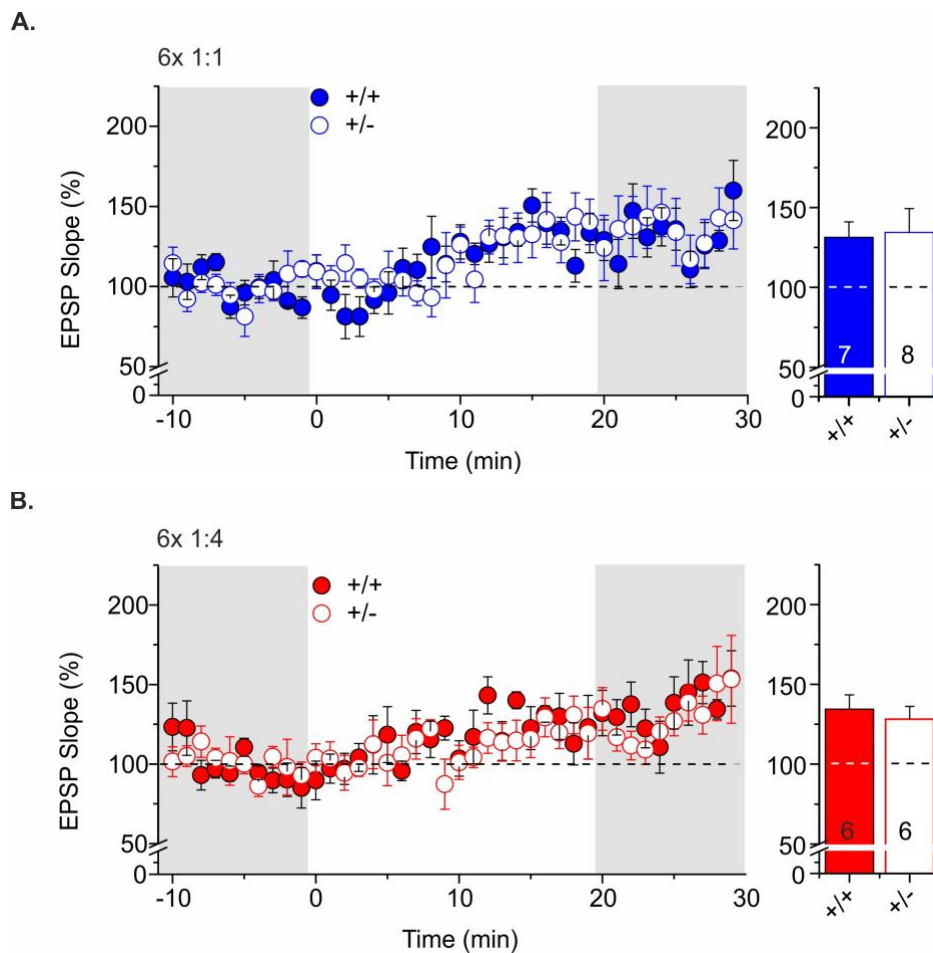


Figure 28. Low repeat t-LTP is not affected in BDNF^{+/-} mice. Time course of experiments and quantification are shown for the respective experiments. **(A)** Effects of BDNF reduction (BDNF^{+/-} mice; open symbols) on t-LTP induced with 6x 1:1 (blue) and **(B)** 6x 1:4 protocol (red) compared to WT mice. The number of measured cells is indicated on the bars. The following number of animals was used for each condition: 6x 1:1 BDNF^{+/-} (N= 7) and WT (N= 8); 6x 1:4 BDNF^{+/-} (N= 5) and WT (N= 6). Data are presented as mean ± SEM.

There is general agreement that 200 nM of K252a affects mainly TrkB receptors (Roux *et al.*, 2002). Then, the K252a effects on 6x 1:1 t-LTP suggest that a possible transactivation of TrkB receptors might be involved. Although the biological functions of transactivation are not very well understood, it could be a cellular strategy to interconnect distinct molecular pathways (Burch *et al.*, 2012). For synaptic plasticity, it has been shown that transactivation of TrkB can be triggered by the influx of zinc (Zn²⁺) via postsynaptic VGCC and NMDAR, and subsequent activation of Src-family kinases (Huang *et al.*, 2008; Hwang *et al.*, 2005; Li *et al.*, 2011). Therefore, here, the potential role of Zn²⁺ in the transactivation of TrkB receptors was investigated by using a specific Zn²⁺ chelator known as TPEN. The results, however, showed no changes in the synaptic efficacy after 6x 1:1 stimulation in response to the bath application of TPEN (10µM) (Mann-Whitney U test, U₍₁₃₎ = 22; p = 0.5358; **Figure 29**), suggesting that possible transactivation of Trk receptors associated to 6x 1:1 stimulation engages other mechanisms, e.g., via G protein-coupled receptors (Rajagopal and Chao, 2006).

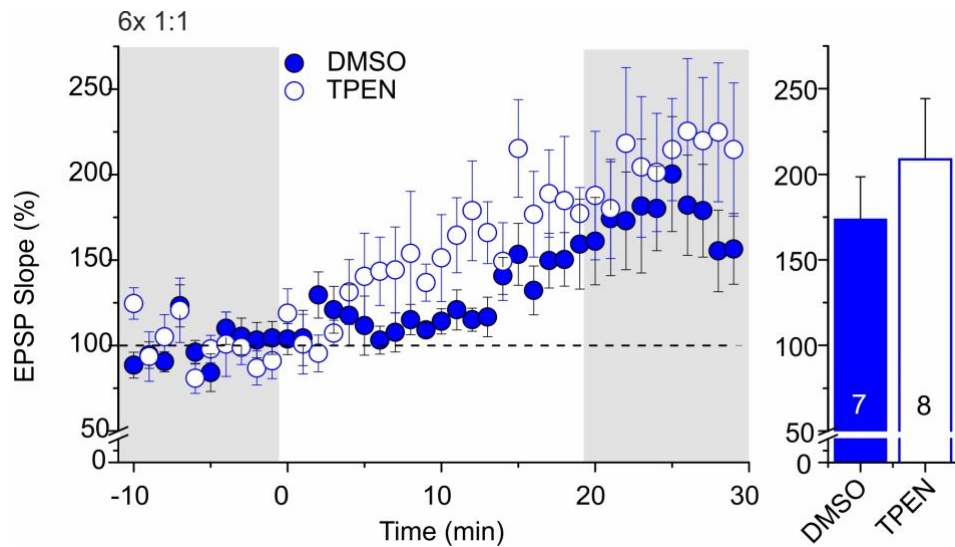


Figure 29. Zn^{2+} signals are not involved in the trans-activation of Trk receptors associated with the molecular mechanisms of 6x 1:1 t-LTP. Time courses show the average of the normalized EPSP slopes in the presence of a specific Zn^{2+} chelator (TPEN, 10 μ M; open symbols) for 6x 1:1 protocol compared with untreated control (ACSF, closed symbols). The number of recorded cells is indicated on the bars. The number of animals used for 6x 1:1 protocol was ACSF / TPEN (N= 4 / N= 3). Data are represented as mean \pm SEM.

Together these data revealed that both 6x 1:1 and 6x 1:4 t-LTP are BDNF-independent, which differ with our previous study showing that 35x 1:4 stimulation induces a BDNF-dependent t-LTP. These findings are stressing the idea that multiple forms of plasticity can be induced and can co-exist at the hippocampal Sc-CA1 synapses, as it was demonstrated by the consecutive activation of both 70x 1:1 and 35x 1:4 t-LTP in the same pyramidal neuron. The recordings clearly showed that both forms of plasticity could be induced without any sign of occlusion (**Figure 30**; Edelmann *et al.*, 2015).

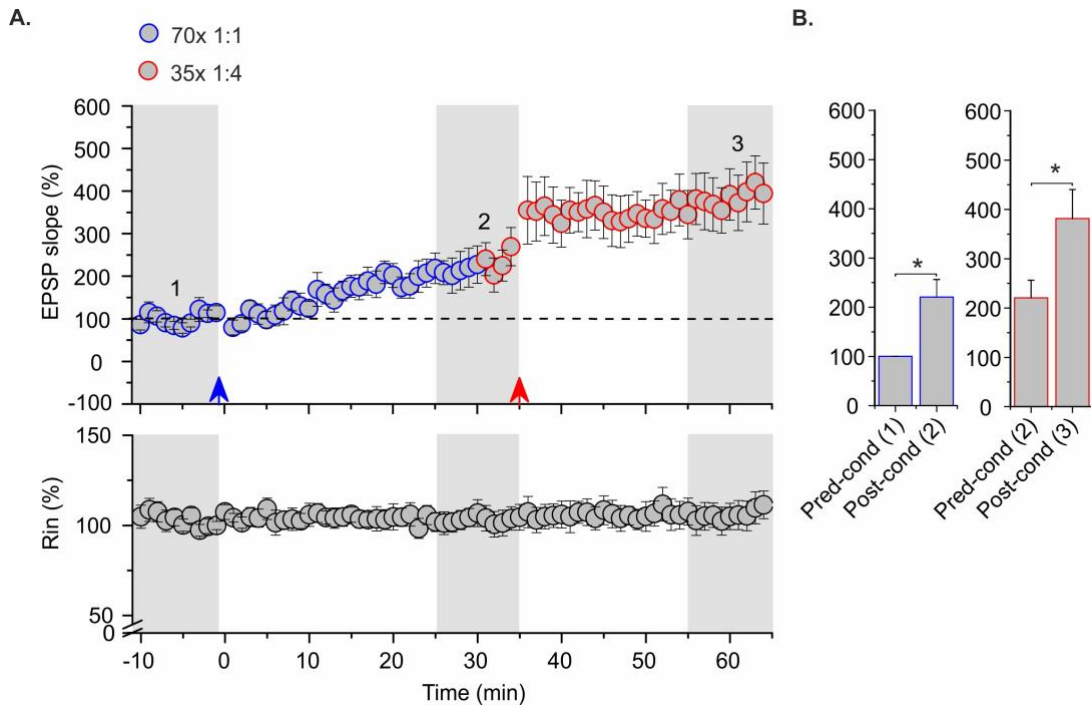


Figure 30. Co-existence of two different forms of synaptic plasticity in the same CA1 pyramidal neuron. (A) After 10 min baseline, Sc-CA1 synapses were conditioning with 70x 1:1 stimulations (blue arrow), then the changes in synaptic transmission were recorded for 30min. Immediately after a second 5 min baseline, the 35x 1:4 protocol was executed (red arrow), and then synaptic responses were monitored for further 30 min. The following number of cells and animals were used: $n=7/ N=7$. **(B)** Bar graphs show robust t-LTP magnitude for both 70x 1:1 versus 100% baseline (blue, Student's t-test $p < 0.05$, one-sample t-test) and 35x 1:4 (red) in comparison with the last 10min of the time course of 70x 1:1 t-LTP (2; two-sample Student's t-test $p < 0.05$). Input resistance (R_{in}) was stable and showed no obvious deflection during the whole recording time. Data are presented as mean \pm SEM. The figure was modified from (Edelmann *et al.*, 2015).

4. Discussion

A single CA1 pyramidal neuron receives thousands of excitatory inputs that arrive onto the dendritic tree to make contact with dendritic spines (Megias *et al.*, 2001). These tiny protrusions have tight regulation of the local Ca₂₊ signals and the biochemical machinery controlling the synaptic plasticity in a compartmentalized fashion (Yuste *et al.*, 2000). Therefore, it is not a surprise that multiple forms of synaptic plasticity are finding at the same synapses. This dissertation shows that the nearly temporal coincidence of only six repeats of one EPSP with either single or multiple postsynaptic spikes lead to distinct types of DA-dependent t-LTP that rely on opposite cellular and different molecular mechanisms.

4.1 Response of hippocampal Sc-CA1 synapses to different numbers of single pre-post pairings

It was notable that the synaptic efficacy at hippocampal Sc-CA1 synapses in response to a distinct number of single pre- and postsynaptic activations in rats and mice show marked differences from each and other (as shown in **Figure 10B** and **Figure 11**). These differences could be due to the variability in active and passive properties in CA1 pyramidal neurons among species of rodents (Routh *et al.*, 2009). Moreover, the minimum number of spike pairings required for successful induction of t-LTP in mice was much lower than in rats, requiring only half of the spike pairings. Besides, the magnitude low repeat t-LTP found in both species of rodents is similar to that reported by other studies using more conventional STDP protocols (Magee and Johnston, 1997; Edelmann *et al.*, 2015; Brzosko *et al.*, 2017; Liu *et al.*, 2017). But even more importantly, this is the first report showing that a robust hippocampal Sc-CA1 t-LTP could be with such as few spike pairings.

Similar findings have been shown in visual cortex at the layer 2/3, in which the authors highlighted that, in some experiments, a significant t-LTP was observed with ≤ 10 spike pairings (Froemke *et al.*, 2006). Also, Cui and collaborators demonstrated that ten spike pairings are sufficient to elicit an NMDAR-independent

t-LTP, which requires the activation of both, endocannabinoid type 1 receptor (eCB1R) and D2 DAR. Interestingly, in the same study, STDP experiments using a higher number of spike pairings (e.g., 100x) result in an opposite form of plasticity, i.e., NMDAR-dependent and unaffected by the inhibition of eCB1Rs (Cui *et al.*, 2015). Later on, the same group report that the differences described above may be due to variations in the endocannabinoids (eCB) levels at the extracellular space caused by the distinct number of pre-post activations, having a repercussion on the magnitude of synaptic plasticity at corticostriatal synapses (Cui *et al.*, 2016). Furthermore, Zhang *et al.* showed that the bath application of exogenous DA increases synaptic efficacy, allowing t-LTP induction with less than ten spike pairings (Zhang *et al.*, 2009). This evidence is consistent with the data presented here, showing that neuromodulation is an essential factor in gating low repeat t-LTP.

4.2 Cellular mechanisms underlying the expression of low repeat t-LTP at hippocampal Sc-CA1 synapses

The current study is showing that t-LTP induced with either 6x 1:1 or 6x 1:4 protocols have different cellular mechanisms. The 6x 1:1 stimulation leads to changes in the release properties of glutamate that were revealed by the significant increase of PPR after t-LTP induction (**Figure 15A**), a phenomenon usually associated to LTD instead of LTP (Foster and McNaughton, 1991). However, these data could be interpreted in a different way in which the increase of PPR after 6x 1:1 stimulation might be due to the incorporation of more release sites with initial low P_r of glutamate, leading to a very small EPSC in response to the first pulse. But, for the second pulse, the EPSC becomes much higher, since the remaining Ca^{2+} build up during the first pulse increases the P_r of glutamate of all new release sites, as has been described (Foster and McNaughton, 1991; Schulz *et al.*, 1994).

It seems to be that changes in P_r of glutamate are more likely to occur in active zones connected with large and mature spines (e.g., mushroom spines) with multivesicular release, than those coupled to small spines (e.g., thin spines) in which the release is mostly unquantal (Bolshakov and Siegelbaum, 1995; Oertner *et al.*,

2002; Conti and Lisman, 2003; Raghavachari and Lisman, 2004). Then it is possible that 1:1 stimulation maybe restricted to large and mature spines in which presynaptic modifications are more likely to occur.

On the other hand, the cellular mechanisms for low repeat STDP, described here, are in agreement with previous studies using the same spike pattern but a higher number of spike pairings (Edelmann *et al.*, 2015), suggesting that the postsynaptic burst is a critical signal to trigger the recruitment of postsynaptic mechanisms rather than the number of spike pairings. In contrast, single spike pairings would be favoring the recruitment of presynaptic mechanisms.

Single and multiple APs are likely to have different functional consequences. At the dendrite, only a burst of APs can produce sufficient depolarization to generate dendritic spikes, which are considered a critical signal for structural and functional modifications linked to small spines (Golding *et al.*, 2002; Kampa *et al.*, 2006). This is also consistent with the data presented here regarding I_{AMPA}/I_{NMDAR} ratio (**Figure 18**), showing that 6x 1:1 stimulation did not cause modifications in postsynaptic AMPARs properties. In contrast, after t-LTP induced with the 6x 1:4 protocol, revealed significant changes in I_{AMPA}/I_{NMDAR} ratio and not variation in PPR (**Figure 15A**). Further experiments in our group using intracellular application of Pep1-TGL (30 μ M), a synthetic peptide interfering with the stabilization of AMPAR GluA1 subunits at the PSD, showed that the 6x 1:4 protocol depends of AMPAR containing GluR1 subunits trafficking, whereas the 6x 1:1 protocol does not (Quiceno G, unpublished data, personal communication).

Ultrastructural analysis in CA1 pyramidal neurons depict that NMDARs densities were stable along dendritic arbor (Nicholson and Geinisman, 2009), whereas AMPARs distribution depended on the size of the spine and its localization (Nusser *et al.*, 1998; Smith *et al.*, 2003; Noguchi *et al.*, 2005; Katz *et al.*, 2009). Moreover, long-lasting morphological modifications in small spines had a positive correlation with an increase in the amplitude of AMPAR evoked EPSCs in CA1 pyramidal neurons. In contrast, in large spines, such structural modifications were only transient and not changes in AMPAR conductance were observed (Matsuzaki *et al.*,

2004). Hence, the size and shape of the dendritic spines might be a determinant factor associated with the locus expression of LTP. Nevertheless, it cannot be ruled out that the recruitment of pre- and postsynaptic mechanisms in response to 1:1 or 1:4 stimulations, respectively, occur in the same set of synapses (Edelmann *et al.*, 2017).

4.3 Low repeat t-LTP induced with single and multiple postsynaptic spikes recruit distinct calcium signals

Here, the data reveal that 6x 1:1 t-LTP requires the activation of both NMDARs and L-type Ca²⁺ channels (**Figure 20A and Figure 21A**). However, intracellular infusion of the Ca²⁺ chelator BAPTA did not affect the synaptic potentiation evoked by the 6x 1:1 protocol (**Figure 23A**), suggesting that postsynaptic Ca²⁺ elevation maybe not required for this type of plasticity.

A possible explanation for these results would be that 6x 1:1 stimulation is not sufficient to produce enough depolarization to relief the Mg²⁺ block from the ion channel of the NMDAR. This is a plausible idea, since the NMDAR antagonist used here was DL-APV, which is a competitive inhibitor that blocks the glutamate-binding site of GluN2 subunit. Interestingly, It has been shown the induction of hippocampal NMDA-dependent LTD can be block by bath application of DL-APV, whereas the application of MK801, a blocker that interferes with the NMDA ion channel opening, does not affect this type of plasticity (Scanziani *et al.*, 1996). This finding brought the idea that NMDAR has metabotropic functions leading to the activation of phosphatases linked to dephosphorylation and endocytosis of AMPAR, resulting in the expression LTD (Dore *et al.*, 2017). Beside, NMDAR metabotropic functions have been only described for LTD (Nabavi *et al.*, 2013), it cannot be ruled out its possible contribute to some forms of LTP. Therefore, it would be important to investigate the potential effects of blocking NMDA ion channel opening on 6x 1:1 t-LTP by using MK801.

An alternative explanation would be that 6x 1:1 stimulation triggers the activation of presynaptic NMDARs (pre-NMDAR) (Sjostrom *et al.*, 2003; Lien *et al.*, 2006; Mapelli *et al.*, 2016; Bouvier *et al.*, 2018), which is implicated in the regulation of neurotransmitter release at the Schaffer collaterals fibers (McGuinness *et al.*, 2010), through the modulation of proteins associated with presynaptic vesicle trafficking (Abrahamsson *et al.*, 2017). Although, the possible contribution of pre-NMDARs to the 6x 1:1 t-LTP is an attractive idea, the suitable experimental settings to have the total control of presynaptic terminals arriving to CA1 region remains to be identified.

Besides that, the role of presynaptic L-type Ca_2^+ channels LTP is describing in mossy fibers-CA3 synapses and the cortico-lateral amygdala synapses (Castillo *et al.*, 1994; Fourcaudot *et al.*, 2009), there is no evidence of the presynaptic expression of L-type Ca_2^+ channels at axon terminals in CA1 region. Indeed, their expression seems to be limited to dendrites, soma, and GABAergic terminals but not axons (Murakami *et al.*, 2002; Tippens *et al.*, 2008). Therefore, further experiments would be required to confirm the role of postsynaptic Ca_2^+ signals in 6x 1:1 t-LTP induction.

In contrast, the 6x 1:4 t-LTP was NMDAR and L-type Ca_2^+ channels independent, which in overall represent the most common sources of Ca_2^+ signals associated to LTP at hippocampal Sc-CA1 synapses (Malenka and Bear, 2004). Furthermore, the presence of either mGluR₁ or mGluR₅ antagonists did not affect the magnitude of the synaptic potentiation. However, it was entirely blocked by the postsynaptic infusion of 10 mM BAPTA (**Figure 23B**). Indeed, NMDAR-independent t-LTP induced with a low number of spike pairings (≤ 10) has been described previously in corticostriatal synapses (Cui *et al.*, 2015), but never in Sc-CA1 synapses.

Although the Ca_2^+ source for 6x 1:4 t-LTP is not defined here, additional experiments in our group revealed that impairment of the internal Ca_2^+ stores by intracellular application of ryanodine (100 μM) hindered 6x 1:4 t-LTP induction (Khodaie B, unpublished data, personal communication). Since the activation of mGluR leads to the mobilization of Ca_2^+ from internal stores (Hong and Ross, 2007), it is essential to reexamine the potential role of mGluR in 6x 1:4 t-LTP induction, because there is

evidence showing overlapping in the function of these receptors in LTP (Le Vasseur *et al.*, 2008; Chen *et al.*, 2017). Thus, the blockade of both mGluR₁ and mGluR₅ simultaneously would be required to examine this possibility. Moreover, the bath application of a selective blocker for GluR₂-lacking AMPAR known as 1-naphthyl acetyl spermine (NASPM, 100 μ M) demonstrated that activation of these receptors is also critical for the induction of 6x 1:4 t-LTP (Khodaie B, unpublished data, personal communication). The transient incorporation of GluR₂-lacking AMPAR previously linked to LTP induction (Kauer and Malenka, 2006; Plant *et al.*, 2006; Man, 2011) in hippocampus (Hainmuller *et al.*, 2014), lateral amygdala (Bissiere *et al.*, 2003), and prefrontal cortex (Xu and Yao, 2010). Activation of GluR₂-lacking AMPAR also increases the synaptic efficacy allowing t-LTP longer temporal windows (Holbro *et al.*, 2010), which could explain the potentiation observed with 6x 1:4 stimulation within a $\Delta t = 30$ ms (**Figure 14B**). However, whether the Ca₂₊ influx via GluR₂-lacking AMPARs alone is sufficient to support the induction of LTP is currently controversial.

At hippocampal Sc-CA1 synapses, LTP can be induced in GluR₂-deficient mice, and impairments in basal transmission or the magnitude of LTP is detected, suggesting that GluR₂-lacking AMPAR are present under resting conditions supporting synaptic transmission (Jia *et al.*, 1996; Asrar *et al.*, 2009). It is bringing a likely scenario in which GluR₂-lacking AMPAR, already present at the PDS, would mediate Ca₂₊ signals required for 6x 1:4 t-LTP, which can be amplified by the mobilization of Ca₂₊ from the internal stores via mGluR_{1/5} or by Ca₂₊ induced Ca₂₊ release.

4.4 Dopaminergic modulation of low repeat t-LTP

In this dissertation is reported that the blockage of both D1-like and D2R-like DARs was required to abolish 6x 1:1 t-LTP, whereas D2-like DARs antagonist alone was sufficient to block 6x 1:4 t-LTP. In fact, the presence of D1-like DAR antagonist alone did not show effects on either 6x 1:1 or 6x 1:4 t-LTP (**Figure 24**), suggesting that D2-like DARs have a dominant role in the modulation of synaptic plasticity induced

with low repeat STDP paradigms. D2-like DAR antagonist also caused effects on action potential firing of CA1 pyramidal neurons that were even more striking by the co-application of both D1-like and D2R-like DARs antagonist (**Table 2**, early adaptation data). Those results are consistent with previous reports indicating that DA raises the threshold of AP initiation through the modulation of K⁺, Na⁺ and Ca²⁺ conductance (Wolfart *et al.*, 2001; Lin *et al.*, 2008; Ford, 2014), controlling the frequency and precision of AP firing (Stanzione *et al.*, 1984). Here, the analysis of the effects of DAR antagonists on AP firing was performed previous to the t-LTP experiments, suggesting that neuronal activity in CA1 region might be controlled by spontaneous tonic DA release (Brzosko *et al.*, 2015; Rice and Cragg, 2008). Then, it is likely that D2R-like DARs control neuronal excitability and synaptic efficacy through the regulation of DA release as well as DA transporters, which may explain the chemical LTP found in the presence of the DA uptake inhibitor (**Figure 25**).

Also, variations in the levels of free DA availability can lead to the activation of different types of DARs with different sensitivities to the ligand. D1-like and D2-like DARs respond to high and low levels of DA, respectively (Richfield *et al.*, 1989). Using optogenetics to control the activation of dopaminergic afferents coming from VTA and SNc to the hippocampus, Rosen and collaborators showed that tonic light stimulation produces low DA ambient, leading to the activation of D2-like DARs. In contrast, the rapid increase of DA concentration in response to phasic light stimulation induces the activation of D1-like DARs (Rosen *et al.*, 2015). Similar effects were found here in response to a high and low number of spike pairings.

Consequently, activation of D1-like DAR is sufficient to support 70x 1:1 t-LTP, whereas 6x 1:1 and 6x 1:4 t-LTP involved mainly D2-like DARs. Thereby, it is possible to propose that variation in the number of spike pairings lead to distinct neuromodulatory ambient, controlling the functional consequences of STDP (see also Cui *et al.*, 2016). The rising question at this point would be why does 6x 1:1 t-LTP need activation of both D1-like and D2-like DARs but 6x 1:4 t-LTP does not?

Because, the 6x 1:1 represent the weakest stimulation capable to inducing successful t-LTP at hippocampal Sc-CA1 synapses (**Figure 10B**), It seems plausible

to assume that the synergism between D1-like and D2-like DARs might be a molecular mechanism to increase synaptic efficacy. Application of exogenous DA converts t-LTD into t-LTP (Zhang *et al.*, 2009). Interestingly, this conversion requires the activation of both D1-like and D2-like DARs (Brzosko *et al.*, 2015). Similar processes occur in the prefrontal cortex, where D2-like DARs at interneuron terminals were found to be essential for t-LTP induction at excitatory L2/3-L5 synapses. Here, the synergism between D2-like DARs and D1-like DARs was required when the spike timing interval was extended from 10 to 30 ms. The authors proposed that D2-like DARs would gate t-LTP, whereas D1-like receptors contribute to the precise temporal coincidence between pre- and postsynaptic activation (Xu and Yao, 2010). Also, the possible role of heteromeric D1-D2 DAR cannot be ruled out neither (Lee *et al.*, 2004).

Activation of D2-like DARs might also represent a critical signal facilitating the back-propagation of the postsynaptic spikes. In CA1 pyramidal neurons, the propagation of a single postsynaptic spike is not attenuated a long distance. The opposite occurs for multiple spikes in which the propagation is sharply reduced at distal dendrites, preferentially, at the branch points (Spruston *et al.*, 1995). This effect is owing to the hyperpolarization of dendritic arbor due to activation of A-type K⁺ channels in order to counteract the strong depolarization caused by the postsynaptic burst (Hoffman and Johnston, 1998). However, during LTP induction, the activation of neuromodulatory inputs such as DA (Hoffman and Johnston, 1998; Magee and Carruth, 1999; Tigerholm *et al.*, 2013) produces the downregulation the A-type K⁺ channels, allowing the postsynaptic burst travel further along distance (Golding and Spruston, 1998; Gasparini *et al.*, 2007) Hence, it would be possible that the activation of D2-like DAR is an essential step that facilitated the back-propagation of postsynaptic burst used for 6x 1:4 t-LTP induction. It may explain why the block of D2-like DAR alone is sufficient to abolish the 6x 1:4 t-LTP expression.

4.5 Contribution of BDNF/TrkB signaling to low repeat t-LTP induction

We previously found that Sc-CA1 synapses from acute hippocampus slices conditioned with 35x 1:4 stimulation elicited a BDNF/TrkB-dependent t-LTP, whereas 70x 1:1 stimulation resulted in a BDNF/TrkB-independent t-LTP. (Edelmann *et al.*, 2015). Since neither the reduced BDNF gene dosage in BDNF^{+/-} mice nor the bath application of BDNF scavenger altered low repeat t-LTP, the most likely explanation would be that the six spike pairings are not sufficient to provoke the release of BDNF. These data in agreement with previous reports in cultured hippocampal neurons, showing that at least 40 spike pairings are needed to detect BDNF secretion at dendritic spines (Lu *et al.*, 2014).

On the other hand, it was shown that K252a significantly impairs 6x 1:1 t-LTP, suggesting potential transactivation as a part of the molecular mechanisms supporting this form of plasticity. Although transactivation of TrkB receptors occurs in response to a transient increase of intracellular concentration of Zn²⁺ (Huang *et al.*, 2008; Hwang *et al.*, 2005; Li *et al.*, 2011), the block of Zn²⁺ signals did not affect 6x 1:1 t-LTP (**Figure 29**). Alternatively, transactivation of Trk receptors could also take place via G protein-coupled receptors in association with Src-family kinases such as Fyn tyrosine kinase (Rajagopal and Chao, 2006). It is the case for primary striatal neurons where either D1-like or D2-like DAR mediates the transactivation of TrkB receptors (Swift *et al.*, 2011). Then, further experiments using specific inhibitors for Src-family kinases would be required. Nevertheless, it has to be considered that 200nM K252a also affects other neurotrophic receptors (Berg *et al.*, 1992; Tapley *et al.*, 1992), such as tyrosine kinase receptors, e.g. platelet-derived growth factor (Nye *et al.*, 1992). Therefore, further experiments are required to clarify the effects of K252a on 6x 1:1 t-LTP.

4.6 General conclusion

Here was demonstrated for the first time that low repeat STDP protocols evoke a robust t-LTP at hippocampal Sc-CA1 synapses. The cellular and molecular

mechanisms underlying low repeat t-LTP seems to be heavily influenced by the pattern and number of the spike pairings, likely through the modulation of passive and active neuronal properties, as well as the levels of neuromodulatory signals along dendritic branches. This study provides evidence that those multiple types of plasticity can coexist in a single CA1 pyramidal neuron (**Figure 30**), expanding our understanding about the integration and processing of information at the single-cell level.

5. References

- Abrahamsson T, Chou CYC, Li SY, Mancino A, Costa RP, Brock JA, Nuro E, Buchanan KA, Elgar D, Blackman AV, Tudor-Jones A, Oyrer J, Farmer WT, Murai KK, Sjöstrom PJ (2017). Differential Regulation of Evoked and Spontaneous Release by Presynaptic NMDA Receptors. *Neuron* **96**(4): 839-855 e835.
- Abrahamsson T, Lalanne T, Watt AJ, Sjöstrom PJ (2016). Long-Term Potentiation by Theta-Burst Stimulation Using Extracellular Field Potential Recordings in Acute Hippocampal Slices. *Cold Spring Harb Protoc* **2016**(6): pdb prot091298.
- Ahmed R, Zha XM, Green SH, Dailey ME (2006). Synaptic activity and F-actin coordinately regulate CaMKIIalpha localization to dendritic postsynaptic sites in developing hippocampal slices. *Mol Cell Neurosci* **31**(1): 37-51.
- Alford S, Frenguelli BG, Schofield JG, Collingridge GL (1993). Characterization of Ca²⁺ signals induced in hippocampal CA1 neurones by the synaptic activation of NMDA receptors. *J Physiol* **469**: 693-716.
- Amitai Y, Friedman A, Connors BW, Gutnick MJ (1993). Regenerative activity in apical dendrites of pyramidal cells in neocortex. *Cereb Cortex* **3**(1): 26-38.
- Andrade-Talavera Y, Duque-Feria P, Paulsen O, Rodriguez-Moreno A (2016). Presynaptic Spike Timing-Dependent Long-Term Depression in the Mouse Hippocampus. *Cereb Cortex* **26**(8): 3637-3654.
- Anwyl R (2009). Metabotropic glutamate receptor-dependent long-term potentiation. *Neuropharmacology* **56**(4): 735-740.
- Ashby MC, Maier SR, Nishimune A, Henley JM (2006). Lateral diffusion drives constitutive exchange of AMPA receptors at dendritic spines and is regulated by spine morphology. *J Neurosci* **26**(26): 7046-7055.
- Asrar S, Zhou Z, Ren W, Jia Z (2009). Ca²⁺ permeable AMPA receptor induced long-term potentiation requires PI3/MAP kinases but not Ca/CaM-dependent kinase II. *PLoS One* **4**(2): e4339.
- Barcomb K, Hell JW, Benke TA, Bayer KU (2016). The CaMKII/GluN2B Protein Interaction Maintains Synaptic Strength. *J Biol Chem* **291**(31): 16082-16089.
- Beaulieu JM, Gainetdinov RR (2011). The physiology, signaling, and pharmacology of dopamine receptors. *Pharmacol Rev* **63**(1): 182-217.
- Bekkers JM, Stevens CF (1989). NMDA and non-NMDA receptors are co-localized at individual excitatory synapses in cultured rat hippocampus. *Nature* **341**(6239): 230-233.
- Bender KJ, Ford CP, Trussell LO (2010). Dopaminergic modulation of axon initial segment calcium channels regulates action potential initiation. *Neuron* **68**(3): 500-511.
- Bender KJ, Trussell LO (2009). Axon initial segment Ca²⁺ channels influence action potential generation and timing. *Neuron* **61**(2): 259-271.

- Benke TA, Luthi A, Isaac JT, Collingridge GL (1998). Modulation of AMPA receptor unitary conductance by synaptic activity. *Nature* **393**(6687): 793-797.
- Berg MM, Sternberg DW, Parada LF, Chao MV (1992). K-252a inhibits nerve growth factor-induced trk proto-oncogene tyrosine phosphorylation and kinase activity. *J Biol Chem* **267**(1): 13-16.
- Bethus I, Tse D, Morris RG (2010). Dopamine and memory: modulation of the persistence of memory for novel hippocampal NMDA receptor-dependent paired associates. *J Neurosci* **30**(5): 1610-1618.
- Bi GQ, Poo MM (1998). Synaptic modifications in cultured hippocampal neurons: dependence on spike timing, synaptic strength, and postsynaptic cell type. *J Neurosci* **18**(24): 10464-10472.
- Bissiere S, Humeau Y, Luthi A (2003). Dopamine gates LTP induction in lateral amygdala by suppressing feedforward inhibition. *Nat Neurosci* **6**(6): 587-592.
- Bliim N, Leshchyns'ka I, Sytnyk V, Janitz M (2016). Transcriptional regulation of long-term potentiation. *Neurogenetics* **17**(4): 201-210.
- Bliss TV, Collingridge GL (1993). A synaptic model of memory: long-term potentiation in the hippocampus. *Nature* **361**(6407): 31-39.
- Bliss TV, Gardner-Medwin AR (1973). Long-lasting potentiation of synaptic transmission in the dentate area of the unanaesthetized rabbit following stimulation of the perforant path. *J Physiol* **232**(2): 357-374.
- Bliss TV, Lomo T (1973). Long-lasting potentiation of synaptic transmission in the dentate area of the anaesthetized rabbit following stimulation of the perforant path. *J Physiol* **232**(2): 331-356.
- Blundon JA, Zakharenko SS (2008). Dissecting the components of long-term potentiation. *Neuroscientist* **14**(6): 598-608.
- Boeckers TM (2006). The postsynaptic density. *Cell Tissue Res* **326**(2): 409-422.
- Bolshakov VY, Siegelbaum SA (1995). Regulation of hippocampal transmitter release during development and long-term potentiation. *Science* **269**(5231): 1730-1734.
- Bosch M, Castro J, Saneyoshi T, Matsuno H, Sur M, Hayashi Y (2014). Structural and molecular remodeling of dendritic spine substructures during long-term potentiation. *Neuron* **82**(2): 444-459.
- Bouvier G, Larsen RS, Rodriguez-Moreno A, Paulsen O, Sjostrom PJ (2018). Towards resolving the presynaptic NMDA receptor debate. *Curr Opin Neurobiol* **51**: 1-7.
- Bredt DS, Nicoll RA (2003). AMPA receptor trafficking at excitatory synapses. *Neuron* **40**(2): 361-379.
- Brzosko Z, Schultz W, Paulsen O (2015). Retroactive modulation of spike timing-dependent plasticity by dopamine. *Elife* **4**.

- Brzosko Z, Zannone S, Schultz W, Clopath C, Paulsen O (2017). Sequential neuromodulation of Hebbian plasticity offers mechanism for effective reward-based navigation. *Elife* **6**.
- Burch ML, Osman N, Getachew R, Al-Aryahi S, Poronnik P, Zheng W, Hill MA, Little PJ (2012). G protein coupled receptor transactivation: extending the paradigm to include serine/threonine kinase receptors. *Int J Biochem Cell Biol* **44**(5): 722-727.
- Caldeira MV, Melo CV, Pereira DB, Carvalho R, Correia SS, Backos DS, Carvalho AL, Esteban JA, Duarte CB (2007a). Brain-derived neurotrophic factor regulates the expression and synaptic delivery of alpha-amino-3-hydroxy-5-methyl-4-isoxazole propionic acid receptor subunits in hippocampal neurons. *J Biol Chem* **282**(17): 12619-12628.
- Caldeira MV, Melo CV, Pereira DB, Carvalho RF, Carvalho AL, Duarte CB (2007b). BDNF regulates the expression and traffic of NMDA receptors in cultured hippocampal neurons. *Mol Cell Neurosci* **35**(2): 208-219.
- Campanac E, Debanne D (2008). Spike timing-dependent plasticity: a learning rule for dendritic integration in rat CA1 pyramidal neurons. *J Physiol* **586**(3): 779-793.
- Caporale N, Dan Y (2008). Spike timing-dependent plasticity: a Hebbian learning rule. *Annu Rev Neurosci* **31**: 25-46.
- Castillo PE, Weisskopf MG, Nicoll RA (1994). The role of Ca²⁺ channels in hippocampal mossy fiber synaptic transmission and long-term potentiation. *Neuron* **12**(2): 261-269.
- Castillo PE, Younts TJ, Chavez AE, Hashimoto Y (2012). Endocannabinoid signaling and synaptic function. *Neuron* **76**(1): 70-81.
- Celikel T, Szostak VA, Feldman DE (2004). Modulation of spike timing by sensory deprivation during induction of cortical map plasticity. *Nat Neurosci* **7**(5): 534-541.
- Chao LH, Stratton MM, Lee IH, Rosenberg OS, Levitz J, Mandell DJ, Kortemme T, Groves JT, Schulman H, Kuriyan J (2011). A mechanism for tunable autoinhibition in the structure of a human Ca²⁺/calmodulin-dependent kinase II holoenzyme. *Cell* **146**(5): 732-745.
- Chen A, Hu WW, Jiang XL, Potegal M, Li H (2017). Molecular mechanisms of group I metabotropic glutamate receptor mediated LTP and LTD in basolateral amygdala in vitro. *Psychopharmacology (Berl)* **234**(4): 681-694.
- Chen HX, Otmakhov N, Lisman J (1999). Requirements for LTP induction by pairing in hippocampal CA1 pyramidal cells. *J Neurophysiol* **82**(2): 526-532.
- Chen L, Chetkovich DM, Petralia RS, Sweeney NT, Kawasaki Y, Wenthold RJ, Brecht DS, Nicoll RA (2000). Stargazin regulates synaptic targeting of AMPA receptors by two distinct mechanisms. *Nature* **408**(6815): 936-943.
- Chen X, Yuan LL, Zhao C, Birnbaum SG, Frick A, Jung WE, Schwarz TL, Sweatt JD, Johnston D (2006). Deletion of Kv4.2 gene eliminates dendritic A-type K⁺ current and enhances

- induction of long-term potentiation in hippocampal CA1 pyramidal neurons. *J Neurosci* **26**(47): 12143-12151.
- Chistiakova M, Bannon NM, Chen JY, Bazhenov M, Volgushev M (2015). Homeostatic role of heterosynaptic plasticity: models and experiments. *Front Comput Neurosci* **9**: 89.
- Chwang WB, O'Riordan KJ, Levenson JM, Sweatt JD (2006). ERK/MAPK regulates hippocampal histone phosphorylation following contextual fear conditioning. *Learn Mem* **13**(3): 322-328.
- Citri A, Malenka RC (2008). Synaptic plasticity: multiple forms, functions, and mechanisms. *Neuropsychopharmacology* **33**(1): 18-41.
- Collingridge GL, Herron CE, Lester RA (1988). Synaptic activation of N-methyl-D-aspartate receptors in the Schaffer collateral-commissural pathway of rat hippocampus. *J Physiol* **399**: 283-300.
- Collingridge GL, Kehl SJ, McLennan H (1983). Excitatory amino acids in synaptic transmission in the Schaffer collateral-commissural pathway of the rat hippocampus. *J Physiol* **334**: 33-46.
- Conti R, Lisman J (2003). The high variance of AMPA receptor- and NMDA receptor-mediated responses at single hippocampal synapses: evidence for multiquantal release. *Proc Natl Acad Sci U S A* **100**(8): 4885-4890.
- Costa RP, Mizusaki BE, Sjostrom PJ, van Rossum MC (2017a). Functional consequences of pre- and postsynaptic expression of synaptic plasticity. *Philos Trans R Soc Lond B Biol Sci* **372**(1715).
- Costa RP, Padamsey Z, D'Amour JA, Emptage NJ, Froemke RC, Vogels TP (2017b). Synaptic transmission optimization predicts expression loci of long-term plasticity. *Neuron* **96**(1): 177-189 e177.
- Cui Y, Paille V, Xu H, Genet S, Delord B, Fino E, Berry H, Venance L (2015). Endocannabinoids mediate bidirectional striatal spike-timing-dependent plasticity. *J Physiol* **593**(13): 2833-2849.
- Cui Y, Prokin I, Xu H, Delord B, Genet S, Venance L, Berry H (2016). Endocannabinoid dynamics gate spike-timing dependent depression and potentiation. *Elife* **5**: e13185.
- Dan Y, Poo MM (2004). Spike timing-dependent plasticity of neural circuits. *Neuron* **44**(1): 23-30.
- Dan Y, Poo MM (2006). Spike timing-dependent plasticity: from synapse to perception. *Physiol Rev* **86**(3): 1033-1048.
- Debanne D, Gahwiler BH, Thompson SM (1994). Asynchronous pre- and postsynaptic activity induces associative long-term depression in area CA1 of the rat hippocampus in vitro. *Proc Natl Acad Sci U S A* **91**(3): 1148-1152.
- Debanne D, Gahwiler BH, Thompson SM (1997). Bidirectional associative plasticity of unitary CA3-CA1 EPSPs in the rat hippocampus in vitro. *J Neurophysiol* **77**(5): 2851-2855.

- Debanne D, Gahwiler BH, Thompson SM (1998). Long-term synaptic plasticity between pairs of individual CA3 pyramidal cells in rat hippocampal slice cultures. *J Physiol* **507 (Pt 1)**: 237-247.
- Del Castillo J, Katz B (1954). Statistical factors involved in neuromuscular facilitation and depression. *J Physiol* **124(3)**: 574-585.
- Dewar KM, Reader TA (1989). Distribution of dopamine D1 and D2 receptors in rabbit cortical areas, hippocampus, and neostriatum in relation to dopamine contents. *Synapse* **4(4)**: 378-386.
- Do T, Kerr B, Kuzhikandathil EV (2007). Brain-derived neurotrophic factor regulates the expression of D1 dopamine receptors. *J Neurochem* **100(2)**: 416-428.
- Dore K, Stein IS, Brock JA, Castillo PE, Zito K, Sjostrom PJ (2017). Unconventional NMDA receptor signaling. *J Neurosci* **37(45)**: 10800-10807.
- Edelmann E, Cepeda-Prado E, Franck M, Lichtenecker P, Brigadski T, Lessmann V (2015). Theta burst firing recruits BDNF release and signaling in postsynaptic CA1 neurons in spike-timing-dependent LTP. *Neuron* **86(4)**: 1041-1054.
- Edelmann E, Cepeda-Prado E, Lessmann V (2017). Coexistence of multiple types of synaptic plasticity in individual hippocampal CA1 pyramidal neurons. *Front Synaptic Neurosci* **9**: 7.
- Edelmann E, Lessmann V (2011). Dopamine modulates spike timing-dependent plasticity and action potential properties in CA1 pyramidal neurons of acute rat hippocampal slices. *Front Synaptic Neurosci* **3**: 6.
- Edelmann E, Lessmann V (2013). Dopamine regulates intrinsic excitability thereby gating successful induction of spike timing-dependent plasticity in CA1 of the hippocampus. *Front Neurosci* **7**: 25.
- Edelmann E, Lessmann V (2018). Dopaminergic innervation and modulation of hippocampal networks. *Cell Tissue Res*: 1-17.
- Edelmann E, Lessmann V, Brigadski T (2014). Pre- and postsynaptic twists in BDNF secretion and action in synaptic plasticity. *Neuropharmacology* **76 Pt C**: 610-627.
- Eichenbaum H, Lipton PA (2008). Towards a functional organization of the medial temporal lobe memory system: role of the parahippocampal and medial entorhinal cortical areas. *Hippocampus* **18(12)**: 1314-1324.
- Ethell IM, Ethell DW (2007). Matrix metalloproteinases in brain development and remodeling: synaptic functions and targets. *J Neurosci Res* **85(13)**: 2813-2823.
- Feldman DE (2012). The spike-timing dependence of plasticity. *Neuron* **75(4)**: 556-571.
- Fifkova E, Van Harreveld A (1977). Long-lasting morphological changes in dendritic spines of dentate granular cells following stimulation of the entorhinal area. *J Neurocytol* **6(2)**: 211-230.

- Figurov A, Pozzo-Miller LD, Olafsson P, Wang T, Lu B (1996). Regulation of synaptic responses to high-frequency stimulation and LTP by neurotrophins in the hippocampus. *Nature* **381**(6584): 706-709.
- Fitzsimonds RM, Poo MM (1998). Retrograde signaling in the development and modification of synapses. *Physiol Rev* **78**(1): 143-170.
- Ford CP (2014). The role of D2-autoreceptors in regulating dopamine neuron activity and transmission. *Neuroscience* **282**: 13-22.
- Foster TC, McNaughton BL (1991). Long-term enhancement of CA1 synaptic transmission is due to increased quantal size, not quantal content. *Hippocampus* **1**(1): 79-91.
- Fourcaudot E, Gambino F, Casassus G, Poulain B, Humeau Y, Luthi A (2009). L-type voltage-dependent Ca(2+) channels mediate expression of presynaptic LTP in amygdala. *Nat Neurosci* **12**(9): 1093-1095.
- Fremaux N, Gerstner W (2016). Neuromodulated Spike-Timing-Dependent Plasticity, and Theory of Three-Factor Learning Rules. *Front Neural Circuits* **9**: 85.
- Froemke RC, Dan Y (2002). Spike-timing-dependent synaptic modification induced by natural spike trains. *Nature* **416**(6879): 433-438.
- Froemke RC, Tsay IA, Raad M, Long JD, Dan Y (2006). Contribution of individual spikes in burst-induced long-term synaptic modification. *J Neurophysiol* **95**(3): 1620-1629.
- Gasbarri A, Packard MG, Sulli A, Pacitti C, Innocenzi R, Perciavalle V (1996). The projections of the retrorubral field A8 to the hippocampal formation in the rat. *Exp Brain Res* **112**(2): 244-252.
- Gasbarri A, Verney C, Innocenzi R, Campana E, Pacitti C (1994). Mesolimbic dopaminergic neurons innervating the hippocampal formation in the rat: a combined retrograde tracing and immunohistochemical study. *Brain Res* **668**(1-2): 71-79.
- Gasparini S, Losonczy A, Chen X, Johnston D, Magee JC (2007). Associative pairing enhances action potential back-propagation in radial oblique branches of CA1 pyramidal neurons. *J Physiol* **580**(Pt.3): 787-800.
- Geisler S, Zahm DS (2005). Afferents of the ventral tegmental area in the rat-anatomical substratum for integrative functions. *J Comp Neurol* **490**(3): 270-294.
- Goggi J, Pullar IA, Carney SL, Bradford HF (2002). Modulation of neurotransmitter release induced by brain-derived neurotrophic factor in rat brain striatal slices in vitro. *Brain Res* **941**(1-2): 34-42.
- Golding NL, Spruston N (1998). Dendritic sodium spikes are variable triggers of axonal action potentials in hippocampal CA1 pyramidal neurons. *Neuron* **21**(5): 1189-1200.
- Golding NL, Staff NP, Spruston N (2002). Dendritic spikes as a mechanism for cooperative long-term potentiation. *Nature* **418**(6895): 326-331.

- Golgi C, Bentivoglio M, Swanson L (2001). On the fine structure of the pes Hippocampi major (with plates XIII-XXIII). 1886. *Brain Res Bull* **54**(5): 461-483.
- Gottmann K, Mittmann T, Lessmann V (2009). BDNF signaling in the formation, maturation and plasticity of glutamatergic and GABAergic synapses. *Exp Brain Res* **199**(3-4): 203-234.
- Gustafsson B, Wigstrom H, Abraham WC, Huang YY (1987). Long-term potentiation in the hippocampus using depolarizing current pulses as the conditioning stimulus to single volley synaptic potentials. *J Neurosci* **7**(3): 774-780.
- Guthrie PB, Segal M, Kater SB (1991). Independent regulation of calcium revealed by imaging dendritic spines. *Nature* **354**(6348): 76-80.
- Hainmuller T, Krieglstein K, Kulik A, Bartos M (2014). Joint CP-AMPA and group I mGlu receptor activation is required for synaptic plasticity in dentate gyrus fast-spiking interneurons. *Proc Natl Acad Sci U S A* **111**(36): 13211-13216.
- Hansen N, Manahan-Vaughan D (2014). Dopamine D1/D5 receptors mediate informational saliency that promotes persistent hippocampal long-term plasticity. *Cereb Cortex* **24**(4): 845-858.
- Hardie J, Spruston N (2009). Synaptic depolarization is more effective than back-propagating action potentials during induction of associative long-term potentiation in hippocampal pyramidal neurons. *J Neurosci* **29**(10): 3233-3241.
- Harris EW, Cotman CW (1986). Long-term potentiation of guinea pig mossy fiber responses is not blocked by N-methyl D-aspartate antagonists. *Neurosci Lett* **70**(1): 132-137.
- Hartmann M, Heumann R, Lessmann V (2001). Synaptic secretion of BDNF after high-frequency stimulation of glutamatergic synapses. *EMBO J* **20**(21): 5887-5897.
- Hering H, Sheng M (2001). Dendritic spines: structure, dynamics and regulation. *Nat Rev Neurosci* **2**(12): 880-888.
- Herwerth M, Jensen V, Novak M, Konopka W, Hvalby O, Kohr G (2012). D4 dopamine receptors modulate NR2B NMDA receptors and LTP in stratum oriens of hippocampal CA1. *Cereb Cortex* **22**(8): 1786-1798.
- Hoffman DA, Johnston D (1998). Downregulation of transient K⁺ channels in dendrites of hippocampal CA1 pyramidal neurons by activation of PKA and PKC. *J Neurosci* **18**(10): 3521-3528.
- Hoffman DA, Johnston D (1999). Neuromodulation of dendritic action potentials. *J Neurophysiol* **81**(1): 408-411.
- Holbro N, Grunditz A, Wiegert JS, Oertner TG (2010). AMPA receptors gate spine Ca²⁺ transients and spike-timing-dependent potentiation. *Proc Natl Acad Sci U S A* **107**(36): 15975-15980.
- Holscher C (1997). Long-term potentiation: a good model for learning and memory? *Prog Neuropsychopharmacol Biol Psychiatry* **21**(1): 47-68.

- Hong M, Ross WN (2007). Priming of intracellular calcium stores in rat CA1 pyramidal neurons. *J Physiol* **584**(Pt 1): 75-87.
- Huang EP (1998). Synaptic plasticity: going through phases with LTP. *Curr Biol* **8**(10): R350-352.
- Huang YZ, Pan E, Xiong ZQ, McNamara JO (2008). Zinc-mediated transactivation of TrkB potentiates the hippocampal mossy fiber-CA3 pyramid synapse. *Neuron* **57**(4): 546-558.
- Hwang JJ, Park MH, Choi SY, Koh JY (2005). Activation of the Trk signaling pathway by extracellular zinc. Role of metalloproteinases. *J Biol Chem* **280**(12): 11995-12001.
- Illario M, Cavallo AL, Bayer KU, Di Matola T, Fenzi G, Rossi G, Vitale M (2003). Calcium/calmodulin-dependent protein kinase II binds to Raf-1 and modulates integrin-stimulated ERK activation. *J Biol Chem* **278**(46): 45101-45108.
- Iwakura Y, Nawa H, Sora I, Chao MV (2008). Dopamine D1 receptor-induced signaling through TrkB receptors in striatal neurons. *J Biol Chem* **283**(23): 15799-15806.
- Jaffe DB, Johnston D, Lasser-Ross N, Lisman JE, Miyakawa H, Ross WN (1992). The spread of Na⁺ spikes determines the pattern of dendritic Ca²⁺ entry into hippocampal neurons. *Nature* **357**(6375): 244-246.
- Jia Z, Agopyan N, Miu P, Xiong Z, Henderson J, Gerlai R, Taverna FA, Velumian A, MacDonald J, Carlen P, Abramow-Newerly W, Roder J (1996). Enhanced LTP in mice deficient in the AMPA receptor GluR2. *Neuron* **17**(5): 945-956.
- Jones MW, Errington ML, French PJ, Fine A, Bliss TV, Garel S, Charnay P, Bozon B, Laroche S, Davis S (2001). A requirement for the immediate early gene Zif268 in the expression of late LTP and long-term memories. *Nat Neurosci* **4**(3): 289-296.
- Kampa BM, Letzkus JJ, Stuart GJ (2006). Requirement of dendritic calcium spikes for induction of spike-timing-dependent synaptic plasticity. *J Physiol* **574**(Pt 1): 283-290.
- Kang H, Schuman EM (1995). Long-lasting neurotrophin-induced enhancement of synaptic transmission in the adult hippocampus. *Science* **267**(5204): 1658-1662.
- Katz B, Miledi R (1967). Ionic requirements of synaptic transmitter release. *Nature* **215**(5101): 651.
- Katz Y, Menon V, Nicholson DA, Geinisman Y, Kath WL, Spruston N (2009). Synapse distribution suggests a two-stage model of dendritic integration in CA1 pyramidal neurons. *Neuron* **63**(2): 171-177.
- Kauer JA, Malenka RC (2006). LTP: AMPA receptors trading places. *Nat Neurosci* **9**(5): 593-594.
- Kempadoo KA, Mosharov EV, Choi SJ, Sulzer D, Kandel ER (2016). Dopamine release from the locus coeruleus to the dorsal hippocampus promotes spatial learning and memory. *Proc Natl Acad Sci U S A* **113**(51): 14835-14840.

- Kennedy MB (2000). Signal-processing machines at the postsynaptic density. *Science* **290**(5492): 750-754.
- Kim HG, Connors BW (1993). Apical dendrites of the neocortex: correlation between sodium- and calcium-dependent spiking and pyramidal cell morphology. *J Neurosci* **13**(12): 5301-5311.
- Kohler C, Ericson H, Radesater AC (1991). Different laminar distributions of dopamine D1 and D2 receptors in the rat hippocampal region. *Neurosci Lett* **126**(2): 107-109.
- Korte M, Carroll P, Wolf E, Brem G, Thoenen H, Bonhoeffer T (1995). Hippocampal long-term potentiation is impaired in mice lacking brain-derived neurotrophic factor. *Proc Natl Acad Sci U S A* **92**(19): 8856-8860.
- Kuczewski N, Porcher C, Gaiarsa JL (2010). Activity-dependent dendritic secretion of brain-derived neurotrophic factor modulates synaptic plasticity. *Eur J Neurosci* **32**(8): 1239-1244.
- Larkum ME, Zhu JJ, Sakmann B (1999). A new cellular mechanism for coupling inputs arriving at different cortical layers. *Nature* **398**(6725): 338-341.
- Larson J, Munkacsy E (2015). Theta-burst LTP. *Brain Res* **1621**: 38-50.
- Laube B, Kuhse J, Betz H (1998). Evidence for a tetrameric structure of recombinant NMDA receptors. *J Neurosci* **18**(8): 2954-2961.
- Lavenex P, Amaral DG (2000). Hippocampal-neocortical interaction: a hierarchy of associativity. *Hippocampus* **10**(4): 420-430.
- Le Vasseur M, Ran I, Lacaille JC (2008). Selective induction of metabotropic glutamate receptor 1- and metabotropic glutamate receptor 5-dependent chemical long-term potentiation at oriens/alveus interneuron synapses of mouse hippocampus. *Neuroscience* **151**(1): 28-42.
- Leal G, Bramham CR, Duarte CB (2017). BDNF and Hippocampal Synaptic Plasticity. *Vitam Horm* **104**: 153-195.
- Leal G, Comprido D, Duarte CB (2014). BDNF-induced local protein synthesis and synaptic plasticity. *Neuropharmacology* **76 Pt C**: 639-656.
- Lee SJ, Escobedo-Lozoya Y, Szatmari EM, Yasuda R (2009). Activation of CaMKII in single dendritic spines during long-term potentiation. *Nature* **458**(7236): 299-304.
- Lee SP, So CH, Rashid AJ, Varghese G, Cheng R, Lanca AJ, O'Dowd BF, George SR (2004). Dopamine D1 and D2 receptor Co-activation generates a novel phospholipase C-mediated calcium signal. *J Biol Chem* **279**(34): 35671-35678.
- Leonard AS, Lim IA, Hemsworth DE, Horne MC, Hell JW (1999). Calcium/calmodulin-dependent protein kinase II is associated with the N-methyl-D-aspartate receptor. *Proc Natl Acad Sci U S A* **96**(6): 3239-3244.
- Lessmann V (1998). Neurotrophin-dependent modulation of glutamatergic synaptic transmission in the mammalian CNS. *Gen Pharmacol* **31**(5): 667-674.

- Lessmann V, Brigadski T (2009). Mechanisms, locations, and kinetics of synaptic BDNF secretion: an update. *Neurosci Res* **65**(1): 11-22.
- Lessmann V, Gottmann K, Heumann R (1994). BDNF and NT-4/5 enhance glutamatergic synaptic transmission in cultured hippocampal neurones. *Neuroreport* **6**(1): 21-25.
- Li C, Dabrowska J, Hazra R, Rainnie DG (2011). Synergistic activation of dopamine D1 and TrkB receptors mediate gain control of synaptic plasticity in the basolateral amygdala. *PLoS One* **6**(10): e26065.
- Liao D, Hessler NA, Malinow R (1995). Activation of postsynaptically silent synapses during pairing-induced LTP in CA1 region of hippocampal slice. *Nature* **375**(6530): 400-404.
- Lien CC, Mu Y, Vargas-Caballero M, Poo MM (2006). Visual stimuli-induced LTD of GABAergic synapses mediated by presynaptic NMDA receptors. *Nat Neurosci* **9**(3): 372-380.
- Lin MT, Lujan R, Watanabe M, Adelman JP, Maylie J (2008). SK2 channel plasticity contributes to LTP at Schaffer collateral-CA1 synapses. *Nat Neurosci* **11**(2): 170-177.
- Lisman J (2017). Glutamatergic synapses are structurally and biochemically complex because of multiple plasticity processes: long-term potentiation, long-term depression, short-term potentiation and scaling. *Philos Trans R Soc Lond B Biol Sci* **372**(1715).
- Lisman J, Yasuda R, Raghavachari S (2012). Mechanisms of CaMKII action in long-term potentiation. *Nat Rev Neurosci* **13**(3): 169-182.
- Lisman JE (2009). The pre/post LTP debate. *Neuron* **63**(3): 281-284.
- Lisman JE, Grace AA (2005). The hippocampal-VTA loop: controlling the entry of information into long-term memory. *Neuron* **46**(5): 703-713.
- Liu Y, Cui L, Schwarz MK, Dong Y, Schluter OM (2017). Adrenergic Gate Release for Spike Timing-Dependent Synaptic Potentiation. *Neuron* **93**(2): 394-408.
- Lømo T (1966). Frequency potentiation of excitatory synaptic activity in the dentate area of the hippocampal formation. *Acta. Physiol. Scand.* **68**(277): 128.
- Lu H, Park H, Poo MM (2014). Spike-timing-dependent BDNF secretion and synaptic plasticity. *Philos Trans R Soc Lond B Biol Sci* **369**(1633): 20130132.
- Luebke JI, Dunlap K, Turner TJ (1993). Multiple calcium channel types control glutamatergic synaptic transmission in the hippocampus. *Neuron* **11**(5): 895-902.
- Lynch GS, Dunwiddie T, Gribkoff V (1977). Heterosynaptic depression: a postsynaptic correlate of long-term potentiation. *Nature* **266**(5604): 737-739.
- Magee JC, Carruth M (1999). Dendritic voltage-gated ion channels regulate the action potential firing mode of hippocampal CA1 pyramidal neurons. *J Neurophysiol* **82**(4): 1895-1901.

- Magee JC, Johnston D (1997). A synaptically controlled, associative signal for Hebbian plasticity in hippocampal neurons. *Science* **275**(5297): 209-213.
- Malenka RC, Bear MF (2004). LTP and LTD: an embarrassment of riches. *Neuron* **44**(1): 5-21.
- Malinow R (1991). Transmission between pairs of hippocampal slice neurons: quantal levels, oscillations, and LTP. *Science* **252**(5006): 722-724.
- Man HY (2011). GluA2-lacking, calcium-permeable AMPA receptors--inducers of plasticity? *Curr Opin Neurobiol* **21**(2): 291-298.
- Mapelli J, Gandolfi D, Vilella A, Zoli M, Bigiani A (2016). Heterosynaptic GABAergic plasticity bidirectionally driven by the activity of pre- and postsynaptic NMDA receptors. *Proc Natl Acad Sci U S A* **113**(35): 9898-9903.
- Markram H, Gerstner W, Sjostrom PJ (2011). A history of spike-timing-dependent plasticity. *Front Synaptic Neurosci* **3**: 4.
- Markram H, Lubke J, Frotscher M, Sakmann B (1997). Regulation of synaptic efficacy by coincidence of postsynaptic APs and EPSPs. *Science* **275**(5297): 213-215.
- Matsuzaki M, Honkura N, Ellis-Davies GC, Kasai H (2004). Structural basis of long-term potentiation in single dendritic spines. *Nature* **429**(6993): 761-766.
- Mayer ML, Westbrook GL, Guthrie PB (1984). Voltage-dependent block by Mg²⁺ of NMDA responses in spinal cord neurones. *Nature* **309**(5965): 261-263.
- McGuinness L, Taylor C, Taylor RD, Yau C, Langenhan T, Hart ML, Christian H, Tynan PW, Donnelly P, Emptage NJ (2010). Presynaptic NMDARs in the hippocampus facilitate transmitter release at theta frequency. *Neuron* **68**(6): 1109-1127.
- McNamara CG, Dupret D (2017). Two sources of dopamine for the hippocampus. *Trends Neurosci* **40**(7): 383-384.
- Megias M, Emri Z, Freund TF, Gulyas AI (2001). Total number and distribution of inhibitory and excitatory synapses on hippocampal CA1 pyramidal cells. *Neuroscience* **102**(3): 527-540.
- Meyer D, Bonhoeffer T, Scheuss V (2014). Balance and stability of synaptic structures during synaptic plasticity. *Neuron* **82**(2): 430-443.
- Miller SG, Kennedy MB (1986). Regulation of brain type II Ca²⁺/calmodulin-dependent protein kinase by autophosphorylation: a Ca²⁺-triggered molecular switch. *Cell* **44**(6): 861-870.
- Mohajerani MH, Sivakumaran S, Zacchi P, Aguilera P, Cherubini E (2007). Correlated network activity enhances synaptic efficacy via BDNF and the ERK pathway at immature CA3 CA1 connections in the hippocampus. *Proc Natl Acad Sci U S A* **104**(32): 13176-13181.

- Moreno-Castilla P, Perez-Ortega R, Violante-Soria V, Balderas I, Bermudez-Rattoni F (2017). Hippocampal release of dopamine and norepinephrine encodes novel contextual information. *Hippocampus* **27**(5): 547-557.
- Moser EI, Krobot KA, Moser MB, Morris RG (1998). Impaired spatial learning after saturation of long-term potentiation. *Science* **281**(5385): 2038-2042.
- Mowla SJ, Farhadi HF, Pareek S, Atwal JK, Morris SJ, Seidah NG, Murphy RA (2001). Biosynthesis and post-translational processing of the precursor to brain-derived neurotrophic factor. *J Biol Chem* **276**(16): 12660-12666.
- Murakami N, Ishibashi H, Katsurabayashi S, Akaike N (2002). Calcium channel subtypes on single GABAergic presynaptic terminal projecting to rat hippocampal neurons. *Brain Res* **951**(1): 121-129.
- Nabavi S, Kessels HW, Alfonso S, Aow J, Fox R, Malinow R (2013). Metabotropic NMDA receptor function is required for NMDA receptor-dependent long-term depression. *Proc Natl Acad Sci U S A* **110**(10): 4027-4032.
- Nadim F, Bucher D (2014). Neuromodulation of neurons and synapses. *Curr Opin Neurobiol* **29**: 48-56.
- Navakkode S, Chew KCM, Tay SJN, Lin Q, Behnisch T, Soong TW (2017). Bidirectional modulation of hippocampal synaptic plasticity by Dopaminergic D4-receptors in the CA1 area of hippocampus. *Sci Rep* **7**(1): 15571.
- Navakkode S, Sajikumar S, Korte M, Soong TW (2012). Dopamine induces LTP differentially in apical and basal dendrites through BDNF and voltage-dependent calcium channels. *Learn Mem* **19**(7): 294-299.
- Neyman S, Manahan-Vaughan D (2008). Metabotropic glutamate receptor 1 (mGluR1) and 5 (mGluR5) regulate late phases of LTP and LTD in the hippocampal CA1 region in vitro. *Eur J Neurosci* **27**(6): 1345-1352.
- Nicholson DA, Geinisman Y (2009). Axospinous synaptic subtype-specific differences in structure, size, ionotropic receptor expression, and connectivity in apical dendritic regions of rat hippocampal CA1 pyramidal neurons. *J Comp Neurol* **512**(3): 399-418.
- Nicoll RA (2017). A Brief History of Long-Term Potentiation. *Neuron* **93**(2): 281-290.
- Nicoll RA, Schmitz D (2005). Synaptic plasticity at hippocampal mossy fibre synapses. *Nat Rev Neurosci* **6**(11): 863-876.
- Nikonenko I, Jourdain P, Alberi S, Toni N, Muller D (2002). Activity-induced changes of spine morphology. *Hippocampus* **12**(5): 585-591.
- Noguchi J, Matsuzaki M, Ellis-Davies GC, Kasai H (2005). Spine-neck geometry determines NMDA receptor-dependent Ca²⁺ signaling in dendrites. *Neuron* **46**(4): 609-622.
- Nowak L, Bregestovski P, Ascher P, Herbet A, Prochiantz A (1984). Magnesium gates glutamate-activated channels in mouse central neurones. *Nature* **307**(5950): 462-465.

- Nusser Z, Lujan R, Laube G, Roberts JD, Molnar E, Somogyi P (1998). Cell type and pathway dependence of synaptic AMPA receptor number and variability in the hippocampus. *Neuron* **21**(3): 545-559.
- Nye SH, Squinto SP, Glass DJ, Stitt TN, Hantzopoulos P, Macchi MJ, Lindsay NS, Ip NY, Yancopoulos GD (1992). K-252a and staurosporine selectively block autophosphorylation of neurotrophin receptors and neurotrophin-mediated responses. *Mol Biol Cell* **3**(6): 677-686.
- Oertner TG, Sabatini BL, Nimchinsky EA, Svoboda K (2002). Facilitation at single synapses probed with optical quantal analysis. *Nat Neurosci* **5**(7): 657-664.
- Ohno-Shosaku T, Kano M (2014). Endocannabinoid-mediated retrograde modulation of synaptic transmission. *Curr Opin Neurobiol* **29**: 1-8.
- Okabe S (2007). Molecular anatomy of the postsynaptic density. *Mol Cell Neurosci* **34**(4): 503-518.
- Oldham WM, Hamm HE (2008). Heterotrimeric G protein activation by G-protein-coupled receptors. *Nat Rev Mol Cell Biol* **9**(1): 60-71.
- Otmakhov N, Tao-Cheng JH, Carpenter S, Asrican B, Dosemeci A, Reese TS, Lisman J (2004). Persistent accumulation of calcium/calmodulin-dependent protein kinase II in dendritic spines after induction of NMDA receptor-dependent chemical long-term potentiation. *J Neurosci* **24**(42): 9324-9331.
- Padamsey Z, Tong R, Emptage N (2017). Glutamate is required for depression but not potentiation of long-term presynaptic function. *Elife* **6**.
- Pare D (2004). Presynaptic induction and expression of NMDA-dependent LTP. *Trends Neurosci* **27**(8): 440-441.
- Pawlak V, Wickens JR, Kirkwood A, Kerr JN (2010). Timing is not Everything: Neuromodulation Opens the STDP Gate. *Front Synaptic Neurosci* **2**: 146.
- Pedarzani P, Storm JF (1995). Dopamine modulates the slow Ca(2+)-activated K⁺ current IAHP via cyclic AMP-dependent protein kinase in hippocampal neurons. *J Neurophysiol* **74**(6): 2749-2753.
- Penn AC, Zhang CL, Georges F, Royer L, Breillat C, Hosy E, Petersen JD, Humeau Y, Choquet D (2017). Hippocampal LTP and contextual learning require surface diffusion of AMPA receptors. *Nature* **549**(7672): 384-388.
- Plant K, Pelkey KA, Bortolotto ZA, Morita D, Terashima A, McBain CJ, Collingridge GL, Isaac JT (2006). Transient incorporation of native GluR2-lacking AMPA receptors during hippocampal long-term potentiation. *Nat Neurosci* **9**(5): 602-604.
- Poirazi P, Kastellakis G (2017). ...with Love, from Post to Pre. *Neuron* **96**(1): 9-10.
- Poo MM (2001). Neurotrophins as synaptic modulators. *Nat Rev Neurosci* **2**(1): 24-32.
- Raghavachari S, Lisman JE (2004). Properties of quantal transmission at CA1 synapses. *J Neurophysiol* **92**(4): 2456-2467.

- Rajagopal R, Chao MV (2006). A role for Fyn in Trk receptor transactivation by G-protein-coupled receptor signaling. *Mol Cell Neurosci* **33**(1): 36-46.
- Rajagopal R, Chen ZY, Lee FS, Chao MV (2004). Transactivation of Trk neurotrophin receptors by G-protein-coupled receptor ligands occurs on intracellular membranes. *J Neurosci* **24**(30): 6650-6658.
- Regehr WG (2012). Short-term presynaptic plasticity. *Cold Spring Harb Perspect Biol* **4**(7): a005702.
- Rellos P, Pike AC, Niesen FH, Salah E, Lee WH, von Delft F, Knapp S (2010). Structure of the CaMKII δ /calmodulin complex reveals the molecular mechanism of CaMKII kinase activation. *PLoS Biol* **8**(7): e1000426.
- Reuter H (1995). Measurements of exocytosis from single presynaptic nerve terminals reveal heterogeneous inhibition by Ca(2+)-channel blockers. *Neuron* **14**(4): 773-779.
- Rice ME, Cragg SJ (2008). Dopamine spillover after quantal release: rethinking dopamine transmission in the nigrostriatal pathway. *Brain Res Rev* **58**(2): 303-313.
- Richfield EK, Penney JB, Young AB (1989). Anatomical and affinity state comparisons between dopamine D1 and D2 receptors in the rat central nervous system. *Neuroscience* **30**(3): 767-777.
- Rosen ZB, Cheung S, Siegelbaum SA (2015). Midbrain dopamine neurons bidirectionally regulate CA3-CA1 synaptic drive. *Nat Neurosci* **18**(12): 1763-1771.
- Routh BN, Johnston D, Harris K, Chitwood RA (2009). Anatomical and electrophysiological comparison of CA1 pyramidal neurons of the rat and mouse. *J Neurophysiol* **102**(4): 2288-2302.
- Roux PP, Dorval G, Boudreau M, Angers-Loustau A, Morris SJ, Makkerh J, Barker PA (2002). K252a and CEP1347 are neuroprotective compounds that inhibit mixed-lineage kinase-3 and induce activation of Akt and ERK. *J Biol Chem* **277**(51): 49473-49480.
- Rozas C, Carvallo C, Contreras D, Carreno M, Ugarte G, Delgado R, Zeise ML, Morales B (2015). Methylphenidate amplifies long-term potentiation in rat hippocampus CA1 area involving the insertion of AMPA receptors by activation of beta-adrenergic and D1/D5 receptors. *Neuropharmacology* **99**: 15-27.
- Scanziani M, Malenka RC, Nicoll RA (1996). Role of intercellular interactions in heterosynaptic long-term depression. *Nature* **380**(6573): 446-450.
- Schneggenburger R, Rosenmund C (2015). Molecular mechanisms governing Ca(2+) regulation of evoked and spontaneous release. *Nat Neurosci* **18**(7): 935-941.
- Schulz PE, Cook EP, Johnston D (1994). Changes in paired-pulse facilitation suggest presynaptic involvement in long-term potentiation. *J Neurosci* **14**(9): 5325-5337.
- Scoville WB, Milner B (1957). Loss of recent memory after bilateral hippocampal lesions. *J Neurol Neurosurg Psychiatry* **20**(1): 11-21.

- Seol GH, Ziburkus J, Huang S, Song L, Kim IT, Takamiya K, Huganir RL, Lee HK, Kirkwood A (2007). Neuromodulators control the polarity of spike-timing-dependent synaptic plasticity. *Neuron* **55**(6): 919-929.
- Shi S, Hayashi Y, Esteban JA, Malinow R (2001). Subunit-specific rules governing AMPA receptor trafficking to synapses in hippocampal pyramidal neurons. *Cell* **105**(3): 331-343.
- Shivarama Shetty M, Gopinadhan S, Sajikumar S (2016). Dopamine D1/D5 receptor signaling regulates synaptic cooperation and competition in hippocampal CA1 pyramidal neurons via sustained ERK1/2 activation. *Hippocampus* **26**(2): 137-150.
- Sjostrom PJ, Turrigiano GG, Nelson SB (2003). Neocortical LTD via coincident activation of presynaptic NMDA and cannabinoid receptors. *Neuron* **39**(4): 641-654.
- Smith CC, Greene RW (2012). CNS dopamine transmission mediated by noradrenergic innervation. *J Neurosci* **32**(18): 6072-6080.
- Smith MA, Ellis-Davies GC, Magee JC (2003). Mechanism of the distance-dependent scaling of Schaffer collateral synapses in rat CA1 pyramidal neurons. *J Physiol* **548**(Pt 1): 245-258.
- Spruston N, Schiller Y, Stuart G, Sakmann B (1995). Activity-dependent action potential invasion and calcium influx into hippocampal CA1 dendrites. *Science* **268**(5208): 297-300.
- Staff NP, Jung HY, Thiagarajan T, Yao M, Spruston N (2000). Resting and active properties of pyramidal neurons in subiculum and CA1 of rat hippocampus. *J Neurophysiol* **84**(5): 2398-2408.
- Stanzione P, Calabresi P, Mercuri N, Bernardi G (1984). Dopamine modulates CA1 hippocampal neurons by elevating the threshold for spike generation: an in vitro study. *Neuroscience* **13**(4): 1105-1116.
- Sudhof TC (2013). Neurotransmitter release: the last millisecond in the life of a synaptic vesicle. *Neuron* **80**(3): 675-690.
- Swift JL, Godin AG, Dore K, Freland L, Bouchard N, Nimmo C, Sergeev M, De Koninck Y, Wiseman PW, Beaulieu JM (2011). Quantification of receptor tyrosine kinase transactivation through direct dimerization and surface density measurements in single cells. *Proc Natl Acad Sci U S A* **108**(17): 7016-7021.
- Tapley P, Lamballe F, Barbacid M (1992). K252a is a selective inhibitor of the tyrosine protein kinase activity of the trk family of oncogenes and neurotrophin receptors. *Oncogene* **7**(2): 371-381.
- Thomas GM, Huganir RL (2004). MAPK cascade signalling and synaptic plasticity. *Nat Rev Neurosci* **5**(3): 173-183.
- Tigaret CM, Olivo V, Sadowski JH, Ashby MC, Mellor JR (2016). Coordinated activation of distinct Ca(2+) sources and metabotropic glutamate receptors encodes Hebbian synaptic plasticity. *Nat Commun* **7**: 10289.

- Tigerholm J, Migliore M, Fransen E (2013). Integration of synchronous synaptic input in CA1 pyramidal neuron depends on spatial and temporal distributions of the input. *Hippocampus* **23**(1): 87-99.
- Tippens AL, Pare JF, Langwieser N, Moosmang S, Milner TA, Smith Y, Lee A (2008). Ultrastructural evidence for pre- and postsynaptic localization of Cav1.2 L-type Ca²⁺ channels in the rat hippocampus. *J Comp Neurol* **506**(4): 569-583.
- Tovar KR, McGinley MJ, Westbrook GL (2013). Triheteromeric NMDA receptors at hippocampal synapses. *J Neurosci* **33**(21): 9150-9160.
- Traynelis SF, Wollmuth LP, McBain CJ, Menniti FS, Vance KM, Ogden KK, Hansen KB, Yuan H, Myers SJ, Dingledine R (2010). Glutamate receptor ion channels: structure, regulation, and function. *Pharmacol Rev* **62**(3): 405-496.
- Tritsch NX, Sabatini BL (2012). Dopaminergic modulation of synaptic transmission in cortex and striatum. *Neuron* **76**(1): 33-50.
- Tse D, Langston RF, Kakeyama M, Bethus I, Spooner PA, Wood ER, Witter MP, Morris RG (2007). Schemas and memory consolidation. *Science* **316**(5821): 76-82.
- Williams JH, Errington ML, Lynch MA, Bliss TV (1989). Arachidonic acid induces a long-term activity-dependent enhancement of synaptic transmission in the hippocampus. *Nature* **341**(6244): 739-742.
- Wittenberg GM, Wang SS (2006). Malleability of spike-timing-dependent plasticity at the CA3-CA1 synapse. *J Neurosci* **26**(24): 6610-6617.
- Witter MP (1993). Organization of the entorhinal-hippocampal system: a review of current anatomical data. *Hippocampus* **3 Spec No**: 33-44.
- Witter MP, Griffioen AW, Jorritsma-Byham B, Krijnen JL (1988). Entorhinal projections to the hippocampal CA1 region in the rat: an underestimated pathway. *Neurosci Lett* **85**(2): 193-198.
- Witter MP, Naber PA, van Haeften T, Machielsen WC, Rombouts SA, Barkhof F, Scheltens P, Lopes da Silva FH (2000). Cortico-hippocampal communication by way of parallel parahippocampal-subicular pathways. *Hippocampus* **10**(4): 398-410.
- Wolfart J, Neuhoff H, Franz O, Roeper J (2001). Differential expression of the small-conductance, calcium-activated potassium channel SK3 is critical for pacemaker control in dopaminergic midbrain neurons. *J Neurosci* **21**(10): 3443-3456.
- Xu TX, Yao WD (2010). D1 and D2 dopamine receptors in separate circuits cooperate to drive associative long-term potentiation in the prefrontal cortex. *Proc Natl Acad Sci U S A* **107**(37): 16366-16371.
- Yang K, Broussard JI, Levine AT, Jenson D, Arenkiel BR, Dani JA (2017). Dopamine receptor activity participates in hippocampal synaptic plasticity associated with novel object recognition. *Eur J Neurosci* **45**(1): 138-146.

- Yang SN (2000). Sustained enhancement of AMPA receptor- and NMDA receptor-mediated currents induced by dopamine D1/D5 receptor activation in the hippocampus: an essential role of postsynaptic Ca²⁺. *Hippocampus* **10**(1): 57-63.
- Yang Y, Calakos N (2013). Presynaptic long-term plasticity. *Front Synaptic Neurosci* **5**: 8.
- Yao H, Dan Y (2001). Stimulus timing-dependent plasticity in cortical processing of orientation. *Neuron* **32**(2): 315-323.
- Yger P, Stimberg M, Brette R (2015). Fast Learning with Weak Synaptic Plasticity. *J Neurosci* **35**(39): 13351-13362.
- Yuste R, Majewska A, Holthoff K (2000). From form to function: calcium compartmentalization in dendritic spines. *Nat Neurosci* **3**(7): 653-659.
- Zenke F, Gerstner W (2017). Hebbian plasticity requires compensatory processes on multiple timescales. *Philos Trans R Soc Lond B Biol Sci* **372**(1715).
- Zhang JC, Lau PM, Bi GQ (2009). Gain in sensitivity and loss in temporal contrast of STDP by dopaminergic modulation at hippocampal synapses. *Proc Natl Acad Sci U S A* **106**(31): 13028-13033.
- Zhang YP, Holbro N, Oertner TG (2008). Optical induction of plasticity at single synapses reveals input-specific accumulation of alphaCaMKII. *Proc Natl Acad Sci U S A* **105**(33): 12039-12044.

Declaration

I hereby declare that I have prepared my dissertation independently on the subject

“Mechanism of spike timing-dependent LTP in CA1 of the hippocampus induced with low repeat of coincident pre- and postsynaptic spiking.”

Facts or ideas taken from other sources, either directly or indirectly, have been marked as such.

Furthermore, I declare that this work has not been submitted either in Germany or abroad to obtain the academic degree of *doctor rerum naturalium* (Dr. rer. nat.).

Magdeburg, 19.06.2018

Efraín Augusto Cepeda-Prado